Metabolic cooperation and the polymorphic secretion of invertase in yeast.

Fuentes Hernandez, Ayari

Award date:
2012

Awarding institution:
University of Bath

Metabolic cooperation and the polymorphic secretion of invertase in yeast.

submitted by

Ayari Fuentes Hernandez

for the degree of Doctor of Philosophy

of the

University of Bath

Department of Biology and Biochemistry

2012

ACKNOWLEDGEMENTS

I would like to express my gratitude to my supervisor Ivana Gudelj, for her guidance and supervision, her patience and for all the time that she spent with me, for introducing me into the field of Evolutionary Biology, and and for giving me the opportunity to collaborate with people in different fields.

I would also like to thank my supervisor Laurence Hurst for his guidance and supervision and for all the help and expertise that he provided me during these years.

I must thank all the people in the Lab. In particular to Robert Beardmore for help and always insightful chats. I would also like to thank Ted for being a great occasional companion.

I wish to thank the people in Duncan Greig's Lab, in particular to Duncan for collaborating with us and for allowing me to be part of his group for a while, and for introducing me to the "experimental world".

To Craig MacLean for experimental data and interesting chats.

I am also thankful with Alan Wheals and Jan-Ulrich Kreft for very helpful and insightful comments about this thesis.

I am grateful to CONACYT for financial support.

This work is dedicated to my parents because they have always been a foundation for achieving my goals. Their love, support and example has made this thesis possible. This work is also theirs.

To Canek for all his support, his love, and for being not just my brother but also my best friend.

To Galia, because she has been one of the greatest joys in my life; she is already one of my favourite people in the world.

And especially to Rafa for being my partner in life and my husband, because with him I have travelled a great journey, for all his love, support and his sense of humour, because without him life would be less interesting.

To all the people that have made me feel at home in England.

To Maya with love.

Contributions

Chapter 2 and Chapter 3 are based on the published article: *R.C MacLean*, A Fuentes-Hernandez*, D Greig, LD Hurst and I. Gudelj.* ***"A mixture of "cheats" and "co-operators" can enable maximal group benefit.*** *PLoS Biology. 2010. Volume 8 (9)* (*Co-first authors).

The experimental data presented in this publication were acquired by Craig MacLean and Duncan Greig . Data analysis was performed by Craig MacLean , Ayari Fuentes-Hernandez, Laurence D. Hurst and Ivana Gudelj . Mathematical modelling and numerical analysis was performed by Ayari Fuentes-Hernandez and Ivana Gudelj.

The mathematical analysis presented Chapter 4 and Chapter 5 was conducted by Ayari Fuentes-Hernandez with guidance by Ivana Gudelj and Laurence Hurst, and the results discussed here are currently being prepared for publication. Experiments presented in Chapter 5 were conceived and conducted by Ayari Fuentes-Hernandez under the supervision of Duncan Greig during an academic visit to the Max Planck Institute for Evolutionary Biology.

CONTENTS

LIST OF FIGURES

Summary

The evolution of cooperation can be seen as a paradox in the light of the theory of natural selection. In simple terms this theory states how evolution is driven mainly by competition. However, nature presents us with multiple examples across different scales, from prokaryotes to humans, of organisms that co-operate and in turn are cheated by other individuals. Co-existence between these two actors is well documented in the literature and understanding the emergence and maintenance of this behaviour is an important challenge for evolutionary biology.

The purpose of this thesis is to analyse a co-operative system where the presence of "cheats" maximises the fitness of the group in competition experiments between two strains of yeast growing under sucrose limitation. The so-called "cooperators" secrete the enzyme invertase hydrolysing sucrose and therefore making glucose available for the rest of the population. Conversely, cells that do not secrete this enzyme but obtain the benefit of the available glucose are referred to as "cheats".

We use a system-biological model constructed from the underlying biochemistry to explore the mechanisms that make the presence of non-producers maximise the fitness of the population. Mechanism that can be summarised as follows: the existence of a well-documented rate-efficiency trade-off, the fact that producing invertase is associated with a metabolic cost, and a spatially-structured environment.

Finally, in this thesis we also examine how temporal structure can affect the population dynamics of the system. We achieve this by introducing a seasonal dynamics where cells compete for the limiting resource during a fixed time interval, before being transferred into a new plate with fresh growth medium. In the final part of this thesis we show that both the length of each season and the transfer protocol under consideration are important factors determining the co-existence patterns and the long-term dynamics of the system.

CHAPTER 1

Introduction

"The great tragedy of Science:
the slaying of a beautiful hypothesis by an ugly fact."
T. H. Huxley

1.1 Evolution and co-operation

Natural selection is one of the most successful theories ever proposed. This theory, postulated by Darwin over 150 years ago, has been able to explain adaptation, survival and reproduction of individuals based on competition and the survival of individuals with a higher fitness. Fitness is defined as the genotype with the highest average reproductive success in a particular environment during their lifetime. Therefore, co-operative behaviour, whereby an individual pays a fitness cost for someone else's benefit [5], seems like an immediate paradox. Understanding the conditions favouring and maintaining co-operation in nature thus presents one of the greatest challenges of evolutionary biology [78].

The problem of altruism sits in the context of the problem of the evolution of social interactions, a process based on changes that are inherited across several generations and, according to their fitness effects, can fix in the population, having consequences

Table 1.1: Social interaction between actor and recipient

	Fitness impact *For recipient +*	Fitness impact *For recipient -*
Fitness impact for actor +	Mutual benefit	Selfishness
Fitness impact for actor -	Altruism	Spite

for both the actor and the recipient. In a simple formulation, any given encounter can present any of the following outcomes: if the actor co-operates the interaction is said to be *mutually beneficial* when it benefits both the actor and the recipient, or *altruistic* if it only benefits the recipient. In contrast, if the actor defects, the interaction can be classified as *selfish* when the actor obtains benefit from the recipient or *spiteful* if neither of them receives a benefit, as shown in Table 1.1 (reproduced from [103]).

Thus, by definition, an altruist produces a benefit to others while paying an individual fitness cost for the benefit of the group. At first sight therefore natural selection should act to increase the abundance of "cheats" (alias "defectors"), individuals that do not pay a cost, but still obtain the benefit. Indeed, in the absence of a co-operation-promoting mechanisms, defectors have a higher average fitness and thus are expected both to invade a population of co-operators and fixate in the population [70], a feature illustrated in Figure 1-1.

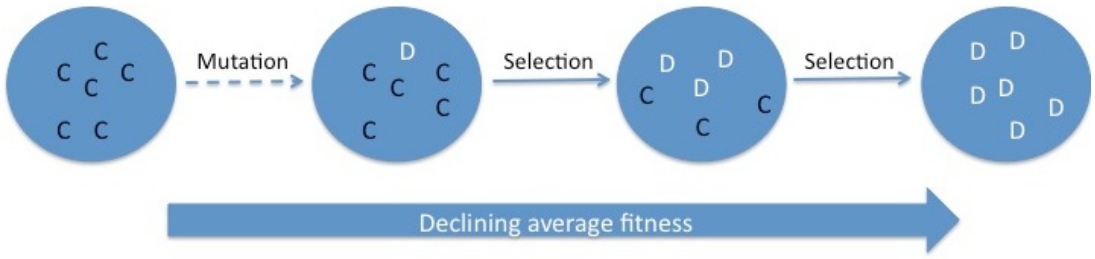

Figure 1-1: In the absence of mechanisms that promote the evolution of co-operation, natural selection favours defectors [70]. Here C indicates a co-operator and D a defector/cheat.

The first and most obvious prediction of this simple conception is that altruistic co-operation should be rare in nature. Putatively co-operative behaviour has, however, been found in humans [101], chimpanzees [20], meerkats [17], fish [13], bats [105], insects

[11, 47, 88], and microbes [62, 42, 2, 103, 29], just to mention a few examples.

Altruistic acts may be understandable in humans, "the kings of co-operation" according to [70], as they have the potential to observe the behaviour of others, remember who has co-operated in the past and assemble reputations, thus enabling discrimination as to whom to punish and whom to favour [74]. The precise conditions favouring co-operation in such psychologically rich organisms as humans remains contentious. This is not the subject of this thesis. Rather I shall examine a circumstance in which such complexities are removed. I shall consider why microbes with a lack of "consciousness" act altruistically "helping" others in detriment of their own benefit. This is arguably one of the most challenging questions of microbial evolution. If we cannot fully understand co-operation in such simple cases what hope have we of understanding it in more complex instances?

1.2 Previous theoretical approaches to understand co-operation

Over the last decades, great efforts have been invested in order to develop a general theory that explains the evolution of co-operation. The most important theory is known as Kin selection or Inclusive fitness, announced by W. D. Hamilton in 1963 as:

"Despite the principle of 'survival of the fittest' the ultimate criterion that determines whether G will spread is not whether the behaviour is to the benefit of the behaver but whether it is to the benefit of gene G". [Hamilton, 1963, p 335]

By shifting the focus of attention from the costs and benefits encountered by a given individual to the costs and benefits encountered by an allele, this theory provides an explanation of broad applicability as to why co-operation can evolve between relatives, using what is known as Hamilton's rule. This notes that altruism is favoured when $rb - c > 0$, where c represents the cost of the altruistic behaviour, r the level of genetic relatedness (genetic similarity) and b the fitness benefit of the beneficiary [40].

These three parameters broadly define the conditions where altruism might be

expected: where the benefits are high compared with the costs and where relatedness between altruist and receiver of the benefits is high. There are two principal mechanisms to obtain high relatedness (r):

- Limited dispersal, whereby kin tend to stay together. In particular, spatial structure allows the benefit of a co-operator to be shared with neighbours, which are most likely to be related.
- Kin discrimination: The altruist distinguishes between relatives and non-relatives and somehow directs the benefits of co-operation disproportionately towards its relatives.

A different approach, often used in economics and sociology, uses game theory as a mathematical framework [66, 58]. In contrast to kin selection, (that subsumes natural selection), this approach argues that natural selection is the main driving force for the evolution of co-operation [72], kin selection is not necessary . Whether this is a merely semantic argument [1] or not, it is not the aim of this thesis to discuss it.

Evolutionary game theory

In its simplest form, evolutionary game theory treats co-operation as an N-player game where individuals have two possible strategies: defect or co-operate. The latter strategy has a cost c for the co-operator and produces a benefit b for the population, while the previous produces no benefit to the population and carries no cost to the player.

The prisoner's dilemma (PD) is based on a game where two prisoners are interrogated separately for a crime they have been accused of. In this game the actors has two possibles strategies, to defect or to co-operate. Co-operation results in a benefit to the opposing player (b) but came with an inherent cost for the actor (c). In this particular case if both actors co-operate the resulting payoff for the actor will be denoted by $R = b - c$, in contrast if the actor defects and the opponent co-operates then the actor gets a better payoff for the action $T = b$ without paying the cost of co-operation. If the

Table 1.2: Payoff matrix for a PD

	Cooperate	Defect
Payoff to Co-operate	$b - c$	$-c$
Payoff to Defect	b	0

Table 1.3: Payoff matrix for a SDG

	Cooperate	Defect
Payoff to Co-operate	$b - c/2$	$b - c$
Payoff to Defect	b	0

actor decides to co-operate but the opponent defects then the payoff will be $S = -c$ and finally, if both actor and opponent defect the payoff for that action will be $P = 0$. If we look closely to these payoffs we notice that the best strategy for both players (*i.e.* the strategy with the lower payoff) is to defect.

If one changes the conditions of the prisoner's dilemma making the one-way defection sufficient for both players to obtain a benefit from the action, we have the snowdrift game (SDG) defined by a payoff matrix shown in Table 1.3 and with the particularity that, in contrast with the PD, a co-operative strategy has an advantage (*i.e.* the strategy with the lower payoff).

As we have seen, different games are represented with different payoff matrices, representing the fitness advantage of adopting different evolutionary strategies. For example Table 1.4 illustrates two possible games that have been used to explain the evolution of co-operation [21]: prisoners dilemma and snowdrift game.

Note that when playing the Prisoners Dilemma, the only stable equilibrium is mutually cheating and therefore co-operation cannot be maintained. Conversely, in

Table 1.4: Optimal strategy when playing PD and SDG

Game		Optimal Strategy	Outcome
Prisoners Dilemma	$T \geq R \geq S \geq P$	Cheat	Cheats win
Snowdrift Game	$T \geq S \geq R \geq P$	Depends on the other player, opposite.	Persistence of co-operation

the Snowdrift game the stable equilibrium is mutual co-operation and therefore co-operation can be maintained, a feature shown in Table 1.4, [21]. In the case of a one-shot play of PD, fixation of co-operation is not possible but including extensions and modifications of the same game like iterated interactions can lead us to find that co-operation can be a stable equilibrium in the population [71].

The fixation of co-operators often depends upon population structure, which not only depends on environmental factors but also on individual behaviour, it is important to notice that this structure can be dynamic [96].

As with kin selection, game theory has been exceptionally successful in capturing general trends of when co-operation is or is not maintained [21, 74, 19, 3], but as well as kin selection, lacks of quantitative predictive power.

Another problem with the theories of co-operation discussed so far, is the use of verbal arguments that resemble the human experience, for instance using words like "altruism" or "cheating". This descriptive language is used metaphorically as it implies conscious decisions that are made to comply ethical rules. Indeed this language has been useful allowing us intuitive understanding of a given biological process but, as discussed in this thesis, can be overly simplistic, misleading and confusing.

1.3 A systems biology of co-operation

In many fields of evolutionary biology, much progress has been made possible through the construction of a theoretical framework that enables strong quantitative predictions (rather than describing broad qualitative trends). For example, Kimura's neutral theory made exact predictions both about the ratio of the variance in the number of substitutions per lineage to the mean (the dispersion index) and the extent to which heterozygosity should vary with population size. That the dispersion index is consistently greater than the predicted unity [73], and that heterozygosity does not increase as much as expected in large populations (although, importantly the qualitative trend

is consistent) [32], have been two pivotal planks on which rejection of strict neutrality was based [73]. Similarly, Kondrashov's mutational deterministic theory [53] generated much research interest, as it predicted not simply that obligate sexual species would have a per genome deleterious mutation rate higher than that seen in obligate asexuals, but also that obligate sexuals will have a per genome deleterious mutation rate greater than one per genome per generation. This enabled attempts to falsify the model on quantitative grounds (see eg. [48]). Although this theories are not mechanistic *i.e.* bottom up models, they highlight the importance of been able to quantify predictions.

If quantitative predictive power is a limitation of both frameworks, kin selection and game theory, can we consider a different approach to co-operation, one that is capable of making quantitative predictions? In this thesis I will deploy tools from systems and population biology to attempt this. My approach follows a bottom-up type of modelling, posing theoretical abstractions but parameterised using known underlying biochemical rate constants. The goal of this approach is to capture, with quantitative accuracy, observed population-level outcomes and dynamics.

This framework is importantly different from others as, rather than defining fitness *apriori*, it considers fitness to be a consequence not only of the underlying molecular and biochemical details but also of the environmental, spatial and temporal dynamics. In short, I model the underlying biology from which I derive fitness, rather than supposing that I know fitness before the fact. An immediate consequence of this approach is that I need to consider the specifics of a given system. The aim of this approach then is to derive a detailed understanding of co-operation in a given system from which one can ask whether lessons learnt may have any relevance to other system. This contrasts with the classical approaches (kin selection/game theory approaches) in which toy models (*i.e.* biologically non-specific) are analysed, with *post hoc* attempts to relate insights to the behaviour observed in any given system. Indeed, the theoretical success of tit-for-tat as a strategy in the iterated prisoner's dilemma, enabling reciprocal altruism, spawned the search for organisms playing this strategy. However, reciprocal altruism, despite receiving considerable theoretical interest, appears to be rare in nature with

few convincing examples [41, 90]. Whether any organism plays tit-for-tat is unresolved and the broader scale relevance of the abundant theoretical literature on the PD can be questioned [41]

1.4 Microbial co-operation

For a systems biological approach to work, I need to be able to quantitatively model and experiment with the co-operative system. The obvious choice is a microbial system. Microbial model systems are an important tool in the field of evolutionary biology [14], not only because of microbes having a "simple" genome (allowing genetic manipulation), but also because their fast generation time allows us to observe evolution in a human time-scale [27].

In the last decades, a wide-range of co-operative behaviours have been observed in microbial systems. These include division of labour [2], cross-feeding between and within species [63, 42] and the production of public goods [12, 36]. The evolution of multicellularity [45, 37] one of the major evolutionary transitions [95] can be configured as a problem of microbial co-operation. We can also find examples where co-operation can be a mechanism for virulence of pathogens that are intrinsically connected with human activities and well-being [52].

1.5 The invertase system in yeast

The system model that I will study in this thesis is one of the most popular examples of a public goods game in microbes: the polymorphic secretion of invertase by yeast (*Saccharomyces cerevisiae*). Invertase is an enzyme that catalyses the hydrolysis of sucrose into fructose and glucose. Although yeast can take up sucrose [6], monosacharides like glucose and fructose are transported into the cell at a higher rate by the same family of transporters (HXT) but these transporters have a higher binding affinity for glucose than for fructose., therefore glucose is the preferred carbon source of yeast (see Figure

1-2). Genes coding for invertase belong to the *SUC* family; in particular *SUC2* plays an important role [67].

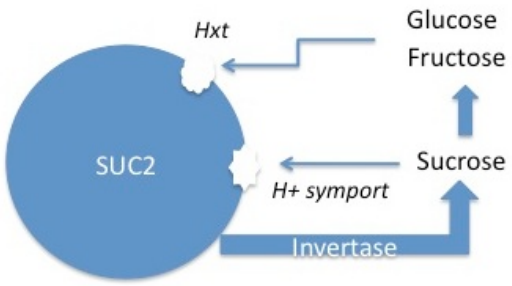

Figure 1-2: Metabolic structure of an Invertase Producer (SUC2).

Invertase enhances growth in yeast by making glucose available in the environment when sucrose is a food substrate. The production of invertase, however, is associated with a metabolic cost. Some strains of yeast do not secrete this enzyme but, in the presence of producers, exploit the monosacharides available in the environment (see Figure 1-3).

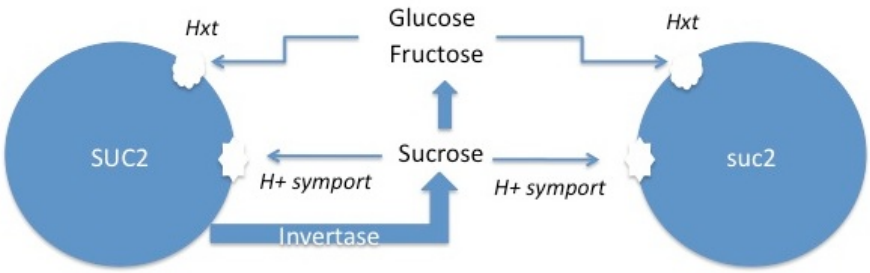

Figure 1-3: Schematic competition between invertase producers (*SUC2*) and non-producers (*suc2*). Both strains can take up the 3 different carbon sources (glucose, fructose and sucrose) , both glucose and fructose compete for the same transporter (*HXT*) although this transporter has a higher binding affinity for glucose, sucrose is take up by the $H^+symport$, with a lower rate of consumption.

Then why does yeast produce costly invertase and share the resulting glucose with the population? What strategy maximises the fitness of the group? Using an engineered

yeast strain that cannot secrete invertase and performing competition experiments in structured environments, Greig and Travisano argue that the Prisoners Dilemma could explain the observed negative frequency dependence [36].

Recently, Gore and van Oudenaarden [34] established that co-operation can be maintained in the population even in well-mixed environments, they proposed that competition between both strains could be explained using a Snowdrift game rather than a Prisoners Dilemma. Other studies, for example [92] argue that contrasting strategies are used in different circumstances, so in order to capture the complexity of the interaction, different games are played at different moments in time.

In general, classical theories of co-operation assume that co-operators by definition increase the average fitness of a group [70, 19]. For instance, when calculating the maximal population payoff in a simple Snowdrift game we find that fitness is maximal when all individuals co-operate, and therefore this strategy is the best for the group.

If x represents the frequency of co-operators in the population, then the population payoff in a SDG is defined as:

$$x^2R + x(1-x)S + x(1-x)T + (1-x)^2P.$$

Therefore population payoff is maximal when:

$$x = \frac{(2P - S - T)}{2(R - S - T + P)}.$$

Incorporating the cost and benefits values from Table 2, we find that populations fitness is maximal when all individuals are co-operating ($x = 1$) (Figure 1-4).

Craig MacLean performed a set of competition experiments between invertase producers and invertase non-producers, starting with different frequencies of each type. This experiment was performed with agar plates with sucrose synthetic medium.

Figure 1-5 shows the outcome of the experiment: fitness of the population is not maximised when everyone "co-operates" as the Snowdrift game predicted. Measuring

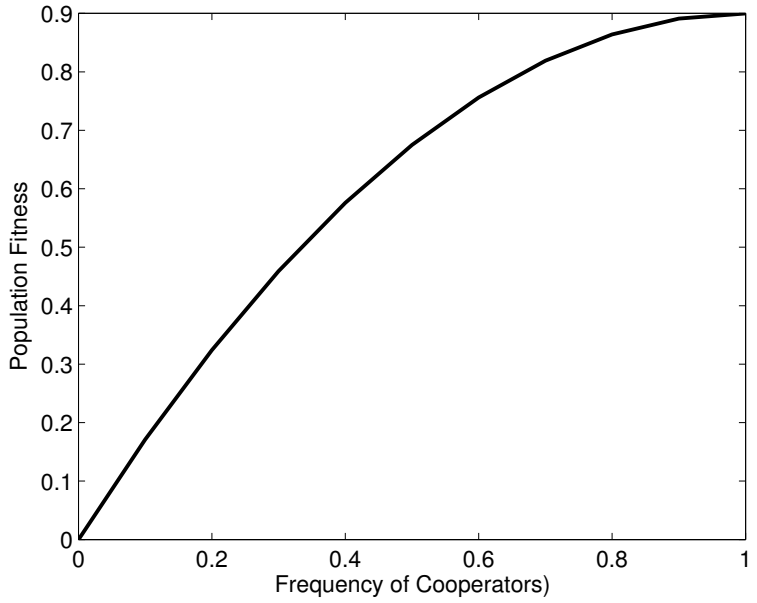

Figure 1-4: In a Snowdrift game the population fitness is maximised when all individual in the population are "co-operators" (Frequency=1).

fitness as the total final population (titre), the maximal fitness is achieved when (maybe wrongly called) "cheats" (non-invertase secretors) and "co-operators" (invertase secretors) are both present in the population [61].

Understanding this unexpected result is the starting point of this thesis. Prior game theoretical models do not capture this result [34]. Can a systems biological model derive this result even though the model is not constructed to enable this result?. Using both theoretical and experimental approaches I will study this model system with the purpose of dissecting the biological mechanisms driving the evolution of co-operation in this particular system: from molecular and metabolic processes to complex ecological interactions.

1.6 Thesis Outline

In Chapter 2 we introduce the core mathematical model: a set of ordinary differential equations that describe the competition experiments of producers and non-producers of invertase in agar plates growing in sucrose synthetic media. Parameterisation of the

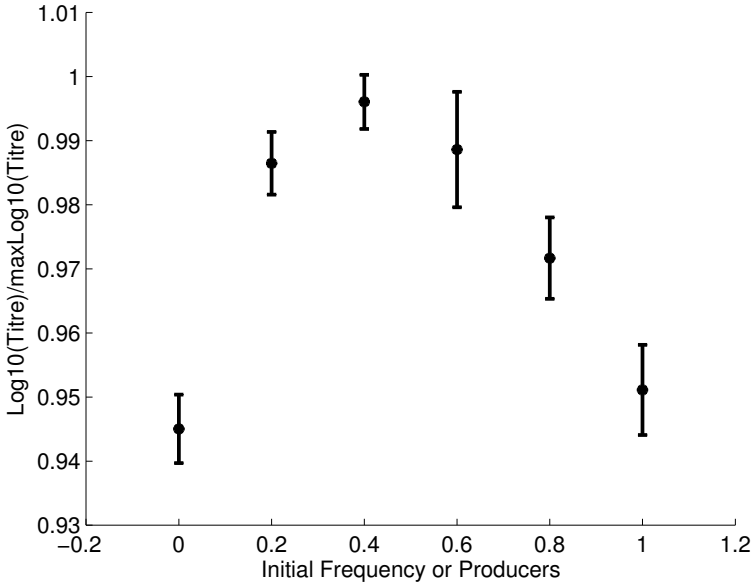

Figure 1-5: Experimental results (data from Craig MacLean) from a 48 hours competition experiment between invertase producers and non-producers growing in agar plates and a sucrose medium. Fitness is measured as Titre. Fitness is maximised when a mix of "co-operators" and "cheats" are present in the population.

model was performed using experimental data obtained by Duncan Greig and Craig MacLean and is also discussed in this chapter. For the purpose of this chapter, spatial structure is considered in a phenomenological way, considering that spatial structure can be defined from who is their neighbour and how many resources can be seen by each competitor.

Chapter 3 is dedicated to discussion of predictions and experimental validation of the model described in Chapter 2 in the context of the theory of co-operation. Here we provide mechanistic explanations as to why fitness is maximised when there is a mixture of "co-operators" and "cheats" in the population. Craig MacLean and Duncan Greig performed the experiments used in this chapter. The main results presented in Chapters 2 and 3 are published in [61].

In Chapter 4 we study how spatial structure can influence coexistence in a competition experiment. For this we propose a spatially explicit model based on partial differential equations, and use it to show that spatial structure is a necessary condition to obtain the same outcome as presented in the previous chapter.

In Chapter 5 we discuss a different temporal structure. By introducing seasonality we present some theoretical results that may be important to understand the generalisability of experimental systems. In particular, we use two different experimental setups, both standard transfer experimental techniques: one representing a migratory regime and the other one a non-migratory regime. From an ecological perspective, these two regimes represent two different forms of re-colonising a summer ground in different seasons.

Although usually ignored when designing experimental protocols, both regimes can have different outcomes in terms of coexistence regarding temporal dynamics. Interestingly, the temporal dynamics introduced by the transfer protocol can result in the system presenting a chaotic behaviour, for instance when using the transfer time as a bifurcation parameter.

To test some of these hypotheses, this chapter also includes a set of preliminary experiments comparing both transfer protocols. The experiments were carried out by me in the Max Planck Institute under the supervision of Duncan Greig and although the results are non conclusive, they seem rather promising and help us to motivate a subsequent study. The ongoing and future work, as well as the general conclusions of this thesis, will be discussed in Chapter 6.

CHAPTER 2

Modelling the polymorphic secretion of invertase by yeast

2.1 *Saccharomyces cerevisiae*

Yeast is an eukaryotic organism that is widespread in nature, with about 1500 different species but only less than 1% of those species has been described. One of these species is *Saccharomyces cerevisiae*, also called "budding" yeast for its ability to reproduce by mitosis in contrast with others species that reproduce by fission and are so-called fission yeast . Another important feature of *S. cerevisiae* is its ability to switch between respiration and fermentation, producing ethanol as a by-product of fermentation using the glycolytic pathway [87, 106]. Humans have taken advantage of this feature and used *S. cerevisiae* to brew alcoholic drinks like beer and wine and to rise bread, and for this reason it has been argued that it was the first organism domesticated by humans [35]. Moreover, in the last 30 years yeast has become one of the most important model organisms to study genetics [24, 109], and the last decade has seen the complete genome of yeast published (available in http://www.yeastgenome.org/), making it one of the best characterised eukaryotic organisms.

Glucose is one of the preferred carbon sources of yeast [31]. Furthermore, glucose is an important messenger molecule, regulating important metabolic traits, such as

growth rate, fermentation capacity and response to stress. Glucose molecules also regulate proteins that are involved in the uptake of other carbon sources such as maltose, galactose and sucrose [87]. This is an important feature that will be further discussed in this chapter.

Yeast cells regulate the transcription of many proteins by sensing the environmental concentration of carbon sources (e.g. glucose) using sensor proteins located in the membrane. To date, the sensing mechanisms are not fully understood, although some glucose-sensing proteins have been identified: Snf3, Rgt2, Gpr1 and Hxk2 [76]. These sensors induce the transcription of the hexoses transporters (*HXT* genes) that are located also on the membrane, being *HXT1* and *HXT3* low affinity transporters (induced at high concentration of glucose) and *HXT6* and *HXT7* high affinity transporters (repressed at high level of glucose) [59, 108].

One of the proteins regulated by glucose, and the one studied in this thesis, is invertase. This enzyme catalyse the hydrolysis of sucrose and breaks this molecule into two monosocharides, glucose and fructose, that are then transported into the cell.

Wild type *S. cerevisiae* secretes the enzyme invertase in order to catalyse the hydrolysis of sucrose. The *SUC* genes, that code for invertase in *S. cerevisiae*, are highly polymorphic [67]. This polymorphism is expressed in number of copies and functionality of the genes; in [67] from 91 laboratory strains, about 80% of the strains carry a single active gene (*SUC2*) and 8% of strains carry at least 2 *SUC* genes. There exist, nevertheless, a minority of strains (about 12%) that don't secrete invertase, carrying a degenerate *suc* pseudogene. We will focus our attention in the *SUC2* gene, and important feature of the expression of this gene is that its regulated by the concentration of glucose in the environment [68].

It is important to notice that glucose is not the only carbon source that can be used by the cell. For instance, sucrose can be also transported into the cell trough an active sucrose-H^+ symport, mediated by two different transport systems: a high-affinity uptake pathway mediated by *AGT*1 permease and a low-affinity pathway mediated by

$MALx1$ maltose transporters [94]. It is known, however, that these transporters are less efficient than the glucose transporters mentioned before [8].

2.2 Modelling growth kinetics

In order to model how yeast cells grow in an environment with a concentration of a limiting resource denoted with the variable R, we will assume that cells can take up resources and convert them into ATP using a simple unbranched metabolic pathway [81]. The rate of ATP production in the pathway will be denoted hereafter by J^{ATP} and can be described by the expression:

$$J^{ATP} = n^R_{ATP} \cdot J^R,$$

where J^R denotes the rate of substrate consumption of the pathway. This is a function of the resource concentration, R, and will be represented mathematically as $J^R(R)$. The term n^R_{ATP} denotes the number of ATP molecules produced in the pathway and is a decreasing function of J^R. Yield of ATP production is known to depend on the rate of resource uptake [82], termed rate-yield trade-off.

When modelling microbial growth rate we used a linear function of the rate of ATP production, namely $r \cdot J^{ATP}$, where r is some proportionality constant [82]. For the purpose of this thesis we will assume, except where stated otherwise, that $r = 1$. In practice, yield of ATP production n^R_{ATP} is not as easy to measure as the efficiency, n^R_e, whereby

$$n^R_e = n^R_{ATP} \cdot b,$$

where b is a constant denoting the amount of biomass formed per unit of ATP.

Therefore we consider a rate-efficiency trade-off instead of rate-yield trade-off. Experimental evidence of this trade-off been has been found for plenty of heterotrophic organisms [69, 9, 82, 30]. Based on [104] the shape of the trade-off function (n^{Hxt}_e) used in this thesis is shown in Figure 2-1.

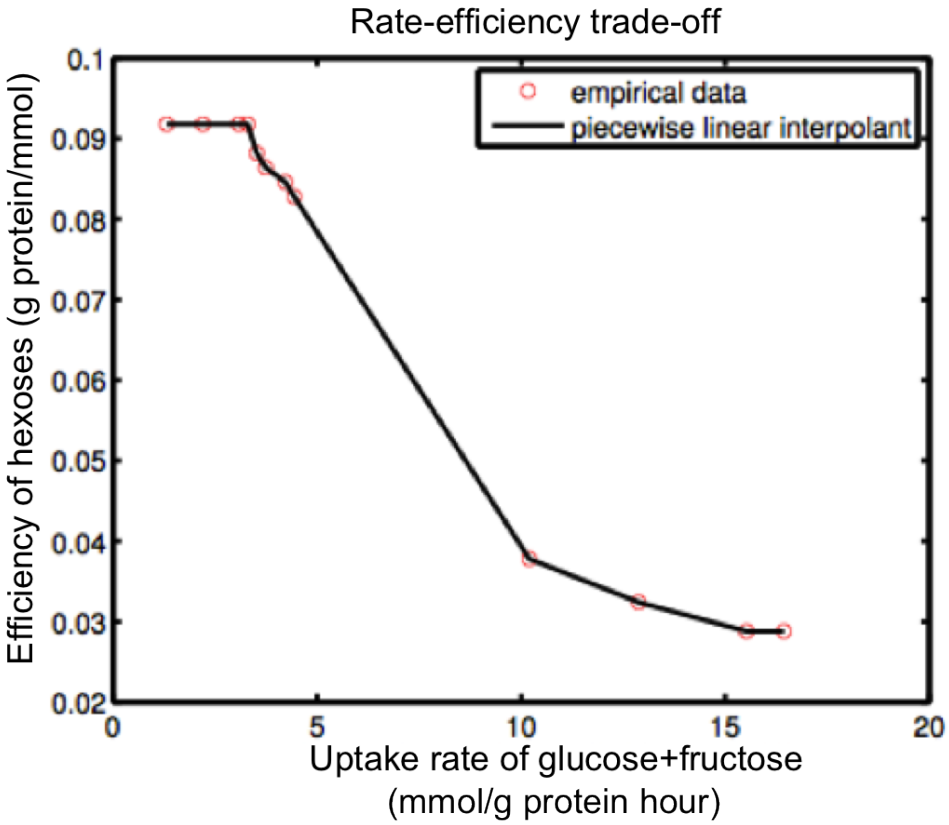

Figure 2-1: Rate-efficiency trade-off, shape of the function taken form [104].

2.3 Sugar uptake

In Section 2.1 we discussed in general how glucose regulates transcription of different proteins. For modelling purposes we will take into account that yeast cells only have sensors for glucose (Snf3 and Rgt2) , so glucose alone is responsible for the activation of *SUC2*, the gene that codes for invertase.

Hexoses (fructose and glucose) enter the cell and are metabolised through the glycolytic pathway together, although it is important to notice the transporters have higher affinity for glucose than for fructose [77, 84]. Sucrose enters the cell through the MAL transporter and for simplicity we will assume that it is metabolised through its own pathway, as illustrated in Figure 2-2.

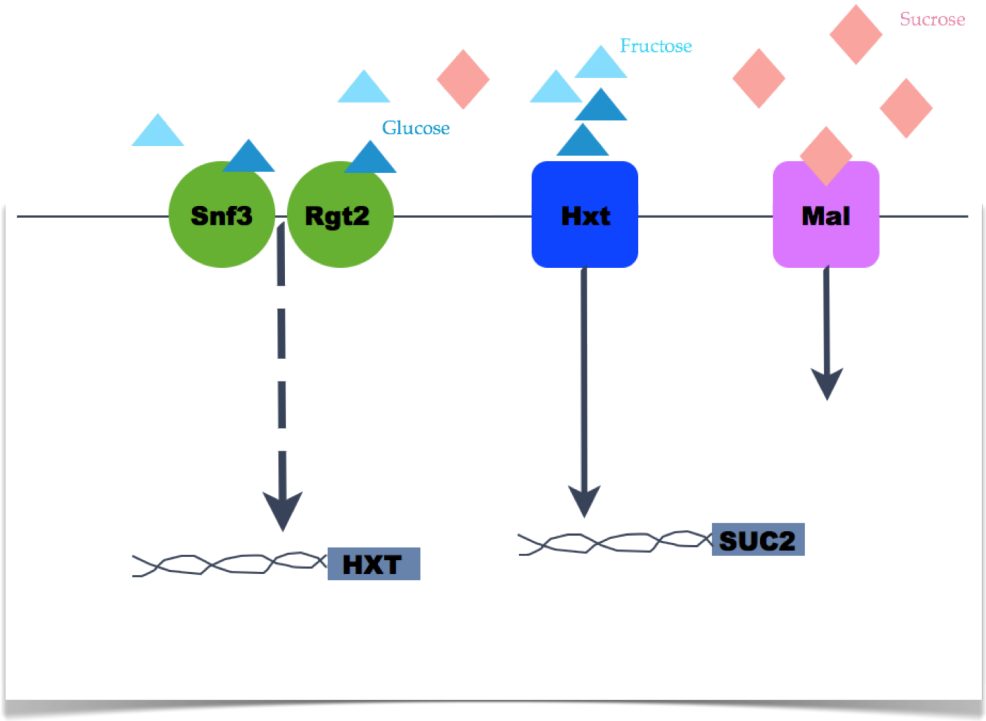

Figure 2-2: Simplification of the pathway: Snf3 and Rgt2 are glucose sensor proteins that activate the transcription of *HXT*, this family of transporters allows hexoses to enter the cell activating *SUC2* producing invertase, *MAL* is a maltose transporter that allows sucrose to enter into the cell.

2.3.1 Hexose uptake

Glucose and fructose are transported into the cell through hexose transporters (HXT) and we will assume that there is one non-specific site for both hexoses to bind. Let us denote with the variables V_{max}^G and V_{max}^F the maximal uptake rate of the pathway for glucose and fructose respectively and K_m^G and K_m^F the half-saturations constants. As we are assuming both sugars compete for one non-specific site, we can model their uptake using a competition for one-site Michaelis-Menten dynamics:

$$J^G = \frac{V_{max}^G \cdot G}{K_m^G \cdot (1 + \frac{F}{K_c^G}) + G} \tag{2.1}$$

$$J^F = \frac{V_{max}^F \cdot F}{K_m^F \cdot (1 + \frac{G}{K_c^F}) + F} \tag{2.2}$$

whereby K_c^G and K_c^F denote the competition constants for glucose and fructose.

The efficiency of the hexose pathway is represented by $n_e^{Hxt}(J^G + J^F)$ and, as discussed in section 2.2, is a function of the concentration of both sugars and exhibits a rate-efficiency trade-off. In simple terms, the rate-efficiency trade-off makes yeast convert hexoses into ATP inefficiently when exposed to abundant resources, compared to the situation when cells are exposed to lower resource levels and therefore are used more efficiently.

2.3.2 Sucrose uptake

Although yeast does not have a specific site for transporting sucrose, this molecule can still be transported inefficiently into the cell. In this thesis, we modelled the uptake and efficiency of this sugar completely separate from the pathway for hexoses, as illustrated in Figure 2-2. While yeast *SUC* knockout strains do not use internal invertase to hydrolyses sucrose, they can nonetheless metabolise it efficiently using maltase [50]. This has been the normal mode of sucrose utilisation lacking invertase [94]. There are plenty of evidence to hypothesis that this is the case, *suc2* strains without maltase cannot grow on sucrose [50], while *suc2* strains missing the hexose import channels grow well [7].

The parameters used to model the uptake of sucrose were obtained using the kinetics of active H^+-sucrose symport activity acquired from [6] (see Figure 2-3) the authors measured the kinetics in 1403-7A strain, $J^S(S)$ will be measure in $\frac{mmol}{g\ protein \cdot hour}$ and S in $mmol$. Using a piece-wise linear fit on the experimental data we estimated the following function:

$$J^S(S) = \left\{ \begin{array}{cc} 64 \cdot S, & 0 \leq S \leq 0.042 \\ 14.8 \cdot S + 2.1, & 0.042 < S \leq 0.043 \\ 2.04 \cdot S + 7.57, & 0.043 < S \leq 0.9 \\ 1.48 \cdot S + 8.08, & 0.9 < S \end{array} \right\}$$

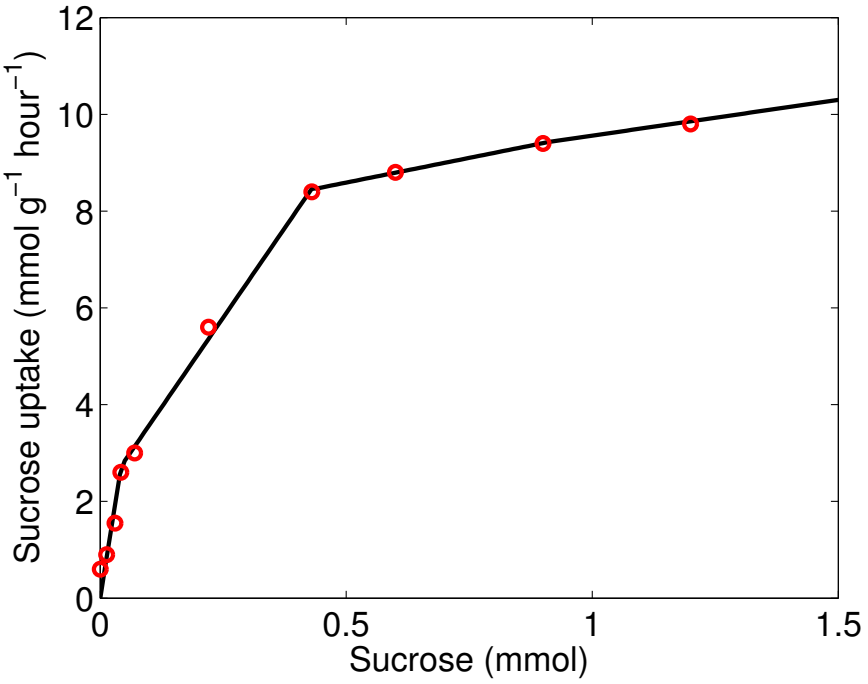

Figure 2-3: Kinetics of active H^+-sucrose symport as a function of the concentration of sucrose. Data points (in red) from [6].

2.4 Invertase production

Wild-type *S. cerevisiae* secretes the enzyme invertase in order to catalise the hydrolysis of sucrose. *SUC2* is the gene responsible for invertase secretion and its expression is regulated by the concentration of glucose in the environment [10].

Secreted invertase hydrolyses sucrose (S), into glucose (G) and fructose (F), and we will model the rate of conversion (Inv) with a function that can be written as:

$$Inv = inv(J^G) \cdot \frac{S}{(k+S)}.$$

where inv is the invertase activity, a term known to be glucose uptake dependent [8], here we will also assume that the rate of sucrose degradation is a saturating function of sucrose concentration therefore k denotes a saturating constant and takes the value $k = 10^{-4}$.

Interestingly, invertase production is associated with a metabolic cost [34, 36]. Here

the cost function c^{Inv} varies with the glucose levels as yeast only has specific sensors for glucose. Then the cost function can be modelled as follows:

$$c^{Inv} = inv(J^G) \cdot U^{Inv},$$

where U^{Inv} denotes the unit cost of producing each molecule of invertase.

In [26] the authors estimated the relationship between invertase activity and glucose consumption rate using KOY.PK2-1C83 wild type strain and its various genetically manipulated derivatives. Using their data we estimated invertase activity, denoted by $inv(J^G)$, as (data and estimated invertase activity is shown in Figure 2-4):

$$inv(J^S) = -2.3453 \cdot (J^G)^2 + 32.609 \cdot (J^G) + 77.109.$$

Note that invertase production is conditioned not on sucrose, but on local glucose levels, high glucose suppress the production on invertase, and absence of glucose resulting in a residual low level production, the maximum of this production is the result of medium levels of glucose concentration.

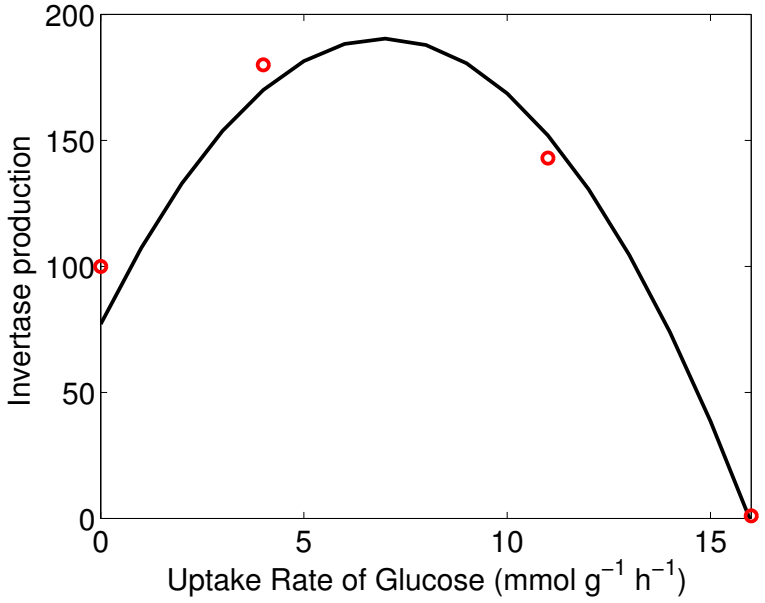

Figure 2-4: Invertase activity ($\frac{mmol}{grams \cdot hour}$) as a function of glucose consumption, data points (in red) from [26] and estimated invertase activity (in black).

2.5 Modelling homogeneous environment

Considering the previous sections, we can put together a model of the growth dynamics of two different types of cells: invertase producers (N_p) and invertase non-producers (N_n), growing in a homogeneous environment (for example a flask that is continuously shaken) with the limiting resources sucrose (S), glucose (G) and fructose (F) with a set of differential equations that can be written as:

$$\begin{aligned}
\frac{dS}{dt} &= -J^S \cdot (N_p + N_n) - Inv \cdot N_p, \\
\frac{dG}{dt} &= -J^G \cdot (N_p + N_n) + Inv \cdot N_p, \\
\frac{dF}{dt} &= -J^F \cdot (N_p + N_n) + Inv \cdot N_p, \\
\frac{dN_p}{dt} &= (1 - c^{Inv}) \cdot (n_e^{Hxt}(J^G + J^F) \cdot (J^G + J^F) + n_e^S \cdot J^S) \cdot N_p, \\
\frac{dN_n}{dt} &= (n_e^{Hxt}(J^G + J^F) \cdot (J^G + J^F) + n_e^S \cdot J^S) \cdot N_n,
\end{aligned}$$

suitably augmented with initial conditions.

This set of ordinary differential equations describe a competition experiment between two competitors growing in a sucrose environment. At the beginning of the experiment sucrose is the only carbon source in the environment but as time increases, the production of invertase makes fructose and glucose available. Note that the only difference between producers and non-producers in the set of equations is that N_p pays a fitness cost represented by the term $(1 - c^{Inv})$.

2.6 A phenomenological approach to modelling space

In addition to the homogeneous environment described in the previous section, we are also interested in modelling structured environments such as agar plates. In order to accomplish this we will use a phenomenological approach to model spatial structure, given by a mixing parameter denoted by the variable m, whereby $0 \leq m \leq 1$.

This parameter represents the proportion of cells of a given type that have a different type as a neighbour, in such a way that when $m = 0$ the two strains are spatially segregated, while when $m = 1$ the two strains are considered to be well-mixed. For $0 < m < 1$ the environment can be viewed as if consisting of three different regions: region 1 where N_p are surrounded only by their own type, region 2 where N_n is surrounded only by their own type and region 3 where N_p and N_n are neighbours. The proportion of N_p in region 3 is equal to m, which is equal to the proportion of N_n also in region 3. The three cases described above are illustrated in Figure 2-5.

Note that while both strains of yeast are non-motile, resources can move throughout the environment at a rate represented by D (Note that D does not refer to classical diffusion). Therefore the spatial structure of the population does not correspond with the spatial distribution of the resources.

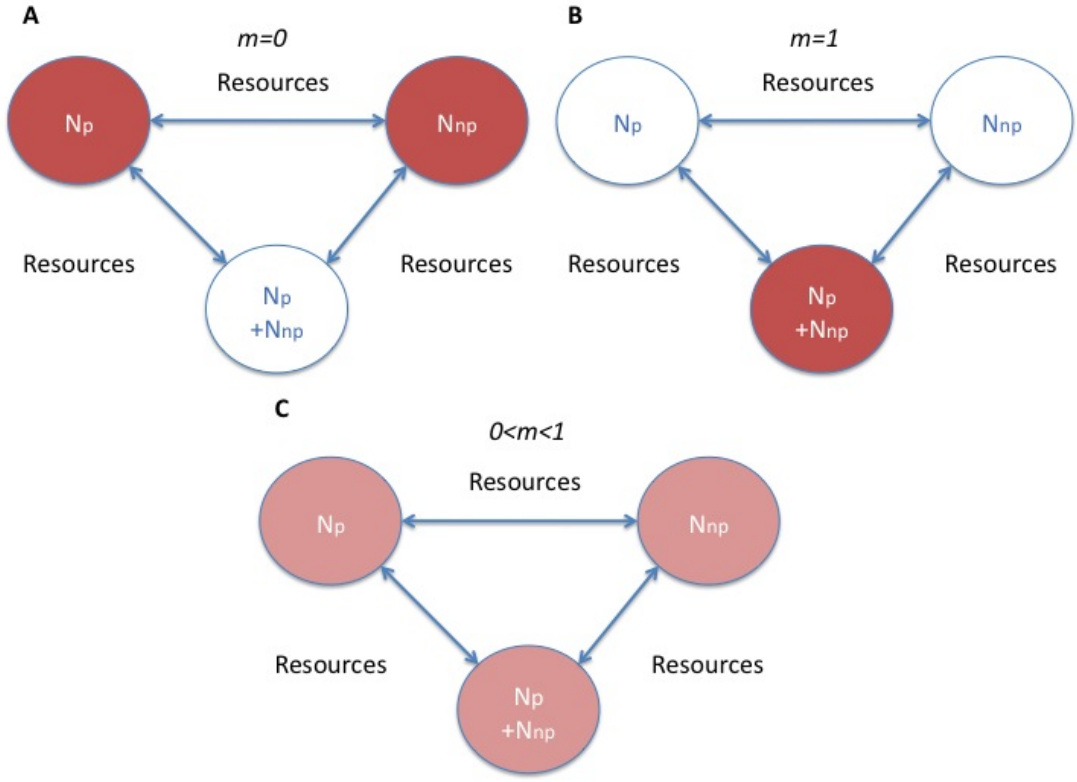

Figure 2-5: Spatial Structure. In panel A when $m = 0$ the two strains are spatially segregated in the two red regions. In panel B when $m = 1$ the two strains coexist together in the red region. In panel C when $0 < m < 1$ the three regions are occupied, in all the three cases resources diffuse from one region to another.

The following set of equations represent a competition experiment between two different types of cells (invertase producers and invertase non-producers) in a heterogeneous environment growing under sucrose limitation:

$$\frac{dS_1}{dt} = -J^{S_1} \cdot N_{1p} - Inv \cdot N_{1p} + \frac{D}{2}(\frac{1}{2} \cdot S_2 + \frac{1}{2} \cdot S_3 - S_1), \tag{2.3a}$$

$$\frac{dG_1}{dt} = -J^{G_1} \cdot N_{1p} + Inv \cdot N_{1p} + D \cdot (\frac{1}{2} \cdot G_2 + \frac{1}{2} \cdot G_3 - G_1), \tag{2.3b}$$

$$\frac{dF_1}{dt} = -J^{F_1} \cdot N_{1p} + Inv \cdot N_{1p} + D \cdot (\frac{1}{2} \cdot F_2 + \frac{1}{2} \cdot F_3 - F_1), \tag{2.3c}$$

$$\frac{dN_{1p}}{dt} = (1 - c^{Inv}) \cdot (n_e^{Hxt}(J^{G_1} + J^{F_1}) \cdot (J^{G_1} + J^{F_1}) + n_e^{S_1} \cdot J^{S_1}) \cdot N_{1p}, \tag{2.3d}$$

$$\frac{dS_2}{dt} = -J^{S_2} \cdot N_{2n} + \frac{D}{2} \cdot (\frac{1}{2} \cdot S_1 + \frac{1}{2} \cdot S_3 - S_2), \tag{2.3e}$$

$$\frac{dG_2}{dt} = -J^{G_2} \cdot N_{2n} + D \cdot (\frac{1}{2} \cdot G_1 + \frac{1}{2} \cdot G_3 - G_2), \tag{2.3f}$$

$$\frac{dF_2}{dt} = -J^{F_2} \cdot N_{2n} + D \cdot (\frac{1}{2} \cdot F_1 + \frac{1}{2} \cdot F_3 - F_2), \tag{2.3g}$$

$$\frac{dN_{2n}}{dt} = (n_e^{Hxt}(J^{G_2} + J^{F_2}) \cdot (J^{G_2} + J^{F_2}) + n_e^{S_2} \cdot J^{S_3}) \cdot N_{2n}, \tag{2.3h}$$

$$\frac{dS_3}{dt} = -J^{S_3} \cdot (N_{3p} + N_{3n}) - Inv \cdot N_{3p} + \frac{D}{2} \cdot (\frac{1}{2} \cdot S_1 + \frac{1}{2} \cdot S_2 - S_3), \tag{2.3i}$$

$$\frac{dG_3}{dt} = -J^{G_3} \cdot (N_{3p} + N_{3n}) + Inv \cdot N_{3p} + D \cdot (\frac{1}{2} \cdot G_1 + \frac{1}{2} \cdot G_2 - G_3), \tag{2.3j}$$

$$\frac{dF_3}{dt} = -J^{F_3} \cdot (N_{3p} + N_{3n}) + Inv \cdot N_{3p} + D \cdot (\frac{1}{2} \cdot F_1 + \frac{1}{2} F_2 - F_3), \tag{2.3k}$$

$$\frac{dN_{3p}}{dt} = (1 - c^{Inv}) \cdot (n_e^{Hxt}(J^{G_3} + J^{F_3}) \cdot (J^{G_3} + J^{F_3}) + n_e^{S_2} \cdot J^{S_1}) \cdot N_{3p}, \tag{2.3l}$$

$$\frac{dN_{3n}}{dt} = (n_e^{Hxt}(J^{G_3} + J^{F_3}) \cdot (J^{G_3} + J^{F_3}) + n_e^{S_3} \cdot J^{S_3}) \cdot N_{3n}. \tag{2.3m}$$

In this set of equations each region of the space is represented by superscripts $1, 2$ and 3. Region 1 contains only cells of type N_{1p}, while Region 2 is inoculated with cells of type N_{2n} and in Region 3, both types N_{3p} and N_{3n}, are present. Sucrose, fructose and glucose are available for all three regions and move between them at a constant rate D in the case of glucose and fructose, and as the sucrose molecule is twice the size as the previous, then we consider its rate of movement between regions to be $D/2$.

The initial conditions for the set of equations (2.3) will depend on the mixing parameter (m), the initial fraction of producers (f), the total population size (N_{in}) and the initial input of sucrose in the environment (S_{in}). Then the initial conditions

Table 2.1: Initial conditions for phenomenological model for the 3 regions.

	Sucrose	Glucose	Fructose	N_p	N_n
Region 1	$(1-m)\cdot f\cdot S_{in}$	0	0	$(1-m)\cdot f\cdot N_{in}$	0
Region 2	$(1-m)\cdot(1-f)\cdot S_{in}$	0	0	0	$(1-m)\cdot(1-f)\cdot N_{in}$
Region 3	$m\cdot S_{in}$	0	0	$m\cdot f\cdot N_{in}$	$m\cdot(1-f)\cdot N_{in}$

for each region are the following:

We will now explore in more detail what happens at the extremes $m = 0$ and $m = 1$. When $m = 1$, the two strains are perfectly mixed so that both producers and non-producers reside solely within the region 3 while regions 1 and 2 do not contain any yeast cells. On the other hand if $m = 0$ the two strains are spatially segregated so that producers can only be found in region 1 while non-producers reside only in region 2 with region 3 remaining empty of yeast cells.

While we assume that yeast are immotile and do not move between the three regions, resources are allowed to move through space. The constant D, reflects the rate at which resources available to one strain become available to the other by moving through regions 1, 2 and 3. This assumption has the following consequence. When $m = 0$ even though region 3 does not contain yeast cells, resources are allowed to diffuse into this region becoming unavailable for the consumption as long as they remain there. Similarly, when $m = 1$ even though regions 1 and 2 do not contain yeast cells resources move in and out of these regions becoming unavailable to both producers and non-producers that solely reside in region 3.

The above leads to the following two artefacts:

- In the case of $m = 1$, even though the environment is perfectly mixed, a substantial chunk of resources are unavailable for consumption, implicitly imposing a spatial structure.
- In the case of both $m = 1$ and $m = 0$, keeping resources away from both producers and non-producers reduces the effect of the rate-yield trade-off and extends the time it takes for all resources to be exhausted.

For these reasons the phenomenological model (2.3) is defined for $0 < m < 1$ while the extreme cases $m = 1$ and $m = 0$ are treated separately.

2.7 Parameter estimation

In order to parameterise the model defined by equations 2.3 we used, when available, estimates from literature.

The following parameters are used in all the simulations and experimental protocols.

1mg protein $= 33 \times 10^6$ cells

Sucrose 1.46 $\frac{mmol}{g\ for\ 25\ mL\ agar\ plate}$

Sucrose 1.17 $\frac{mmol}{g\ for\ 20\ mL\ agar\ plate}$

In the case where the corresponding parameters were not available for *S. cerevisiae* we used metabolic estimates of different strains than the one studied in this thesis. The values and references of such parameters are the following:

- From [75] we obtained growth parameters for glucose, in this study the measurement was done for a strain derived from CEN.PK2-1C (*MATa leu2-3,112 ura3-52 trp1-289 his3-*Δ *MAL 2-8*^{c} *SUC2 hxt 14*Δ) grown in minimal media with 2% glcuose at 30°.

$$V_{max}^G = 40 \frac{mmol}{g\ protein \cdot\ hour}.$$

$$K_m^G = \left\{ \begin{array}{c} 1.9 \frac{mmol}{25\ mL\ agar\ plates} \\ 1.52 \frac{mmol}{20\ mL\ agar\ plates} \end{array} \right\}$$

- For fructose K_m^F was obtained from [84], in this study the strain used was a wild type from MC996A (*MATa ura 3-52 his 3-11,15 leu 2-3 112 MAL2 SUC2 GAL MEL*)

$$K_m^F = \left\{ \begin{array}{c} 3.125 \frac{mmol}{25\ mL\ agar\ plates} \\ 2.5 \frac{mmol}{20\ mL\ agar\ plates} \end{array} \right\}$$

- The uptake for sucrose was obtained from [6] in this study a 1403-7A strain is used, this strain is a *MAL* constitutive strain that lacks invertase activity, grown in rich YP media containing 20g/L sucrose.

$$J^S(S) = \left\{ \begin{array}{cc} 64 \cdot S, & 0 \leq S \leq 0.042 \\ 14.8 \cdot S + 2.1, & 0.042 < S \leq 0.043 \\ 2.04 \cdot S + 7.57, & 0.043 < S \leq 0.9 \\ 1.48 \cdot S + 8.08, & 0.9 < S \end{array} \right\}$$

- Using data from [25] we estimated the invertase activity $inv(J^G)$ as

$$inv(J^S) = -2.3453 \cdot (J^G)^2 + 32.609 \cdot (J^G) + 77.109$$

in this study the strains used are isongenic strains derived from CEN.PK2-1 (*MATa leu2-3 122 ura3-52 trp1-289 his3-*Δ *MAL2-8*^{c} *SUC2 hxt12*Δ).

2.8 Growth experiments

Unfortunately we could not find all parameter values in the literature and therefore we estimated the remaining using our own growth experiments. In our experiments yeast cells were placed in two 5 μl patches 5 cm apart on 25 mL agar plates (for detailed experimental methods see Appendix A).

Results from these experiments are summarised in Table 2.2. Each experiment is based on six replicates with two different initial concentration of resources, and the obtained data were used to fit the growth curves as explained in the remaining of this chapter.

Table 2.2: Growth experiments

	Cell type	Carbon source	Initial cell biomass g protein/per patch (replica average n=6)	Length of experiment (days)	Final cell biomass g protein/per patch (replicate average n=6)
Experiment 1a	np	sucrose 0.2%	$9.737 \cdot 10^{-6}$	4	0.00215
Experiment 1b	np	sucrose 2%	$9.737 \cdot 10^{-6}$	4	0.0083
Experiment 2a	np	glucose 0.2%	$9.17 \cdot 10^{-6}$	2	0.0029
Experiment 2b	np	glucose 2%	$9.17 \cdot 10^{-6}$	2	0.0047
Experiment 3a	np	fructose 0.2%	$9.17 \cdot 10^{-6}$	2	0.0025
Experiment 3b	np	fructose 2%	$9.17 \cdot 10^{-6}$	2	0.0053
Experiment 4a	p	fructose 0.2%	$9.4 \cdot 10^{-6}$	2	0.0023
Experiment 4b	p	fructose 2%	$9.4 \cdot 10^{-6}$	2	0.005
Experiment 5a	np	glucose 0.2% & fructose 0.2%	$9.17 \cdot 10^{-6}$	2	0.0032
Experiment 5b	np	glucose 2% & fructose 2%	$9.17 \cdot 10^{-6}$	2	0.0043
Experiment 6a	p	sucrose 0.2%	$7.663 \cdot 10^{-6}$	4	0.0071
Experiment 6b	p	sucrose 2%	$7.663 \cdot 10^{-6}$	4	0.011

2.8.1 Rate-efficiency trade-off of hexoses transport

In order to estimate the value for the rate efficiency trade-off we modelled growth of non-producers (N_n) on glucose. This can be represented by a simple model:

$$\frac{dG}{dt} = -J^G \cdot N_n, \tag{2.4}$$

$$\frac{dN_n}{dt} = n_e^{Hxt} \cdot J^G \cdot N_n. \tag{2.5}$$

In the absence of fructose, $F = 0$, we obtain $J^G = \frac{V_{max}^G \cdot G}{K_m^G + G}$. Furthermore, as mentioned in 2.7, the values of V_{max}^G and K_m^G were fixed (obtained from the literature). The value of n^{Hxt} as a function of the uptake of hexose (for this particular case glucose) can be estimated from the Experiments 2a and 2b from Table 2.2, the shape of the efficiency function was taken from [104] and is shown in Figure 2-1. Note that the values obtained from [104] were not used as these have been obtained in the chemostat. As pointed out in [98], biomass yields estimates are found to be lower in chemostats than when obtained from agar plates.

Fitting the model (2.4) to the experiments we have the following values (values are measure in $\frac{gprotein}{mmol \cdot sucrose}$):

- $a_2 = 0.048$
- $b_2 = 0.00632$
- $c_2 = 0.001$

The parameters x_1, x_2 and x_3 denote the maximal uptake rate at 0.2%, 2% and 4% of glucose (values are measure in $\frac{mmol}{gprotein \cdot h}$). In this case:

- $x_1 = 2.4$
- $x_2 = 12$

- $x_3 = 16$

2.8.2 Estimating maximal uptake-rate of fructose

Growth of non-producers in Fructose can be represented as:

$$\frac{dF}{dt} = -J^F \cdot N_n \tag{2.6}$$

$$\frac{dN_n}{dt} = n_e^{Hxt}(J^F) \cdot J^F \cdot N_n, \tag{2.7}$$

In the absence of glucose $G = 0$, $J^F = \frac{V_{max}^F \cdot F}{K_m^F + F}$, therefore the only parameter that is not fixed is V_{max}^F. From the experimental results presented in Table 2.2 we have two values for the cell density of the final population (Experimental data 3a, 3b) that correspond to growth in 2% and 0.2% of fructose. Solving the equation we obtained $V_{max}^F = 54.93 \frac{mmol}{g\ protein \cdot hour}$.

2.8.3 Estimating the rate-efficiency trade-off of $H^+ - symport$

Finally, the growth of non-producers on sucrose can be represented by:

$$\frac{dS}{dt} = -J^S \cdot N_n \tag{2.8}$$

$$\frac{dN_n}{dt} = n_e^S \cdot J^S \cdot N_n. \tag{2.9}$$

Having obtained from the literature the value for J^S and using the value from Table 2.2 (Experiment 1a,1b) we have

$$n_e^S(J^S) = \left\{ \begin{array}{ll} 0.0295 \frac{g\ protein}{mmol sucrose}, & 0 \leq J^S \leq maximal\ uptake\ rate\ at\ 0.2\% sucrose \\ 0.0094 \frac{g\ protein}{mmol sucrose}, & J^S > maximal\ uptake\ rate\ at\ 0.2\% sucrose. \end{array} \right\}$$

2.8.4 Estimating the cost of invertase production

For estimating the cost of invertase production we competed producer and non-producer strains in glucose-limited chemostats under conditions that induce secretion of invertase without any possible benefit. For details of this experiment see AppendixA (Experimental Methods A).

Using [22] as a motivation and using the results from the experiment just described, we estimated:

$$U^{Inv} = 0.00054e^{0.000001 \cdot inv(J^G)}.$$

U^{Inv} is the cost for every unit of invertase produced, and hence the total cost will be expressed as follows:

$$c^{Inv} = inv(J^G) \cdot U^{Inv}.$$

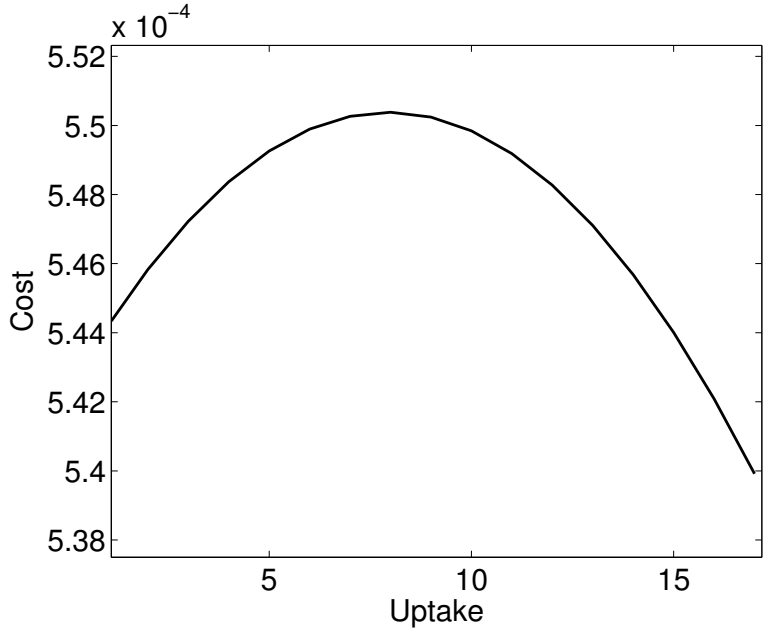

Figure 2-6: Cost of invertase production (this is a dimensionless parameter) as a function of uptake rate of glucose ($\frac{mmol}{grprotein \cdot hour}$) .

Notice that $inv(J^G)$ is the production of invertase that was previously fitted, this is just dependent on glucose uptake. Figure 2-6 illustrates the cost of invertase as a

function of glucose uptake.

2.8.5 Estimating the hexose transporter competition functions for glucose (K_c^G) and fructose (K_c^F)

To estimate the competition parameters between fructose and glucose for the same non-specific site (the HXT transporter), notice that growth of non-producers in these two sugars can be expressed as:

$$\frac{dG}{dt} = -J^G \cdot N_n, \tag{2.10}$$
$$\frac{dF}{dt} = -J^F \cdot N_n, \tag{2.11}$$
$$\frac{dN_n}{dt} = n_e^{Hxt}(J^G + J^F) \cdot (J^G + J^F) \cdot N_n, \tag{2.12}$$

where J^G and J^F are defined as

$$J^G = \frac{V_{max}^G \cdot G}{K_m^G \cdot (1 + \frac{F}{K_c^G}) + G},$$

$$J^F = \frac{V_{max}^F \cdot F}{K_m^F \cdot (1 + \frac{G}{K_c^F}) + F}.$$

The growth of producers on sucrose can also be represented by:

$$\frac{dS}{dt} = -J^S \cdot N_p - Inv \cdot N_p, \tag{2.13}$$
$$\frac{dG}{dt} = -J^G \cdot N_p + Inv \cdot N_p, \tag{2.14}$$
$$\frac{dF}{dt} = -J^F \cdot N_p + Inv \cdot N_p, \tag{2.15}$$
$$\frac{dN_p}{dt} = (1 - c^{Inv}) \cdot (n_e^{Hxt}(J^G + J^F) \cdot (J^G + J^F) + n_e^S \cdot J^S) \cdot N_p. \tag{2.16}$$

Using experiments 5 and 6 and fixing the remaining parameters, we obtained values of K_m^G and K_m^F (measure in $\frac{mmol}{agar}$) and therefore the expressions representing the competition functions are the following:

For 20 mL plates:

$$K_c^G = \left\{ \begin{array}{cc} 0.53, & 0 \leq J^G \leq y_1^G \\ 0.024, & y_1^G \leq J^G \leq y_2^G \\ 0.10, & J^G > y_2 \end{array} \right\}$$

and

$$K_c^F = \left\{ \begin{array}{cc} 0.04, & 0 \leq J^F \leq y_1^F \\ 0.00704, & y_1^F \leq J^F \leq y_2^F \\ 0.01392, & J^F > y_2^F \end{array} \right\}.$$

For 25 mL plates:

$$K_c^G = \left\{ \begin{array}{cc} 0.67, & 0 \leq J^G \leq y_1^G \\ 0.03 & y_1^G \leq J^G \leq y_2^G \\ 0.132, & J^G > y_2 \end{array} \right\}$$

and

$$K_c^F = \left\{ \begin{array}{cc} 0.05, & 0 \leq J^F \leq y_1^F \\ 0.0088, & y_1^F \leq J^F \leq y_2^F \\ 0.0174, & J^F > y_2^F \end{array} \right\}.$$

In the last expressions the constants y_1^G,y_1^F denote the degradation of glucose and fructose of 0.2% of sucrose while y_2^G ,y_2^F denote de concentrations of glucose and fructose created from the degradation of 2% of sucrose. Fitting the set of equations (2.10) and (2.13) to the data from experiments 6a and 6b we estimate the first part of the equation corresponding to $0 \leq J^{G(F)} \leq y_1^{G(F)}$. For the next part corresponding to $y_1^{G(F)} \leq J^{G(F)} \leq y_2^{G(F)}$ we fitted the model (2.13) to the experimental data from experiment 6b. Finally fitting the model (2.10) to the experimental data in 5b we find the last part corresponding to $J^{G(F)} > y_2^{G(F)}$.

For each component of the fit we have two free parameters and one experimental data point. We then use the criteria that glucose is used preferentially over fructose and

the sum of the maximal glucose uptake rate should be such that there is a rate-efficiency trade-off as observed in Figure 2-1.

2.8.6 Estimating resource movement parameter D

The last free parameter of the system of equations defined in 2.3 is D. In order to estimate the value of this parameter we used data from experiments where yeast cells of each types (producers and non-producers) were distributed in two 5 μL patches of liquid culture (grown overnight in YEPD broth) and placed in 25 mL agar plates (in sucrose growth media) 5 cm apart form each other.

In agreement with the experimental design, of which the results are summarised in Table 2.3, let us assume the two types of cells are placed in two different regions and, as yeast is a non-motile organism, they are unable to move between regions. Resources, however, are shared between regions and move between them at a rate D. Now, given that the molecule of sucrose is twice the size of glucose and fructose, we assume that this molecule moves between regions at a rate $D/2$, in contrast to glucose and fructose that moves at a rate D. Then if Region 1 contains N_{1p} and region 2 contains N_{2n}, we obtain the following system of ordinary differential equations suitably augmented with initial conditions:

$$
\begin{aligned}
\frac{dS_1}{dt} &= -J^{S_1} \cdot N_{1p} - Inv \cdot N_{1p} + \frac{D}{2} \cdot (S_2 - S_1), \\
\frac{dG_1}{dt} &= -J^{G_1} \cdot N_{1p} + Inv \cdot N_{1p} + D \cdot (G_2 - G_1), \\
\frac{dF_1}{dt} &= -J^{F_1} \cdot N_{1p} + Inv \cdot N_{1p} + D \cdot (F_2 - F_1), \\
\frac{dN_{1p}}{dt} &= (1 - c^{Inv}) \cdot (n_e^{Hxt}(J^{G_1} + J^{F_1}) \cdot (J^{G_1} + J^{F_1}) + n_e^{S_1} \cdot J^{S_1}) \cdot N_{1p}, \\
\frac{dS_2}{dt} &= -J^{S_2} \cdot N_{2n} + \frac{D}{2} \cdot (S_1 - S_2), \\
\frac{dG_2}{dt} &= -J^{G_2} \cdot N_{2n} + D \cdot (G_1 - G_2), \\
\frac{dF_2}{dt} &= -J^{F_2} \cdot N_{2n} + D \cdot (F_1 - F_2), \\
\frac{dN_{2n}}{dt} &= (n_e^{Hxt}(J^{G_2} + J^{F_2}) \cdot (J^{G_2} + J^{F^2}) + n_e^{S_2} \cdot J^{S_2}) \cdot N_{2n}.
\end{aligned}
$$

Based on the fact that parameters are already estimated using experimental data summarised in Table 2.3, we then estimate $D = 0.007$.

Using the system of equations 2.3 with the parametrisation presented in this chapter, in the following chapter we will present the results obtained after simulating numerically competition experiments between populations composed of different fractions of producers and non-producers growing under resource limitation.

Table 2.3: Experiment 8: Experimental data for estimating resources movement rate D.

Carbon source	Initial cell biomass producers g protein/patch 1	Initial cell biomass of non-producers g protein/patch 2	Length of experiment (days)	Final cell biomass of producers g protein/ patch 1 (n=6)	Final cell biomass of non-producers g protein/patch 2 (n=6)
0.2% sucrose	$1.28x10^{-5}$	9.710^{-6}	4	0.0063	0.0035

CHAPTER 3

"Cheats" stimulate population growth in a public goods game.

Evolution is one of the most successful theories ever posed in biology, this theory takes into account the competition between species. Despite the fierce competition, cooperative behaviour exists and several examples can be found in nature. If co-operation is defined as an act performed by an individual that enhances fitness of the other reducing their own fitness, then in the natural selection context cooperation is an apparent paradox. Altruistic co-operators, where individuals act in benefit of others reducing their own fitness, are widespread in nature. This highlights the question of how cooperators can survive, evolve and spread when they are not the fittest?

Co-operative behaviour is not exclusive for higher organisms, for instance several examples have been reported in microbes [58, 18, 102, 15, 14]. Invertase secretion by yeast is one of the classical examples of cooperation (public goods) in microorganisms [36, 33, 92]. A public good is a product that was costly to produce for one of the actors before being shared between all the population enhancing the overall fitness. The production of invertase can be seen as a cooperative trait because it enhances growth of cells by making glucose (yeast preferred carbon source) available to the group, and thus increases their fitness. As discussed in the previous chapter, the production of this enzyme is associated with a fitness cost.

In this chapter we will use the mathematical model developed in Chapter 2 in order to study the polymorphic invertase secretion in yeast, addressing one question in particular: is it best for the group that all individuals co-operate? Classical cooperation theory often considers that the best for a group is when every individual co-operates, because by definition fitness is increased by co-operators. The competition between producers and non-producers of invertase has been modelled as a snowdrift game [33], in this framework, cooperation is the strategy that maximised the fitness of a group. Despite this theoretical result, we found at least one experimental case where this assumption does not hold.

Measuring population fitness as titre of cells after 48 hours (when all sucrose has been exhausted), Figure 3-1 illustrates that fitness peaks when both producers and non-producers are present. This result suggests a new reason why a diversity of strategies is seen in social interactions. In such situations, in both nature and in humans, it is quite common [36, 18, 46] to observe the co-existence of apparent cheats and co-operators. This is also the case for invertase production: most strains of yeast secrete invertase, but approximately 10% of strains do not [67]. Our results suggest that competition between groups (the net productivity effect that we observe) as well as within groups, mediated as negative frequency dependent selection (Figure 3-3), can both select for a diversity of strategies. The independence of the within- and between-group effects needs emphasis. In a snowdrift game formulation of the yeast system, for example, co-operators and cheats can be stably maintained even in approximately homogeneous environments [33]. In part this is because invertase is retained in the vicinity of *SUC2* strains, ensuring that producer strains receive a disproportionate amount of free glucose. This, however, is independent of any effect on population fitness, as the games predicting polymorphism also predict maximal population fitness when cheats are absent [33].

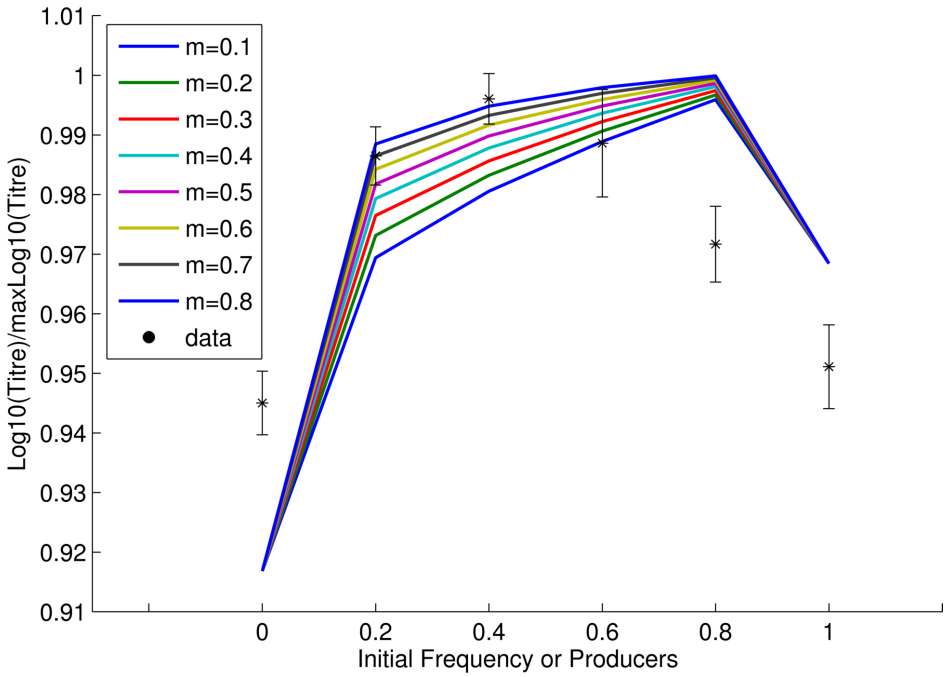

Figure 3-1: Final population size(Log(titre,normalised to maximum observed titre)) after exhaustion of resources as a function of initial invertase producer frequency, in theory (lines) and practice (points(*);mean ± s.e.m.; n=9).

3.1 "Cheats" can enable maximal group benefit.

The model described in Chapter 2 captures the population fitness maximisation when non-producers are present (Figure 3-1). Note too that the model was not constructed in a manner designed to recover this result but rather to reflect known details of the biology and biochemistry of yeast. That such an "end-blind" model can capture unexpected experimental results suggests it to be fit for purpose. For this simulation the two extreme points (0% producers and 100% producers) use a one region model.

This result is also, at least in theory, independent of the definition of population fitness. The population fitness we defined above as the total cell productivity after all sucrose is exhausted. This is equivalent to population fitness for K selected organisms. Were r selection more relevant, one might prefer to consider population growth rate (per unit time) instead. Using this definition of population fitness does not, at least in theory, importantly affect our conclusion that population fitness is maximal when pro-

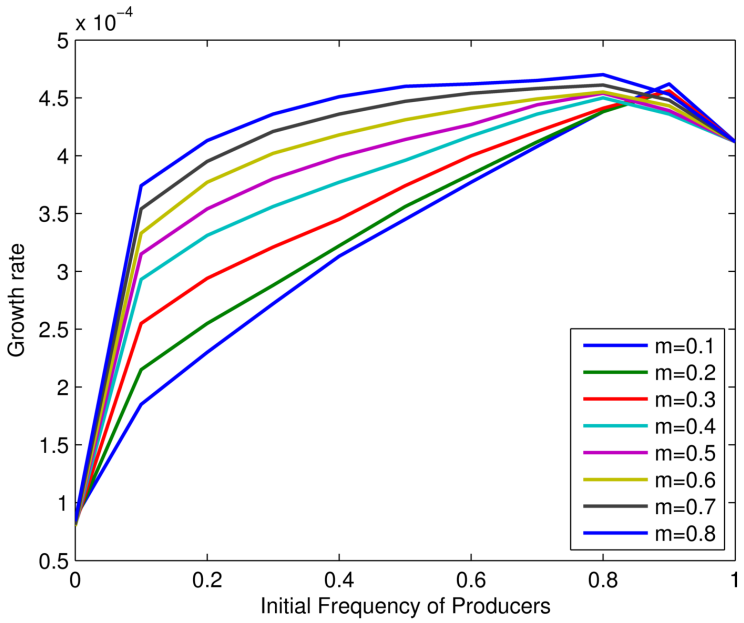

Figure 3-2: Using population growth as a measure of fitness. We observed that the peak is in an intermediate fraction of producers and non-producers.

ducers and non-producers co-exist (Figure 3-2). Using population growth rate instead of titre as measure of fitness as defined by [44]:

$$growth\ rate = \frac{(N_{end} - N_{start})/2}{t_{mid}}$$

where N_{start} denotes the initial population size and N_{end} denotes the population size just after the resources have been exhausted. The value t_{mid} is the time at which the population size reaches $\frac{N_{end}-N_{start}}{2}$.

The expected population growth rate as a function of initial producer frequency is shown in Figure 3-2 and confirms, in theory, that population fitness is maximal when producers and non-producers co-exist regardless again from the mixing conditions.

We can further establish whether the model is fit for purpose by examining additional predictions. Our model, for example, predicts negative frequency dependence of relative fitness (Figure 3-3). Although in contrast to Hamilton's theoretical result [40] that inclusive fitness of co-operators is not a function of co-operator frequency, this result is not without precedent (e.g. [33, 89, 62]). Our competition experiments

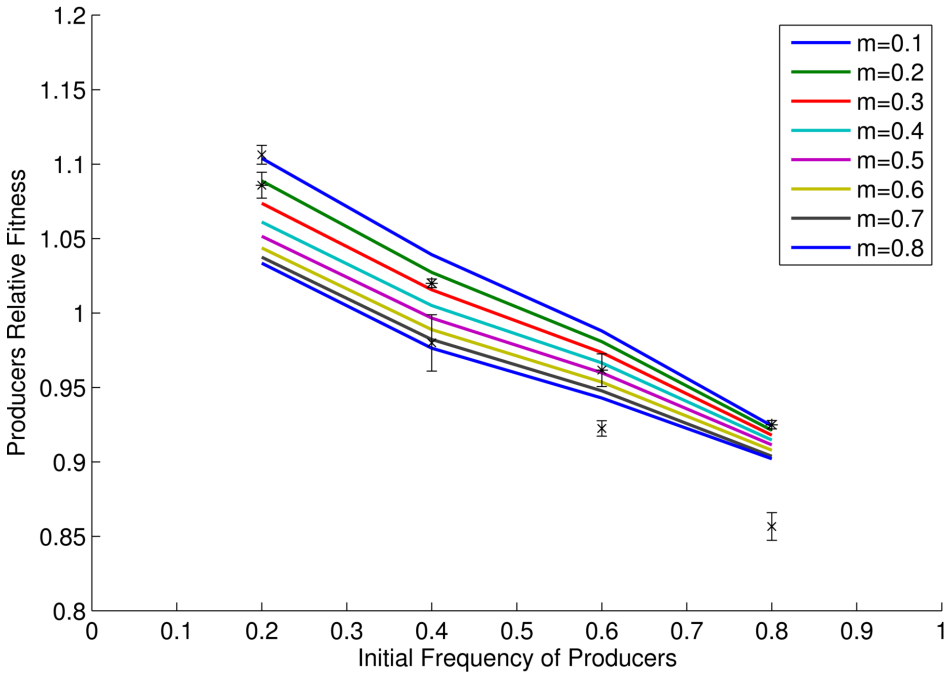

Figure 3-3: Relative producer fitness as a function of initial frequency in theory (lines) and practice (points (*); mean ± s.e.m.; n=3). Asterisks represent poorly mixed cultures (m low) while data points marked with an x represent better mixed cultures (m high).

between isogenic *SUC2* and *suc2* knock-out strains of yeast confirm that selection for invertase production is indeed negatively frequency-dependent (Figure 3-3). Our model also predicts that increasing population structure modestly increases relative fitness of producers, as a higher proportion of glucose goes to the producers (note different intercepts of approximately parallel lines in (Figure 3-3). This result is also confirmed by our experiments (Figure 3-3).

Given the observed negative frequency dependence, our model can also predict the stable equilibrium frequencies of producers and non-producers under different experimental regimes, these occurring when the relative fitnesses are the same. By fitting a quadratic function to the observed data in Figure 3-3, for high m the experimental equilibrium is estimated to be around 0.38 producers. The model predicts for m between 0.5 and 0.8 an equilibrium in the range of 0.31-0.39. For low m the observed equilibrium position is estimated to be around 0.46, the predicted range (m from 0.4-0.1) is between

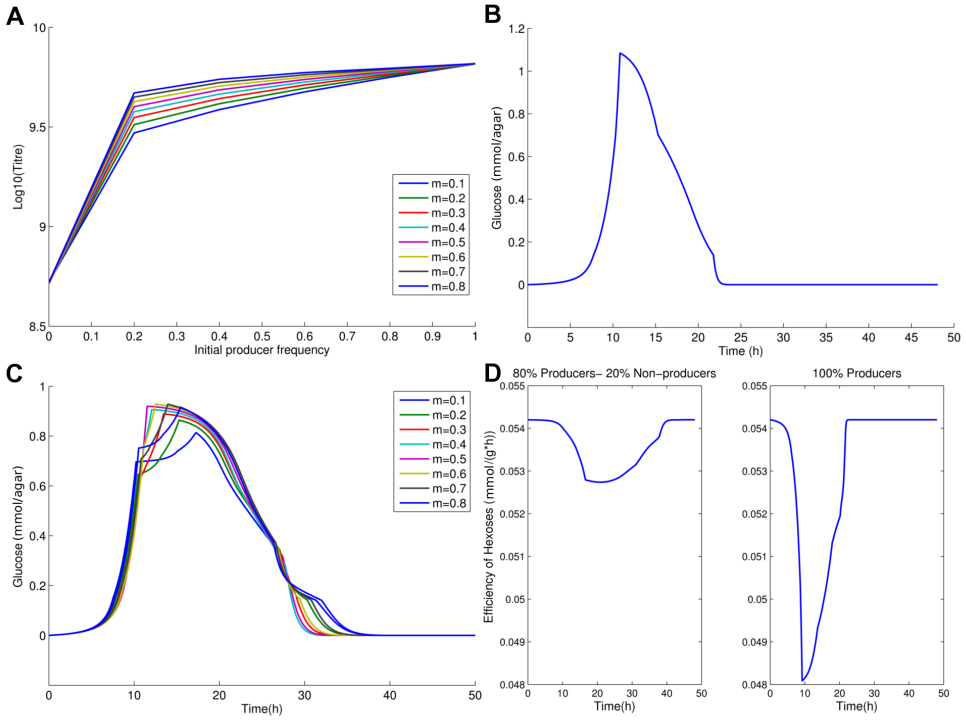

Figure 3-4: The role of the rate-efficiency trade-off and the dynamics of sugar metabolism. (a) Expected final population size(Log(titre)) after exhaustion of resources as a function of initial producer frequency in the absence of rate-efficiency trade-off. The temporal glucose spike, with glucose measured in $\frac{mmol}{agar}$ and time represented in hours, (b) when initially all the population are producers and (c) when 80% are producers with glucose measured in $\frac{mmol}{agar}$ and time is in hours. Note that the spike in (c) is lower and longer-lived, hence glucoseis used more efficiently. (d) Efficiency of hexose usage by producers (g protein/mmol hexose) when non-producers are present (80:20 ratio:left hand panel) and when they are absent, i.e. 100% producers (right hand panel). Here we average across spatial structures.

0.42 and 0.55. We conclude that the model has a respectable ability to quantitatively predict equilibrium frequencies. At equilibrium the population is predicted to have a higher fitness than a population of only producers. The model equilibrium frequencies are not the same as those that maximise population fitness. At equilibrium, there thus remains a conflict between individual and group "best interests".

3.1.1 Assumptions of benefits and costs and the peculiar behaviour of population titre

Why does this model find that apparent cheats promote population growth where a prior snowdrift formulation did not [33]? Might it be a consequence of features specific to yeast and incorporated in our model or might it be owing to factors that are likely to be more broadly applicable? To approach this we modify the model so as to determine the necessary conditions for the maintenance of the core result, namely that population growth is maximal in the presence of non-producers.

Our model makes assumptions about costs and benefits that are appropriate for our situation but that are typically not configured in the more general-purpose heuristic models of co-operation discussed above. We highlight two evident differences. First, snowdrift assumes the benefit to be fixed and constant, such that the b term is the same for all players gaining a benefit. More generally, game theoretical models usually presume that each unit of resource gained represents one unit of benefit. This is not true in yeast. While the growth rate is dependent on glucose concentrations, high local concentrations lead to inefficient utilisation on a per molecule basis.

Similarly, the snowdrift game considers costs to be equally shared by all co-operators, that cost is linearly proportional to work done, and that there is a fixed total cost to removal of snow, this dictated by the amount of snow to be shoveled (e.g. co-operators stop shoveling when the road is cleared). Importantly, yeast are prone to violating this last assumption as they adjust their invertase production to the local glucose level, not to the sucrose level, ensuring a disconnect between the amount of "co-operation" needed (sucrose to be digested; snow to be shoveled) and the amount of "co-operation" offered (invertase production; snow shoveled).

3.1.2 Removing rate-efficiency trade-off

Might modification of either of these biologically verified assumptions explain why non-producers stimulate population growth? Leaving the observed costs in place, we

find that removal of the assumption of the rate-efficiency trade-off restores the usual assumption that population fitness is highest in the absence of cheats (Figure 3-4 A). We can test the proposal that the rate-efficiency trade-off is important by making use of a particular feature of yeast's metabolism, namely that at very low sucrose levels the rate efficiency trade-off is very weak or non-existent [104]. We thus repeated our experiments at a very low sucrose level (0.01%) (see Appendix A Experimental Design E) and observe just the predicted behaviour (Figure 3-5 A). This does not, however, mean that the space in which maximal population fitness is associated with a mixture of producers and non-producers need be limited. If we consider an intermediate sucrose level, for example, we experimentally recover the humped distribution (Figure 3-5 B), as predicted.

The rate-efficiency trade-off matters most if one considers the temporal trajectory of co-operation and population growth. When producers are especially common, the invertase production results in a large immediate spike, both spatial and temporal, in glucose. This would enable rapid but inefficient growth. If we replace a few producers with non-producers, the glucose spike would be smaller, so the population burns the finite resource more efficiently. The net effect then is to ensure sucrose is more efficiently converted to growth, but only if there is a rate-efficiency trade-off.

Consistent with this explanation, when producers are common, a high but short-lived temporal (and spatial) peak in free-glucose is observed in the model (Figure 3-4 B), compared with the rather slower and more protracted production seen when producers are a little less common (Figure 3-4 C). An even lower level of producers ensures, however, that internally metabolised sucrose is the predominant nutrient and this is also inefficient. As then expected, the efficiency (conversion of hexose to protein) of producers is radically degraded when the spike in glucose is observed, while a relatively small reduction is seen when cheats are present, even in an 80:20 mix (Figure 3-4 D).

From examination of the time course we also observe that sucrose is typically exhausted early on, but with invertase production being conditional on low glucose import rates, the producers make expensive, but useless, invertase through much of the latter

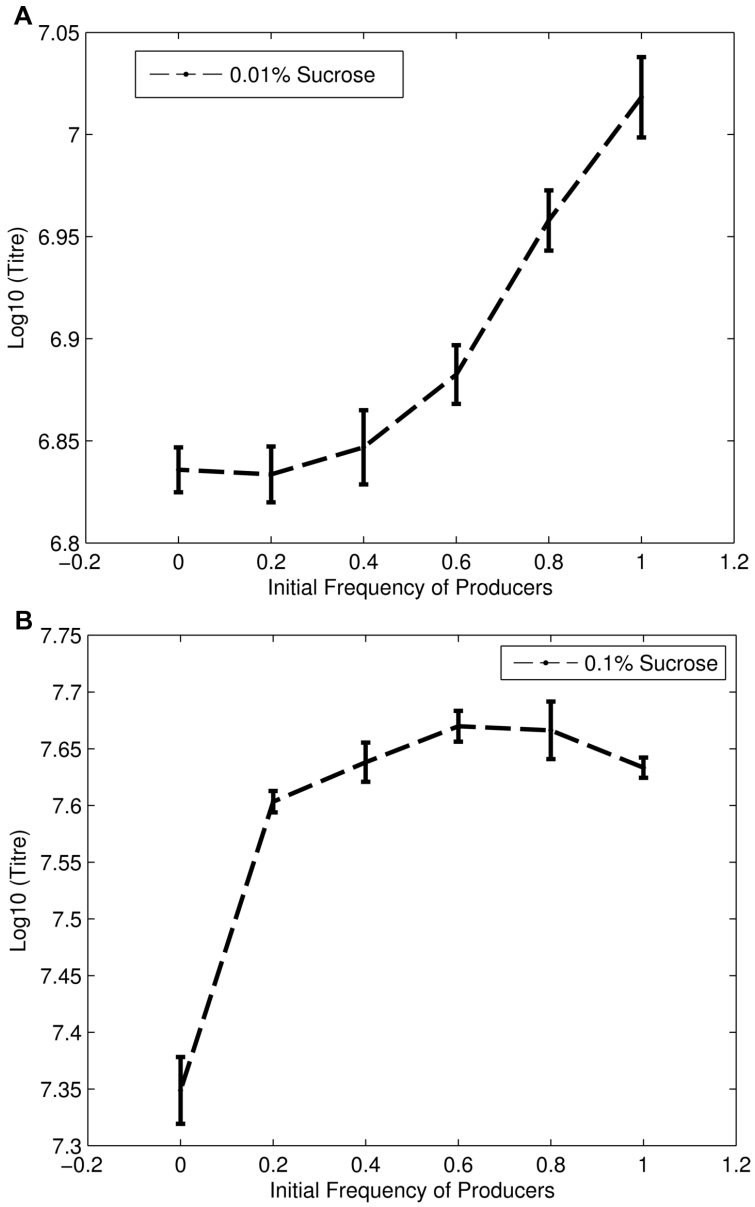

Figure 3-5: Experimental data for different sucrose levels. (A) Competition experiments is performed in 0.01% of sucrose, in this case the rate-efficiency trade-off is weak or not existing. In (B) the competition experiment is performed in 0.1% of Sucrose recovering the hump distribution.

part of the experiment (Figure 3-6 A-B). To employ the metaphor of the snowdrift game, they are shoveling snow after the path is cleared. If invertase production is costly, producers thus retard population growth rates once all the sucrose has been hydrolysed. We should then expect that the population titre peak is more likely to disappear as costs tend to zero. Indeed, we observe this in the model (Figure 3-6 C).

3.1.3 Having perfect information

Moreover, if yeast make invertase at a rate dependent upon the amount of sucrose available (and don't make invertase when sucrose is absent), we might also expect to find the classical result of maximum productivity when cheats are absent. To examine this we consider a model in which invertase production follows Michealis-Menten dynamics as a function of sucrose levels, rather than glucose levels, with zero production when sucrose is absent. This is equivalent to yeast having perfect information. As expected we find that, even with a rate-efficiency trade-off and costly invertase production, maximum population productivity occurs in the model when cheats are absent (Figure 3-7). Thus imperfect information is also required to yield the unexpected result. While we provide an experimental test of the other predictions of our model (see above and below) this one is not obviously amenable to experimental manipulation.

3.1.4 Removing spatial structure

Aside from these two assumptions, we also model a spatially structured population. This is expected to be important as well- mixed populations share resources equally. To this end we can consider what happens when m = 1. When this occurs the model again recovers the classical result (Figure 3-8). We test this prediction by considering what happens in very well shaken flasks (see Appendix A Experimental Design F), thus providing the best approximation of an absence of population structure. As predicted, in well-mixed populations there is no evidence (to any measurable degree) that population fitness is highest when producers and non-producers co-exist (Figure 3-9).

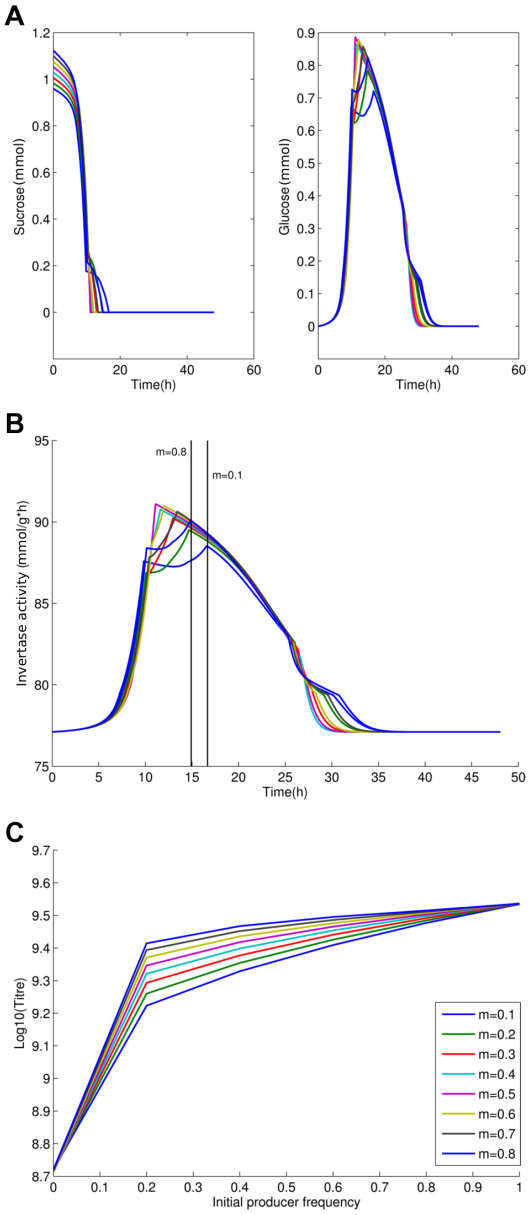

Figure 3-6: The importance of costly invertase production and its coupling with sucrose levels. (a) Sucrose and glucose levels ($\frac{mmol}{agar}$) across the time course of the experiment (in the vicinity of region 3); (b) corresponding invertase activity levels($\frac{mmolglucose}{gprotein \cdot hour}$); time of sucrose exhaustion is indicated by vertical black lines for m=0.8 and m=0.1. Note sucrose has disappeared relatively early but invertase is still produced thereafter; (c) expected final population size (Log(titre)) after exhaustion of resources as a function of initial co-operator frequency when cost of invertase production is reduced from 4% to 2% for invertase production of 86.7 mmol glucose/g protein /hour that is 12% higher than the base-level invertase production.

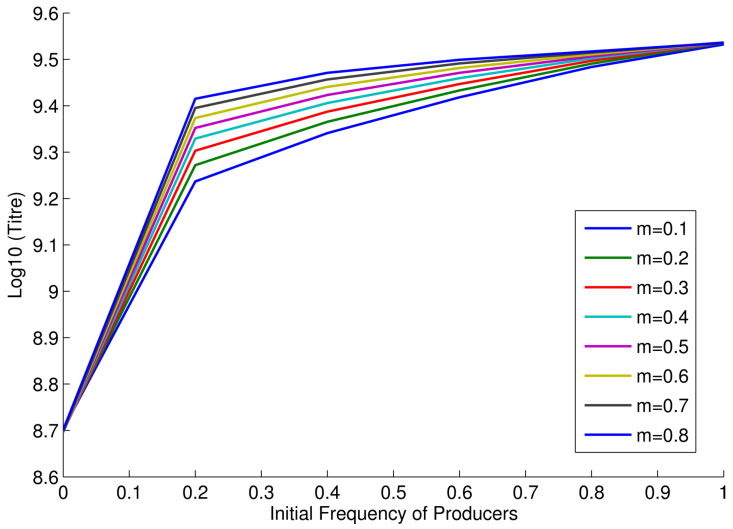

Figure 3-7: Theoretical expectations for titre when invertase production matches sucrose levels (perfect information).

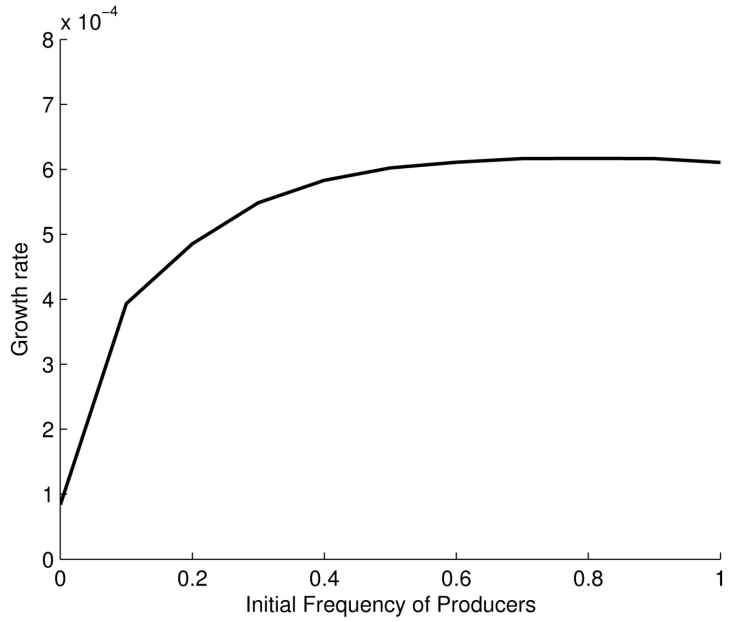

Figure 3-8: Theoretical prediction of a homogeneous environment

3.1.5 The economics of inefficiency

The above demonstrates that three features are required to recover our non-classical result that population fitness is maximal in the presence of non-producers. Modifications of some of these features can be seen as removal of an inefficiency that would otherwise

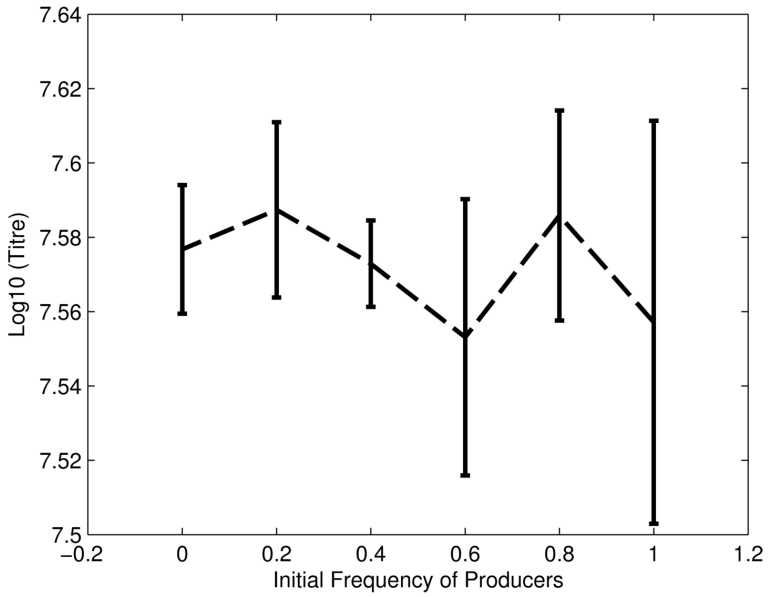

Figure 3-9: Experimental data of the competition experiment performed in flask: homogeneous environment

retard population growth when producers are especially common: the rate-efficiency trade-off ensures that glucose is not used as efficiently as it might be; the costly invertase production being uncoupled to sucrose levels provides an evident inefficiency. Population structure contributes to inefficiency by ensuring that some cells suffer costs while reaping poor benefits, owing to the rate- efficiency trade-off and to being exposed to the spike in glucose.

Given this, why is it that removal of just one inefficiency, leaving the others, can restore the classical result? To see this consider that, while producers may be inefficient in some regards, they also diminish an inefficiency, as they convert inefficiently used sucrose into more efficiently used glucose. The question is not whether there are any inefficiencies but rather whether their net decelerating effects outweigh their net accelerating effects (removal of inefficiency). Importantly, modification of just one cost/inefficiency has consequences for the others, potentially amplifying effects. For example, removal of cost has the direct consequence of faster growth of producers. However, as a knock-on effect, the population uses less sucrose, thus diminishing a further inefficiency. The effect is non-trivial, however, as it is further modulated by the

rate-efficiency trade-offs.

CHAPTER 4

Spatial Structure and the polymorphic secretion of invertase.

Natural environments are inherently spatially structured. For instance soil, biofilms and the sea have a heterogeneous spatial structure that allows the formation of different niches, supporting a wide diversity of species. The sea, for example, despite its continuous movement producing turbulent mixing, has several structured environments. For instance light creates degrees of luminosity and non-uniform temperature gradients, with sharp transitions known as thermoclines that in turn are responsible for changes in the local density of water. All these differences in physicochemical properties of the sea are particularly relevant for microorganisms and therefore diversity of microbes in the sea is enormous [93].

This spatial structure is not exclusive of natural environments, truly homogeneous environments are difficult to find even in laboratory systems; microbial microcosms present gradients on a small scale like vessel walls, colony growth, biofilms or the formation of clumps. Moreover, spatial structure can emerge from a homogeneous environment due to the interaction between the environment and a heterogeneous population composed of different phenotypes. For this reason, understanding how microorganisms behave and evolve in structured environments is an important ecological and evolutionary question.

In particular, spatial structure is known to be an important factor in the maintenance and evolution of co-operation [65, 74, 21, 56, 100, 86]. For instance, one of the most widely-accepted theories explaining the emergence of multicellularity is based on unicellular organisms co-operating in a spatially structured environment [80, 54, 45, 37]. This major evolutionary transition could be a consequence of different cells clustering and grouping together as individuals.

Previous theoretical results focus on understanding the consequences of spatial structure using evolutionary game theory. For example, a Prisoner's Dilemma in which a one-shot play makes defection a stable strategy can switch to a dynamics where co-operation is a stable strategy when spatial structure is taken into consideration [70], although, this is not always the case, there are examples showing that under certain conditions, spatial structure can inhibit cooperation [43].

The fact that spatial structure is important for the maintenance of co-operation is not a surprising result, particularly when competition for consumption and exploitation of common resources are involved (as is the case presented in this thesis). Spatial structure can help individuals paying high costs to remain in the vicinity of the public goods they produce for longer, allowing them to exploit the resources themselves. Spatial structure can also limit the dispersal of the good produced, and increased inclusive fitness by allow them to share the goods preferentially with their kin. This process can lead to the creation of patchy structures that support co-operators. Of course, this argument is not as straightforward as it appears, because as discussed in the previous chapter, individuals with a high amount of resources available may use them inefficiently, and therefore this may only be relevant under resource limitation. Temporal structure is also relevant for the maintenance of co-operation, as will be discussed in the following chapter.

In this chapter we will use a theoretical approach to evaluate the effect of spatial structure in the public goods game presented in the previous chapters. To achieve this, we will modify the model constructed in Chapter 2 in order to consider the spatial component of the system explicitly by formulating a system of PDEs. Subsequently

we will use numerical simulations to show that the results presented so far in this thesis are robust to different spatial distribution of cells and resources. Finally, we will discuss how spatial structure can affect the long-term co-existence between producers and non-producers.

4.1 Modelling spatial structure explicitly

Mathematical and computational models of spatially structured biological systems come in different shapes and sizes. Classically, reaction-diffusion models have widely been used for describing physical situations such as heat conduction in a one-dimensional solid body, spread of a dye in a stationary fluid, population dispersion, and other similar processes. One of the most important contributions regarding this topic was done by Alan Turing who in 1952 studied the emergence of structures in a developing embryo using a reaction-diffusion system [97].

To derived a one dimension reaction diffusion equation, consider a particle moving in a line located at $x = 0$ at the time $t = 0$. The particle can move to the right (r) or to the left (l) a distance δx in a time δt with a probability $p(x,t)$ As both movements are independent therefore:

$$p_l = l[p(x + \delta x, t - \delta t)]$$

$$p_r = r[p(x - \delta x, t - \delta t)].$$

if we consider the particle can't stay in the same place then $p(x,t) = p_l(x,t) + p_r(x,t)$. Expanding $p(x + \delta x, t - \delta t)$ and $p(x - \delta x, t - \delta t)$ in a Taylor series in the vicinity of (x,t)

$$p(x + \delta x, t - \delta t) = p(x,t) + \delta x \frac{\partial p}{\partial x} - \delta t \frac{\partial p}{\partial t} + \frac{(\delta x)^2}{2} \frac{\partial^2 p}{\partial x^2} + ...$$

$$p(x - \delta x, t - \delta t) = p(x,t) - \delta x \frac{\partial p}{\partial x} - \delta t \frac{\partial p}{\partial t} + \frac{(\delta x)^2}{2} \frac{\partial^2 p}{\partial x^2} + ...$$

therefore

$$p(x,t) = l(p(x,t)+\delta x\frac{\partial p}{\partial x}-\delta t\frac{\partial p}{\partial t}+\frac{(\delta x)^2}{2}\frac{\partial^2 p}{\partial x^2}+...)+r(p(x,t)-\delta x\frac{\partial p}{\partial x}-\delta t\frac{\partial p}{\partial t}+\frac{(\delta x)^2}{2}\frac{\partial^2 p}{\partial x^2}+...)+...$$

notice that $l + r = 1$ and introducing $\beta = r - l$

$$p(x,t) = p(x,t) - \beta\delta x\frac{\partial p}{\partial x} - \delta t\frac{\partial p}{\partial t} + \frac{(\delta x)^2}{2}\frac{\partial^2 p}{\partial x^2} + O(\delta t^2, \delta x^3),$$

as $(\delta t > 0)$

$$\frac{\partial p}{\partial t} = -(\frac{\beta\delta x}{\delta t})\frac{\delta p}{\delta x} + \frac{(\delta x)^2}{2\delta t}\frac{\delta^2 p}{\delta x^2}.$$

defining the finite limits :

$$v = \lim_{\delta x,\delta t\to 0}\frac{-\beta\delta x}{\delta t}$$

$$D = \lim_{\delta x,\delta t\to 0}\frac{(\delta x)^2}{2\delta t}$$

then

$$\frac{\partial p}{\partial x} = v\frac{\partial p}{\partial x} + D\frac{\partial^2 p}{\partial x^2}$$

where v is the advection coefficient and D is the diffusion coefficient. If the medium is homogeneous, (*i.e.* $l = r = \frac{1}{2}$) then $\beta = 0$ and $v = 0$ and the equation can be written as follows:

$$\frac{\partial p}{\partial t} = D\frac{\partial^2 p}{\partial x^2}.$$

With the increase in computing power individual-based models and cellular automata have increased in popularity and have proven particularly successful in modelling spatially complex ecological interactions [55, 107].

Individual based models focus on how macroscopic behaviour emerges from local interactions of individuals, if they are spatially explicit the individuals are associated with a particular location in the domain. Each individual in these simulations is autonomous and interact with each other and the environment under given autonomous rules.

In contrast, cellular automata models assume a fixed spatial grid where all individuals are identical and the space is dense and uniform. Individuals evolve through a number of discrete time steps under a certain set of rules depending on their own state and the state of their neighbours, such rules are iterated for a determined length of time.

Here we will use a continuous model, based on reaction-diffusion as we will assume that the three carbon sources (glucose, fructose and sucrose) act as reactants and diffuse throughout space. In contrast to the assumption of the previous chapter, where yeast has been considered non-motile, here we take into account that as colonies grow, The spreading of the cells in a colony is a passive, mechanical process, due to generation of pressure inside the colony due to volume increase due to growth, then yeast cells will disperse slowly through the domain (*ie.* the diameter of colonies will increase in size, as observed experimentally).

For simplicity we will consider a one-dimensional spatial domain $\Omega = [0, l]$, this can be done because the dynamic of the system is the same in all direction, adding more dimension wouldn't change the outcome, and without loss of generality we set $l = 1$. We define $N_p(t, x)$ and $N_{np}(t, x)$ as the densities of producers and non-producers, respectively, at time t and in the spatial location x with $x \in \Omega$. Similarly $S(t, x), G(t, x)$ and $F(x, t)$ denote sucrose, glucose and fructose concentrations, respectively, at time t and in the spatial location x. Extending the metabolic model described in Chapter 2 to include the above elements we arrive at:

$$\frac{\partial S}{\partial t} = D_s \frac{\partial^2 S}{\partial x^2} - J^S \cdot (Np + Nn) - Inv \cdot Np \tag{4.1a}$$

$$\frac{\partial G}{\partial t} = D_g \frac{\partial^2 G}{\partial x^2} - J^G \cdot (Np + Nn) + Inv \cdot Np \tag{4.1b}$$

$$\frac{\partial F}{\partial t} = D_f \frac{\partial^2 F}{\partial x^2} - J^F \cdot (Np + Nn) + Inv \cdot Np \tag{4.1c}$$

$$\frac{\partial N_p}{\partial t} = D_{Np} \frac{\partial^2 N_p}{\partial x^2} + (1 - c^{Inv}) \cdot (n_e^{Hxt}(J^G + J^F) \cdot (J^G + J^F) + n_e^S \cdot J^S) \cdot Np \tag{4.1d}$$

$$\frac{\partial N_{np}}{\partial t} = D_{Nnp} \frac{\partial^2 N_{np}}{\partial x^2} + (n_e^{Hxt}(J^G + J^F) \cdot (J^G + J^F) + n_e^S \cdot J^S) \cdot Nn. \tag{4.1e}$$

where different D_s' denote diffusion constants with subscripts referring to each state variable. In particular $D_s = \frac{D_g}{2}; D_{np} = D_p << D_f = D_g$. For simulation proposes

diffusion coefficients have the following values: $D_{np} = D_p = 1 \times 10^{-6}$ finally $D_g = D_f = 1 \times 10^{-3}$ and $D_g = \frac{1}{2}D_s$, x has dimensionless space units and therefore diffusion coefficients has units of $\frac{space^2}{time}$.

In order to ensure that outcomes of the model are determined completely by the interactions described in the model (4.1a-e), we impose no-flux boundary conditions at $x = 0$ and $x = 1$:

$$S_x(t,0) = G_x(t,0) = F_x(t,0) = 0,$$
$$S_x(t,1) = G_x(t,1) = F_x(t,1) = 0.$$
$$Np_x(t,0) = Nnp_x(t,0) = 0,$$
$$Np_x(t,1) = Nnp_x(t,1) = 0.$$

We define the initial conditions as

$$S(0,x) = S_0, \quad G(0,x) = G_0, \quad F(0,x) = F_0, \quad N_{p0}(x) \quad \text{and} \quad N_{np}(0,x) = N_{np0}(x)$$

where S_0, G_0 and F_0 are constants and the form of $N_{p0}(x)$ and $N_{np0}(x)$ will depend on the case under consideration, as discussed in the following section. In this simulations $S_0 = 1.17\frac{mmol}{g}$ and it is uniformly distributed in the domain. Numerical simulations presented in this chapter were performed using Matlab's built-in solver *pdepe*. Space is measured in dimensionless spacial units, and time in dimensionless time units.

4.2 Outcomes of the model for varying initial population structures

In the simulations presented in this chapter, the only resource that is initially present in the environment is sucrose which is uniformly distributed throughout the domain. Here we consider different initial spatial distributions of producers ($N_{p0}(x)$) and non-producers ($N_{np0}(x)$) and explore their effect on the overall fitness of the population.

We will examine interactions between producers and non-producers over short-time scale and genetic and regulatory changes will no be taken into account and instead the system will be considered from a purely ecological perspective.

In particular we consider the following two cases:

- **Case I**: Both cell types (producers and non-producers) are uniformly distributed across the entire domain (Figure 4-1) .
- **Case II**: Each cell type is placed in a patch with varying distances between the patches (Figure 4-4) and varying number of patches (Figure 4-9).

In order to compare the outcome of the spatially explicit system (eq 4.1) and the one where space is modelled phenomenologically (eq 2.3) the parameters that do not relate to mass transfer are kept the same in the two models.

Case I: Uniform distribution of both cell types

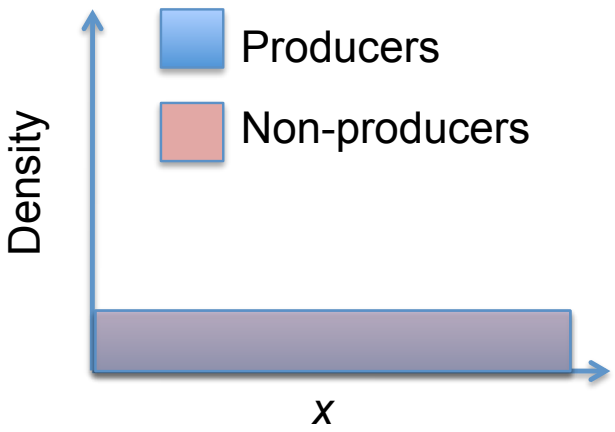

Figure 4-1: Uniform initial distribution for both populations; producers and non-producers

Using the initial yeast distribution illustrated in Figure 4-1 we perform a series of numerical simulations differing in the initial frequency of producers while keeping constant the total cell density of producers and non-producers put together. The simulations are run for t^* (until the resources have been exhausted) and, as in Chapter

2, for each initial producer frequency we record the total population size at the end of the numerical run $\int_0^1 (N_p(t^*, x) + N_{np}(t^*, x))dx$.

The initial conditions of the distribution of cells is as follows where $x \in [0, 1]$ denotes a position in the space, N_p denotes the initial distribution of Producers at $t = 0$, and N_n the initial distribution of Non-producers at $t = 0$.

Lets denote f the fraction of Producers in the initial population and N the initial amount of biomass in the population.

$f = \frac{N_p}{N_p + N_{np}}$
$N = 6.5 \times 10^{-7}$

$$N_p = \left\{ \begin{array}{ll} f \cdot N & 0 \leq x \leq 1 \end{array} \right\}$$

$$N_n = \left\{ \begin{array}{ll} (1 - f) \cdot N & 0 \leq x \leq 1 \end{array} \right\}$$

As for the case where spatial structure is modelled phenomenologically (Chapter 2) we find that population fitness (measured as the population density - Titre) peaks when a combination of both producers and non-producers are present in the population as shown in Figure 4-2 B. However, in contrast to the phenomenological model (eq. 2.3), the relative fitness of producers for the spatially explicit system (eq. 4.1) is always less than 1 (Figure 4-2 A). Given that the stable equilibrium frequency of producers and non-producers occurs when the relative fitness of producers (to non-producers) is 1, in this case our model predicts that eventually non-producers will outcompete producers.

The above finding can be explained as follows. Focusing on the spatial and temporal distribution of resources we find that at any given time point all three resources are uniformly distributed across the domain (Figure 4-3) making all resources equally accessible to both producers and non-producers. The cost that producers pay to break down sucrose into glucose and fructose ensures that the fitness of producers is always lower than that of non-producers.

Figure 4-2: Relative Fitness of Producers and Titre as a function of initial frequency of producers. Uniform distribution of a mixed population at the beginning of the simulation

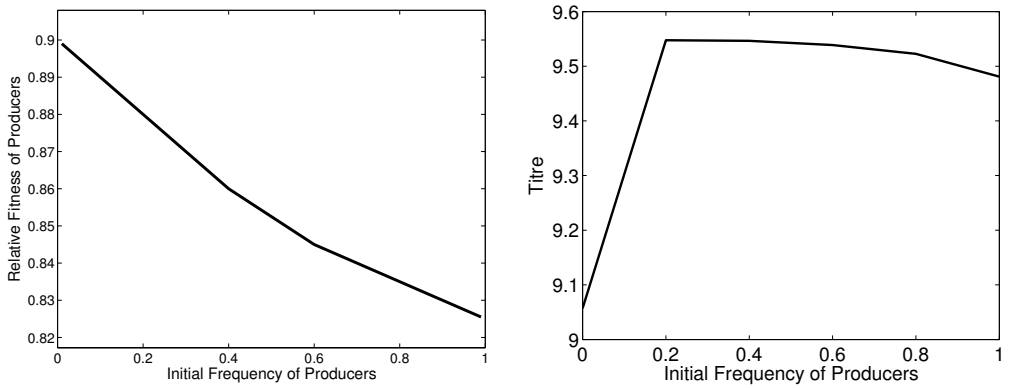

(a) Relative Fitness (b) Titre

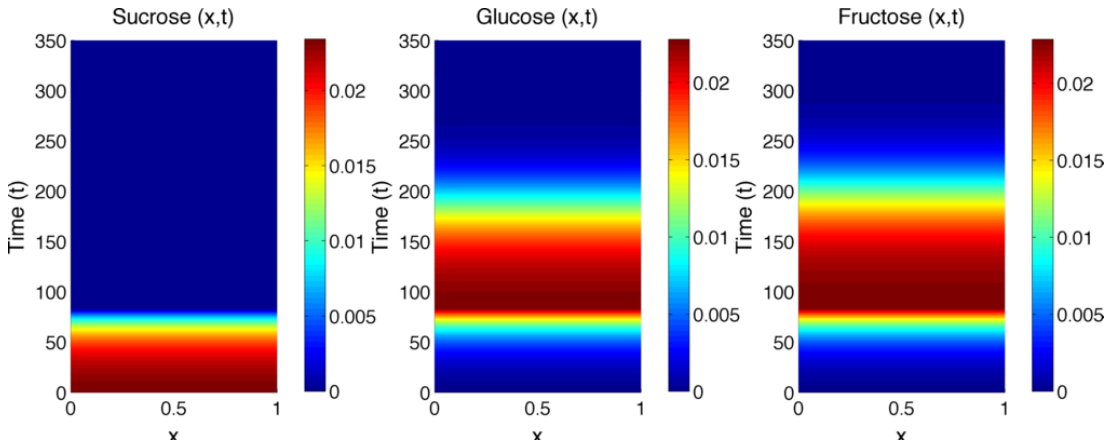

Figure 4-3: Dynamic of resources (sucrose, glucose and fructose) in time when producers and non producers start at $0.5 - 0.5$ in frequency.

Case II:Distribution of two patches with each patch containing one of the two different cell types.

Using the yeast distribution illustrated in Figure 4-4 we perform a series of numerical simulation as described above in Case I. In addition we consider the robustness of these results with respect to varying distances between the two patches.

The first simulation has an initial distribution of cells as follows, parameters had been previously define in Case I.

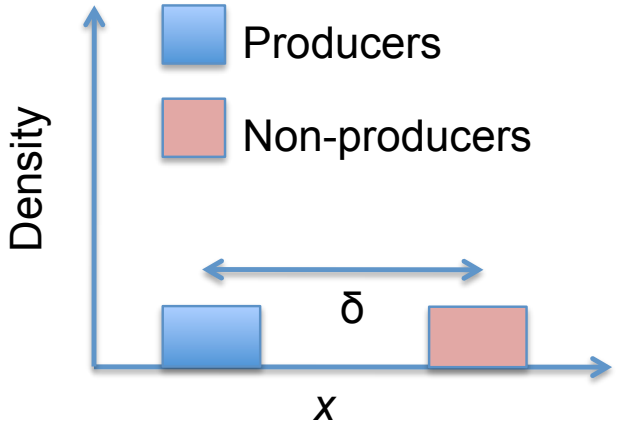

Figure 4-4: Initial distribution of cells: two different patches of producers and non-producers separated by a distance δ.

$$N_p = \left\{ \begin{array}{cc} 0 & 0 \leq x < 0.46 \\ f \cdot N & 0.46 \leq x \leq 0.53 \\ 0 & 0.53 < x \leq 1 \end{array} \right\}$$

$$N_n = \left\{ \begin{array}{cc} 0 & 0 \leq x < 0.53 \\ (1-f) \cdot N & 0.50 \leq x \leq 0.57 \\ 0 & 0.57 < x \leq 1 \end{array} \right\}$$

For a fixed distance between the producer and non-producer patch (δ), we find that as in Case I, population fitness peaks when a combination of both producers and non-producers are present in the population as shown in Figure 4-5 (b). However, contrary to Case I there is a stable equilibrium frequency of producers and non-producers since the relative fitness of producers crosses the line of equal fitness (Figure 4-5 (a)).

On inspection of the spatial and temporal dynamics of the three resources (Figure 4-6), we observe that the highest concentrations of glucose and fructose can be found in the left part of the domain where producers are initially located. This provides sufficient benefit to producers, which counteracts the cost of making invertase preventing the extinction of producers.

Increasing the distance between the initial patches (by increasing the value of δ)

increases the equilibrium frequency of producers (Figure 4-7 A) but removes the beneficial contribution of non-producers to the population fitness with population fitness now being maximised if everyone in the population is a producer (Figure 4-7 B).

Increasing the distance between the patches results in a initial distribution of cells as follows. The parameters were defined in Case I.

$$N_p = \left\{ \begin{array}{cc} 0 & 0 \leq x < 0.30 \\ f \cdot N & 0.30 \leq x \leq 0.35 \\ 0 & 0.35 < x \leq 1 \end{array} \right\}$$

$$N_n = \left\{ \begin{array}{cc} 0 & 0 \leq x < 0.65 \\ (1-f) \cdot N & 0.63 \leq x \leq 0.70 \\ 0 & 0.70 < x \leq 1 \end{array} \right\}$$

Figure 4-5: Relative Fitness of Producers and Titre as a function of the Initial Frequency of producers. The cells are initially located in two different patches, producers to the left and non producers in the right side of the domain,($\delta = .04$).

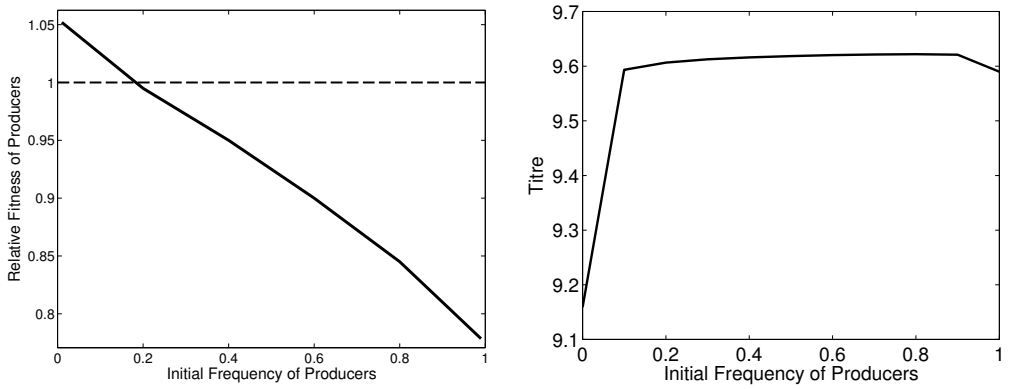

(a) Relative Fitness (b) Titre

Increasing the number of patches in the initial cell distribution (Figure 4-9) does not qualitatively change the outcome which can be seen by comparing Figure 4-5 with Figure 4-7. We increased the number of patches to be four, two of each strain , and the initial spatial distribution at time $t = 0$ is as follows:

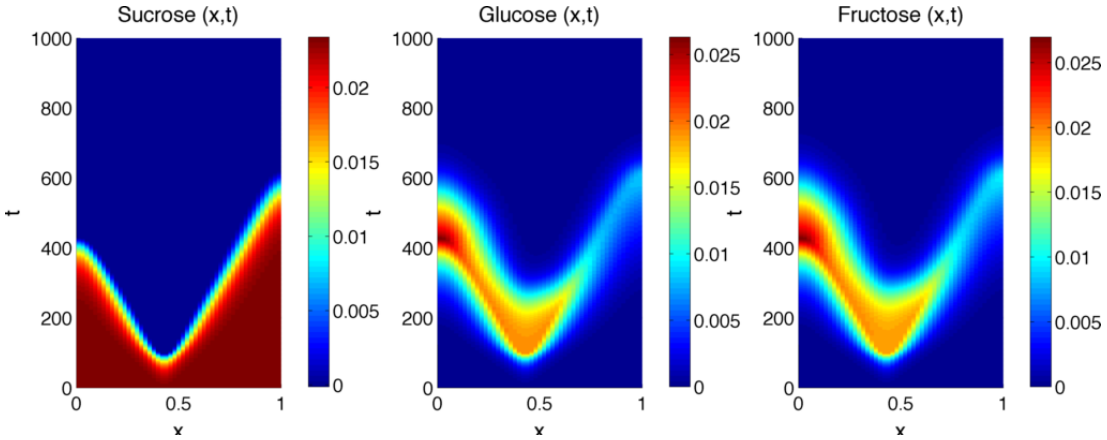

Figure 4-6: Consumption of resources in time when producers and non producers start at equal frequencies.

Figure 4-7: Relative Fitness of Producers and Titre as a function of the Initial Frequency of producers. The cells are initially located in two different patches, producers to the left and non producers in the right side of the domain($\delta = .34$)

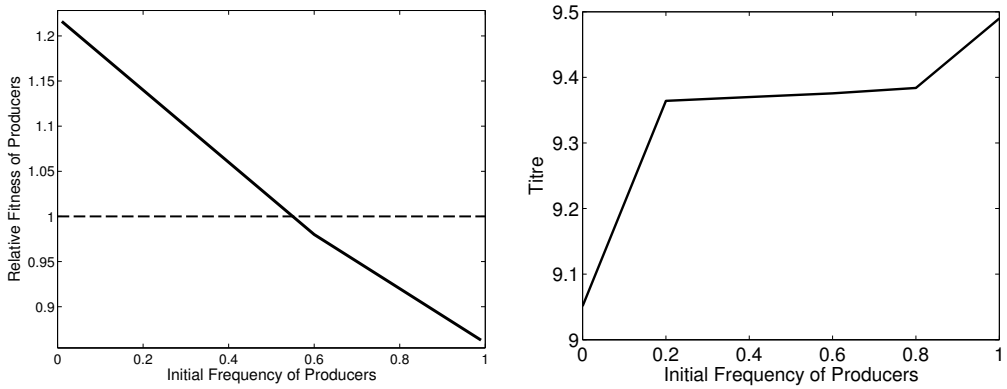

(a) Relative Fitness (b) Titre

$$N_p = \left\{ \begin{array}{cc} 0 & 0 \leq x < 0.30 \\ f \cdot N \cdot 0.5 & 0.30 \leq x \leq 0.35 \\ 0 & 0.35 < x \leq 0.45 \\ f \cdot N \cdot 0.5 & 0.45 \leq x 0.50 \\ 0 & 0.50 < x \leq 1 \end{array} \right\}$$

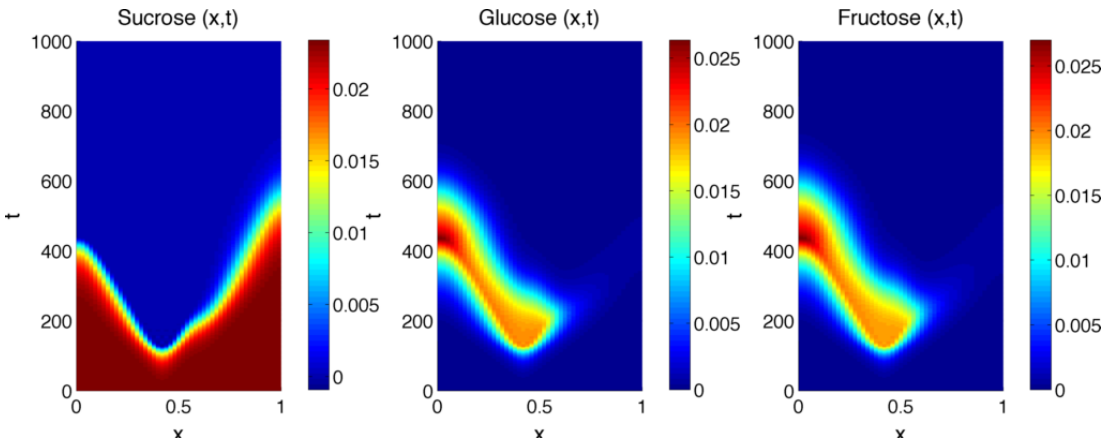

Figure 4-8: Dynamics of resources in time when producers and non producers starts at $0.5 - 0.5$ in frequency.

$$N_n = \begin{Bmatrix} 0 & 0 \leq x < 0.37 \\ (1-f)\cdot N \cdot 0.5 & 0.37 \leq x \leq 0.42 \\ 0 & 0.42 < x < 0.52 \\ (1-f)\cdot N \cdot 0.5 & 0.52 \leq x \leq 0.57 \\ 0 & 0.57 < x \end{Bmatrix}$$

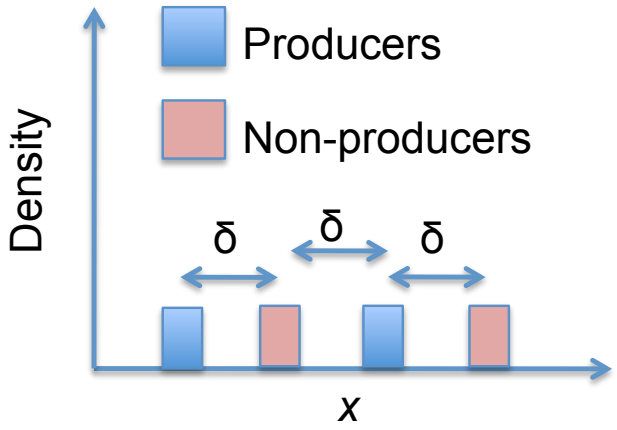

Figure 4-9: Initial distribution of four intercalated patches

Summary

In this section we have demonstrated that the result obtained in Chapter 3, namely that the population fitness is maximised when a combination of both producers and non-

Figure 4-10: Relative Fitness of Producers and Titre as a function of the Initial Frequency of Producers for the 4 patches initial distribution of cells, ($\delta = 0.07$)

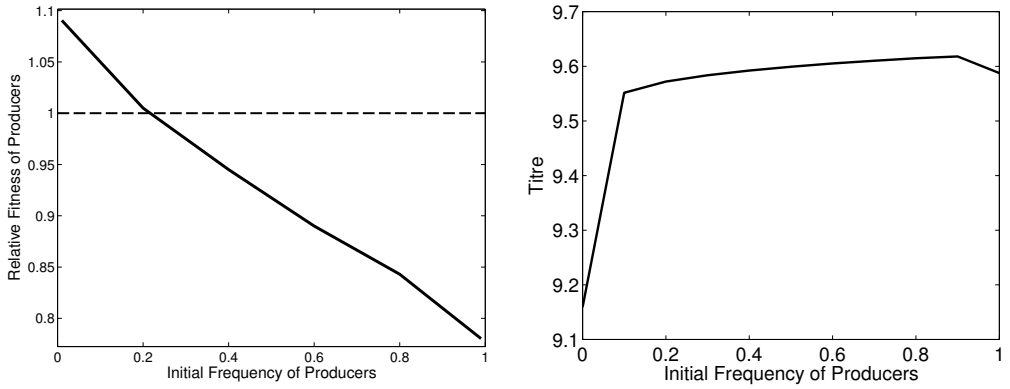

(a) A Relative Fitness (b) B Titre

producers is present in the population, is not just a peculiarity of the way the spatial structure was modelled. We find that both the phenomenological and spatially explicit models give rise to the same result. The fact that cheats can sometimes actually benefit the population they are in is therefore a result of the ecological dynamics between yeast cells and their environment.

In addition we find that spatial structure of a population affects the long-term coexistence between invertase producers and non-producers. We observe that the availability of glucose and fructose in the spatial locations containing non-producers must be smaller than the resource availability in the spatial locations containing producers for the coexistence to be possible. In agreement with prior theoretical studies our results support the idea that patchy structure supports the maintenance of cooperation while homogeneous environments support cheating. This can be explained in the following way. A patchy structure allows producers to retain the glucose that they produce for longer periods of time than would otherwise be the case in well-mixed environments. This ensures that at least some of the benefit of producing invertase is kept by the producers without having to share it with non-producers. However, if the diffusion of resources is high, the environment becomes more homogeneous and producers can end up losing their produced resources to non-producing individuals.

Although in our model patchy structure is artificially introduced through the initial

distribution of cells, there are some recent studies suggesting that clumping can be advantageous for both nutrient acquisition and protection, therefore can be the initial step for the evolution of multicellularity [37, 83].

4.3 Predicting the long-term coexistence of producers and non-producers

It is important to point out that the experimental data and the numerical simulations presented so far in this thesis have been conducted for a fixed time period representing dynamics within a single season. We define the length of a season as the time it takes for all resources to be exhausted and for the population to reach a stationary phase.

However, the negative-frequency dependence plots produced in this thesis (e.g Figure 4-2(a) and Figure 4-6(a)) do not identify all possible long-term equilibria of our system. In particular the temporal structure such as the length of a season will have an effect on the long-term dynamics and this will be explored in the final chapter of this thesis.

CHAPTER 5

Seasonal dynamics and long-term coexistence

What maintains diversity, be it in ecosystems or within populations, remains one of the central issues in biology. In particular, spatial and temporal heterogeneity are well-established drivers of diversity [16]. In this chapter we will consider both spatially and temporally heterogeneous environments and ask a different set of questions. Does the way a population disperses and re-colonises affect the long-term equilibrium? Will there be a unique outcome? Could any equilibrium be derived from considering a single-season dynamics? Alternatively, are there multiple stable solutions depending on the initial conditions? These questions are relevant not only to real-world ecology and evolution but also to the design of protocols for laboratory-based evolutionary experiments.

In the previous chapters, we analysed our model system in order to find conditions that maximised population fitness when producers and non-producer of invertase were competing in a spatially structured environment, within one season and with limiting availability of resources. Here we are interested in answering what is the long-term equilibrium, and what are the necessary conditions for maintaining long term co-existence in this system? Furthermore, we will discuss a set of experimental results based on the system studied throughout this thesis, examining the robustness of different ex-

perimental protocols with respect to the mechanism in which the spatial structure is maintained between seasons.

5.1 Seasonality and the invertase system

Imagine a population of invertase producers and non-producers growing on sucrose in a spatially structured environment. Imagine too that such a population is allowed to mature until all the sugar (sucrose, glucose and fructose) is exhausted, when resources are completely depleted we will call it a complete season.

The second season is initiated by transferring cells from the end of the first season into a new environment with the same initial sugar content as the previous one. We consider two ways of transferring between environments that mirror real-world between-season ecologies. The first protocol is such that spatial structure is not maintained between seasons, which may be comparable to migratory species that re-colonise a summer feeding ground randomly [51, 79] and therefore will be referred to as *migratory regime*. Alternatively, we consider what might happen if spatial structure is maintained between seasons, a protocol that we will call *non-migratory regime*. This is similar to a non-migratory species in which over-wintering is done at the physical location at which an organism is found at the end of the summer growing season.

In practice the migratory transfer method is performed by washing cells off the old plate, mixing them thoroughly and then spreading a sample across the surface of a new plate; we expect a unique long-term equilibrium between producers and non-producers to be established. In contrast, the non-migratory transfer can be achieved experimentally using replica-plating to maintain spatial structure, under this method cells from the old plate are transferred to a sterile velvet stamp that is used to inoculate the new plate, maintaining the spatial position between cells. This regime has historically had two main applications: isolation of new mutants and the classification of colonies that are different from each other in the nutritional requirements [28, 57, 85].

In both protocols the initial resource concentrations are the same between seasons, as well as the initial population sizes. The duration of each season is defined as the moment when all resources have been exhausted, taking complete seasons. At first sight, it is not obvious that the transfer regimes make a big difference to the population dynamics. Indeed, very few studies in the experimental evolution literature discuss the significance of such differences [49, 39, 38].

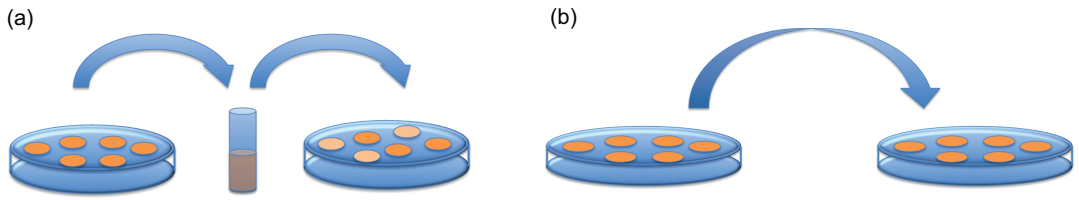

Figure 5-1: In panel (a) the spatial structure is not maintained between seasons: in each transfer the population is taken out of the plate and vortexed in a test tube, before a sample of this mixture is re-inoculated in an agar plate with fresh growth medium. In panel (b) the protocol preserves (as much as possible) the spatial structure between seasons by using a velvet and a velvet tool to press the old agar plate into it. This method leaves an impression which is then transferred into an agar plate with fresh medium.

5.2 Long-term experiments for the invertase system

In order to examine experimentally the difference between both experimental protocols (Figure 5-1) we decided to perform long-term experiments. I was invited by Dr. Duncan Greig to visit his lab at the Max Planck Institute of Evolutionary Biology in Plön, Germany, to undertake the experiments described in the following section.

5.2.1 Experimental methods

We used two isogenic strains, *SUC2 (a/α, leu2/leu2, his5/his5, ura3/ura3, SUC2/SUC2)* and *suc2*, an isogenic diploid strain in which both copies of *SUC2* have been replaced by *KanMX*. For all experiments, initial cultures of yeast were grown overnight in standard YEPD medium at a temperature of 30° c in the incubator. For the propagation of mixed communities, cultures were inoculated and grown in sucrose synthetic medium

Producers (%)	Non-producers (%)
10	90
30	70
50	50
70	30
90	10

Table 5.1: Initial population cultures in percentage.

in 25 mL agar plates with a concentration of sucrose of 20 g/L (2%) .

For the long-term experiment, mixed communities of invertase producers and non-producers were propagated and the frequency of each type was tracked each season under the transfer protocols previously discussed. To determine the size of the sample that will be transferred each season, ten plates were replica plated and both the old and the new samples were cut using a sterile scalpel and placed into tubes containing $5mL$ of sterile water. The tubes were vortexed and a sample of the solution was counted in the hemocytometer to determine the percentage of cells of each sub-population.

The initial populations started with five different initial frequencies (proportion of producers/non-producers) and five replicas of each experiment were done:

Suspensions containing the five initial frequencies were prepared and the frequencies were tested by counting growing colonies. One single patch of 5 μL of each initial frequency was placed in the middle of a 25 mL Petri dish containing 2% sucrose in the medium. All populations were allowed to grow for six days at a temperature of 30°C in the incubator. After the sixth day, a sample from each population was transferred into fresh plates and the cycle was repeated.

The frequency of the producers and non-producers was determined after each cycle by diluting the suspension 4-fold and then cultivating a sample of the resulting population into standard YEPD and YEPD with added antibiotic G148 plates and counting colonies to determine the resulting frequency. The *suc2* strain is the only one that can survive in G148 YPD media because the marker *KanMX* make them antibiotic resistant.

For **Protocol 1** (Migratory Regime), after 6 days patches from each plate were cut from the plates with a sterile scalpel and placed into tubes containing 5 mL of sterile water. Then the tubes were vortexed for 1 minute and a 5 μL of the suspension was placed in a new plate with fresh medium.

For **Protocol 2** (Non-Migratory Regime), after 6 days each plate was transferred using replica plating tool where a sterile velvet was placed, an exact printing of the plate was taken by pressing the plate on the velvet, then a new plate with fresh medium was pressed on the same velvet, obtaining an exact copy of the old plate.

The experiment lasted seven seasons for both protocols and each season lasted six days.

5.2.2 Results

At the end of each season, the proportion of producers in the resulting population was counted. As we can observe from the results presented in Figure 5-2(a) and Figure 5-2(b), the data obtained is inconclusive. There is not a clear difference in the population dynamics of both protocols, and in seven seasons our experiment failed to reach an equilibrium (due to time constraints we could not continue the experiments).

For both protocols, however, there is a clear tendency for the fraction of producers to increase over time, although for **Protocol 2** this is not the case for all initial conditions.

Our experiment was conducted for seasons of fixed length (6 days) and a fixed number of seasons (7 seasons). To systematically explore the dynamics between seasons under different parameter ranges, we carried out a theoretical analysis by introducing temporal structure into the mathematical model described by equations (eq. 2.3). The reason for using the model described in Chapter 2 is its proven ability to consistently make not just qualitatively but also quantitatively predictions. Furthermore, extending this model allows us to test experimentally the predictions of the model.

5.2.3 Theoretical approach to studying seasonal environments

The system of equations (eq. 2.3) developed in Chapter 2 describes the competition dynamics between two yeast types within a single season. Here we adapt this model to evaluate what happens to the competing types after a number of seasons. In order to optimise the numerical simulations some of the functions estimated in Chapter 2 were re-fitted using polynomial fitting included later in this chapter.

At the beginning of the first season, all environments are initiated with the same amount of sucrose (S_0) and the same total cell number (N_0), but we allow the ratio of producers to non-producers (f) and the degree of mixing (m) to vary. Note that initially there is no glucose or fructose present in the environment, these resources only appear once sucrose is hydrolysed through invertase. The initial conditions at the beginning of the first season can therefore be defined as follows:

$$\begin{aligned}
&S_1(0) = (1-m)fS_0, && N_{p1}(0) = (1-m)fN_0,\\
&S_2(0) = (1-m)(1-f)S_0, && N_{n2}(0) = (1-m)(1-f)N_0,\\
&S_3(0) = mS_0, && N_{p3}(0) = mfN_0 \text{ and } N_{n3}(0) = m(1-f)N_0,
\end{aligned}$$

with $G_i(0) = 0$ and $F_i(0) = 0$ for $i = 1, 2, 3$ denoting the different regions of the model. Cells grow and compete for resources until all sugars (sucrose, glucose and fructose) are exhausted, denoting the end of the season. The subsequent season is initiated by transferring a small fraction of the total number of cells from the previous season into the fresh environment. The beginning of each season is denoted by the time T_0^j while the time it takes for the resources to be depleted is denoted by T_{end}^j, where the superscript j represents the season number.

As mentioned before, we will consider two mechanisms by which the transfer between seasons can be achieved: a migratory regime (Figure 5-1 a) and a non-migratory regime (Figure 5-1 b).

5.2.4 Migratory regime

If $N_p(T^j_{end})$ and $N_n(T^j_{end})$ denote respectively the total number of producers and non-producers at the end of j-th season, then the fraction of producers at the end of j-th season is defined as:

$$f^j = \frac{N_p(T^j_{end})}{N_p(T^j_{end}) + N_n(T^j_{end})}.$$

Then the initial conditions for the $j+1$-st season can be written as:

$$\begin{aligned}
&S_1(T_0^{j+1}) = (1-m)f^j S_0, && N_{p1}(T_0^{j+1}) = (1-m)f^j N_0,\\
&S_2(T_0^{j+1}) = (1-m)(1-f^j) S_0, && N_{n2}(T_0^{j+1}) = (1-m)(1-f^j) N_0,\\
&S_3(T_0^{j+1}) = m S_0, && N_{p3}(T_0^{j+1}) = m f^j N_0,\\
&\text{and } \ N_{n3}(T_0^{j+1}) = m(1-f^j) N_0,
\end{aligned}$$

with $G_i(T_0^{j+1}) = 0$ and $F_i(T_0^{j+1}) = 0$ for $i = 1, 2, 3$.

5.2.5 Non-migratory regime

The initial condition for the $j+1$-st season can be written as

$$g^j = \frac{1}{N_p(T^j_{end}) + N_n(T^j_{end})}$$

$$\begin{aligned}
&S_1(T_0^{j+1}) = (1-m)f^j S_0, && N_{p1}(T_0^{j+1}) = g^j N_{p1}(T^j_{end}) N_0,\\
&S_2(T_0^{j+1}) = (1-m)(1-f^j) S_0, && N_{n2}(T_0^{j+1}) = g^j N_{n2}(T^j_{end}) N_0,\\
&S_3(T_0^{j+1}) = m S_0, && N_{p3}(T_0^{j+1}) = g^j N_{p3}(T^j_{end}) N_0,\\
&\text{and } \ N_{n3}(T_0^{j+1}) = g^j N_{n3}(T^j_{end}) N_0,
\end{aligned}$$

with $G_i(T_0^{j+1}) = 0$ and $F_i(T_0^{j+1}) = 0$ for $i = 1, 2, 3$.

In both regimes the transfers were carried out while $|f^{j+1} - f^j| > \epsilon$, where ϵ denotes a constant associated with a numerical error with $\epsilon \approx O(10^{-7})$.

5.2.6 Competition in seasonal environments and stability analysis

Note that for the non-migratory regime the population structure is in itself a changing trait: even if producers and non-producers start with the same proportion, the following season this structure may well be different and therefore the end-result can also be different.

In contrast, under the migratory regime at the start of each season the population-structure, m, is reset and thus m cannot evolve. Therefore the only parameter changing between seasons is the proportion of producers, as defined in Section 5.2.4. For this reason, although the long-term equilibria for the migratory regime can be determined using stability analysis, this method cannot be employed for the non-migratory regime.

Furthermore, as the migratory regime can be written as an iterative map, we can use a cobweb method to describe its dynamics and find the long-term equilibria of the system from a single-season dynamics.

Let us define a map as a function of the form $R_{n+1} = \Gamma(R_n)$ where R_0 is a set of initial conditions. If R^* satisfy $\Gamma(R^*) = R^*$ then R^* will be a fix point of the system. In this thesis we will use the cobweb method to determine the stability of the fix points, as explained below. Graphically the steady states are intersections of the curve $R_{n+1} = \Gamma(R_n)$ and $R_{n+1} = R_n$ and the dynamic evolution of the solution R_n can be obtained graphically as follows. Suppose we start with R_0 then R_1 is given by drawing a vertical line through R_0 until it intersects the curve $R_{n+1} = \Gamma(R_n)$ which gives $R_1 = \Gamma(R_0)$. Next we draw a horizontal line through $\Gamma(R_0)$ until it intersects the diagonal $R_{n+1} = R_n$ which gives us a new initial condition R_1 and the process starts again with R_1 in place of R_0.

In our system, using single-season dynamics (cobweb maps) in a complete season scenario (when all resources have been exhausted), we should observe a unique stable equilibrium and this is indeed the case for the values $m = 0.2$ and $m = 0.8$, as illustrated in Figure 5-3(a-b).

We are also interested in studying what happens when resources have not been exhausted, a condition that will be referred to as an incomplete season. Using again stability analysis, we find that different equilibria are achieved for incomplete seasons. For example, in Figure 5-4(a) we find that there is no co-existence, and 0 and 1 are both stable equilibria of the system. Similarly, Figure 5-4(b) illustrates a case where we still find two different stable equilibria, but in contrast with the previous case, those equilibria present co-existence at different fractions of producers.

In order to compare the two different protocols, we constructed bifurcation diagrams of both regimes (Migratory and Non-Migratory). For each one we simulated different initial conditions and plotted the stable equilibria of the system at each transfer time, $0 < T < 250$. For each value of T we iterate the system a fixed number of times ($N = 300$) with initial conditions described in Section 5.2.4 for the migratory regime and Section 5.2.5 for the non-migratory regime. Using different initial proportion of producers we iterated the system and plotted the values computed for the last 50 iterations, and thus visualising both stable equilibria and periodic orbits.

For each transfer regime we considered two different mixing parameters, one with a high degree of mixing ($m = 0.8$) and one with a low degree of mixing ($m = 0.2$) and obtained the bifurcation diagrams shown in Figure 5-5. Note that for both regimes and for both values of m, no co-existence is found if the transfer time is short ($0 < T < 100$). The final equilibrium is determined by the initial proportion of producers, and either strain can outcompete the other. Furthermore, notice that for $m = 0.8$ and $T \geq 100$, the stable equilibrium is unique for all initial conditions and the system presents co-existence between both strains (Figures 5-5(b) and 5-5(d)).

In contrast, for $m = 0.2$ the result is rather different, as illustrated in Figure 5-5(a) and Figure 5-5(c). After the value of T at which no co-existence is found ($T = 100$), the system presents multiple stable equilibria. For the migratory regime at some intermediate times ($100 < T < 180$) we observe two different equilibria for each value of T, as was indeed predicted from the stability analysis. As the time increases ($T \geq 180$), the bubble collapses into a single stable equilibrium.

The non-migratory regime presents a more complex dynamics, as illustrated in Figure 5-5(c). Instead of just possessing at most two stable equilibria for each value of T, there appears to be a cascade of period-doubling bifurcations, an indicator of chaotic dynamics. This feature is illustrated in more detail in Figure 5-6. Performing a rigorous mathematical analysis is beyond the scope of this thesis and a matter for further research.

5.3 Polynomial fitting

Polynomial fitting were estimated using Matlab's built-in polynomial fitting tool in the least squares sense from the functions described in Chapter 2.

- Efficiency of hexoses $n^{Hxt} = 3.9 \times 10^{-9} \cdot (J^G + J^F)^5 - 6.728 \times 10^{-7} \cdot (J^G + J^F)^4 - 5.9 \times 10^{-4} \cdot (J^G + J^F)^3 - 1 \times 10^{-3} \cdot (J^G + J^F)^2 + 1.044 \times 10^{-3} (J^G + J^F) + 4.777 \times 10^{-2}$.
- Efficiency of Sucrose $n^S = 4.182785 \times 10^{-9} \cdot J^{S^8} - 3.00355268 \times 10^{-7} \cdot J^{S^7} + 8.660780388 \times 10^{-6} \cdot J^{S^6} - 1.26960896486 \times 10^{-}4 \cdot J^{S^5} + 9.77018981074 \times 10^{-4} \cdot J^{S^4} - 3.543231508268 \times 10^{-4} \cdot J^{S^3} + 3.639336246873 \times 10^{-3} \cdot J^{S^2} + 1.130598427030 \times 10^{-3} \cdot J^S + 2.9024713958809 \times 10^{-2}$.
- Sucrose Uptake Rate $J^S = -62.90 \cdot S^8 + 429.7 \cdot S^7 - 1193.0 \cdot S^6 + 1723.3 \cdot S^5 - 1381.0 \cdot S^4 + 616.7 \cdot S^3 - 162.9 \cdot S^2 + 38.8 \cdot S$.
- Competition parameter for Fructose $K_c^F = -2.12 \times 10^{-2} \cdot (F^6) + 5.08 \times 10^{-2} \cdot F^5) + 1.259 \times 10^{-1} \cdot F^4 - 5.430 \cdot F^3 + 6.493 \times 10^{-1} \cdot F^2 - 2.990 \times 10^{-1} \cdot F + 519 \times 10^{-2}$.
- Competition parameter for Glucose $K_c^G = -0.1167 \cdot (G^6) - 0.3946 \cdot (G^5) + 4.4219 \cdot (G^4) - 10.7498 \cdot (G^3) + 11.0073 \cdot (G^2) - 4.777 \cdot G + 0.7248$.

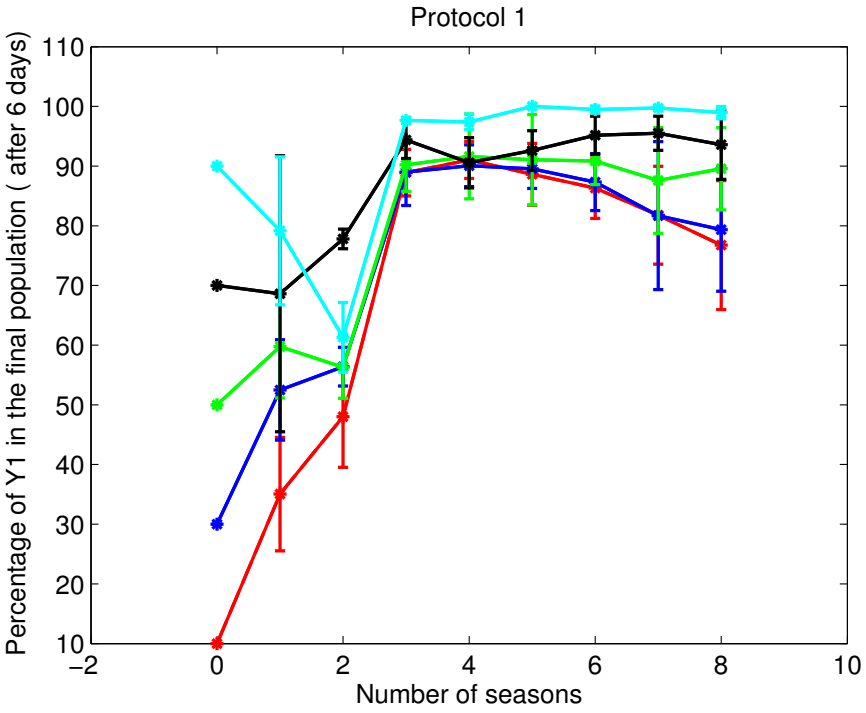

(a) Experimental data under **Protocol 1**: Migratory Regime (Y1 represents the population of invertase producers)

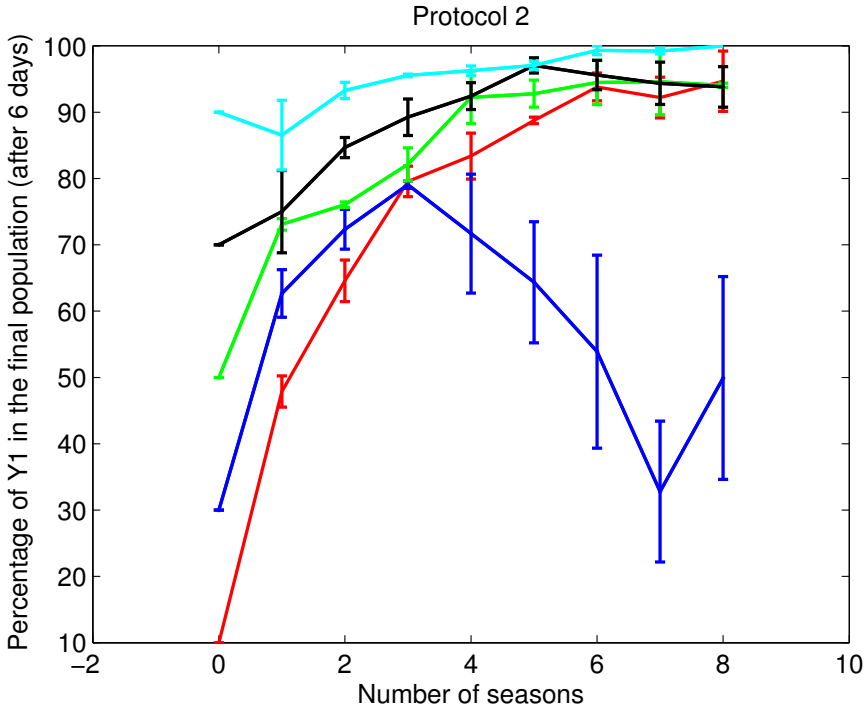

(b) Experimental data under **Protocol 2**: Non-Migratory Regime (Y1 represents the population of invertase producers)

Figure 5-2: Experimental data from both protocols, migratory regime and non-migratory regime, each season correspond to 6 days..

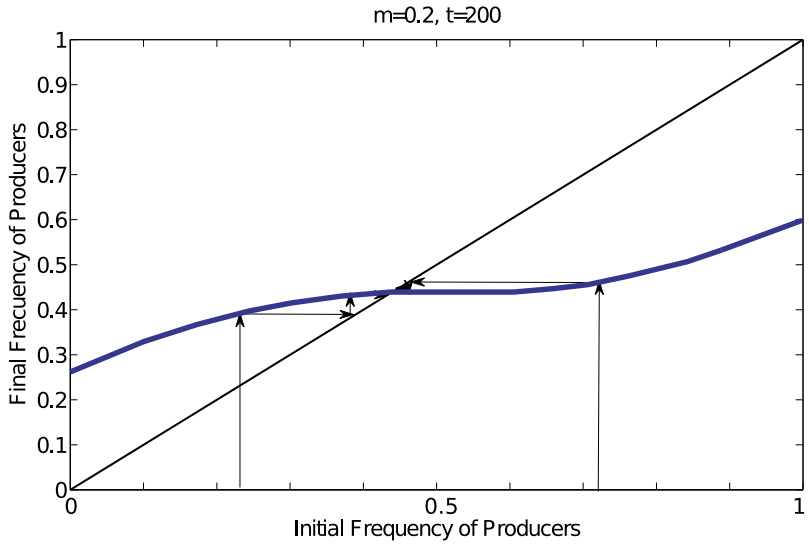

(a) For $m = 0.2$ and $T = 200$ the system presents a single stable equilibrium.

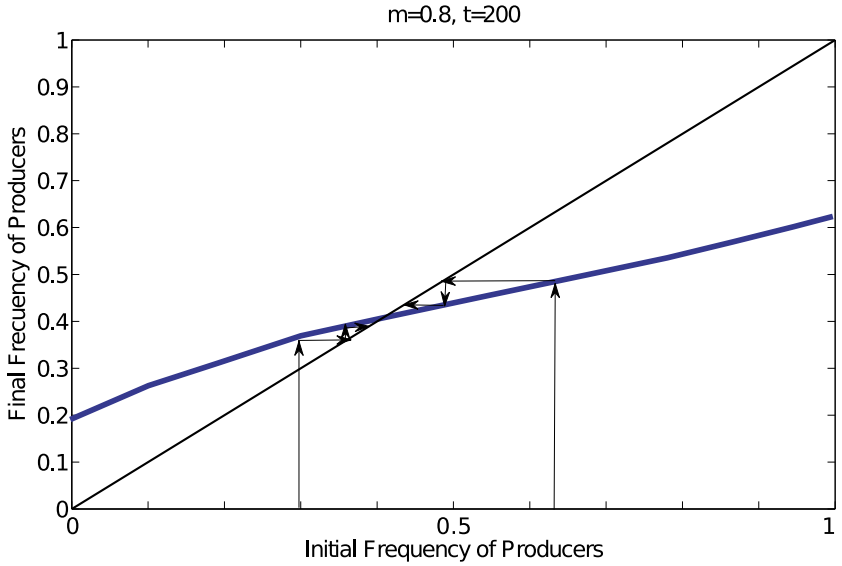

(b) For $m = 0.8$, $T = 200$ the system presents a single stable equilibrium.

Figure 5-3: Cobweb map for a complete season scenario where all resources have been depleted for different mixing parameters.

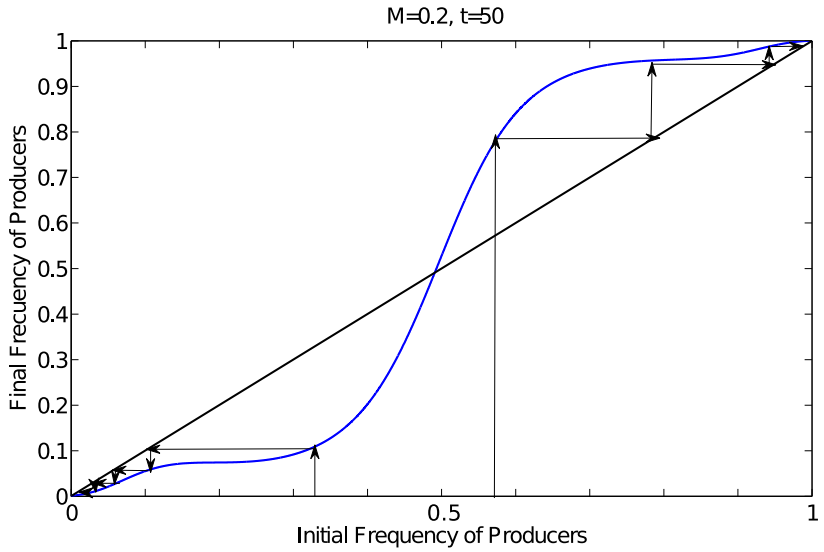

(a) $m = 0.2$ and $T = 50$

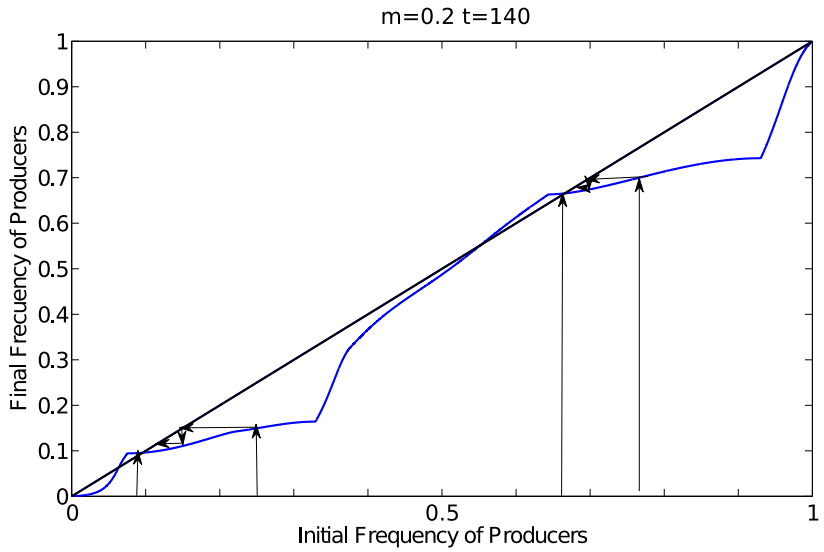

(b) $m = 0.2$ and $T = 140$

Figure 5-4: In an incomplete season ($T = 50$ and $T = 140$) different equilibria are found. (a) Two stable equilibria are found in 0 and 1, showing no co-existence of the two strains. (b) This case also presents two stable equilibria, but in this case co-existence is observed at two different proportions of producers and non-producers.

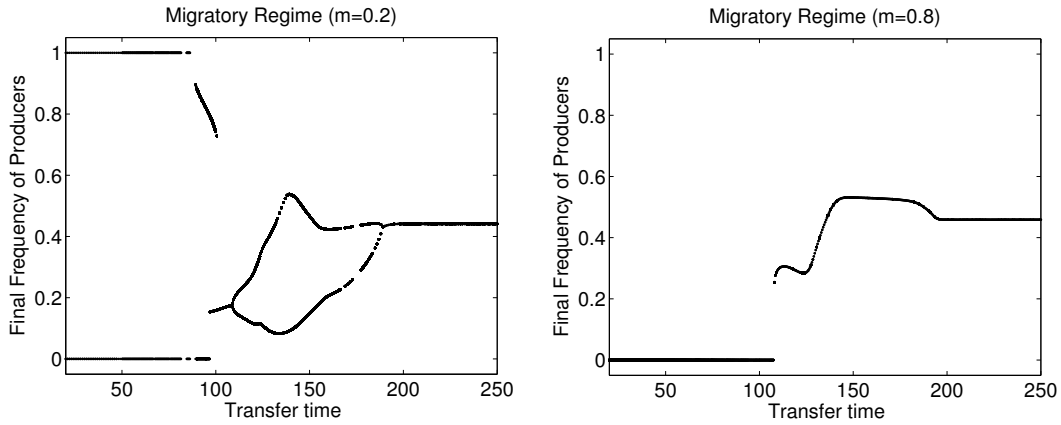

(a) Migratory Regime m=0.2

(b) MigratoryRegime m=0.8

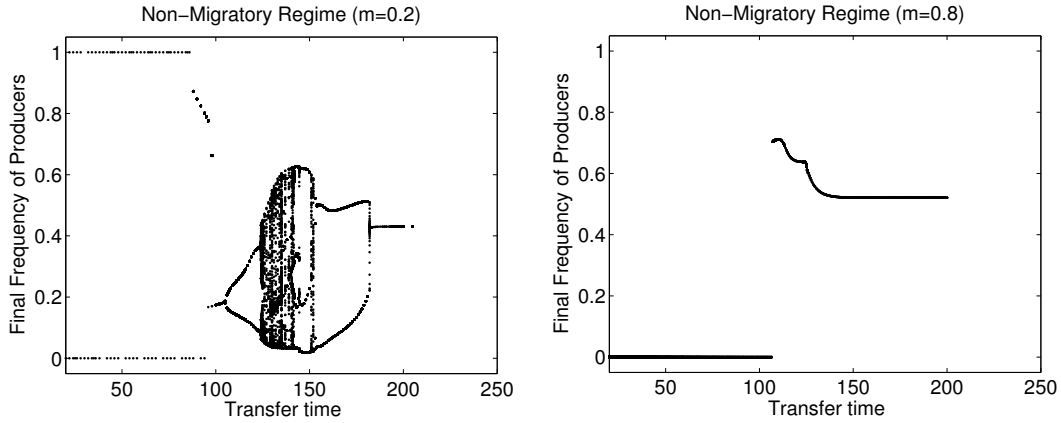

(c) Non-Migratory Regime m=0.2

(d) Non-Migratory Regime m=0.8

Figure 5-5: Bifurcation diagrams comparing the migratory and non-migratory regimes for values $m = 0.2$ and $m = 0.8$.

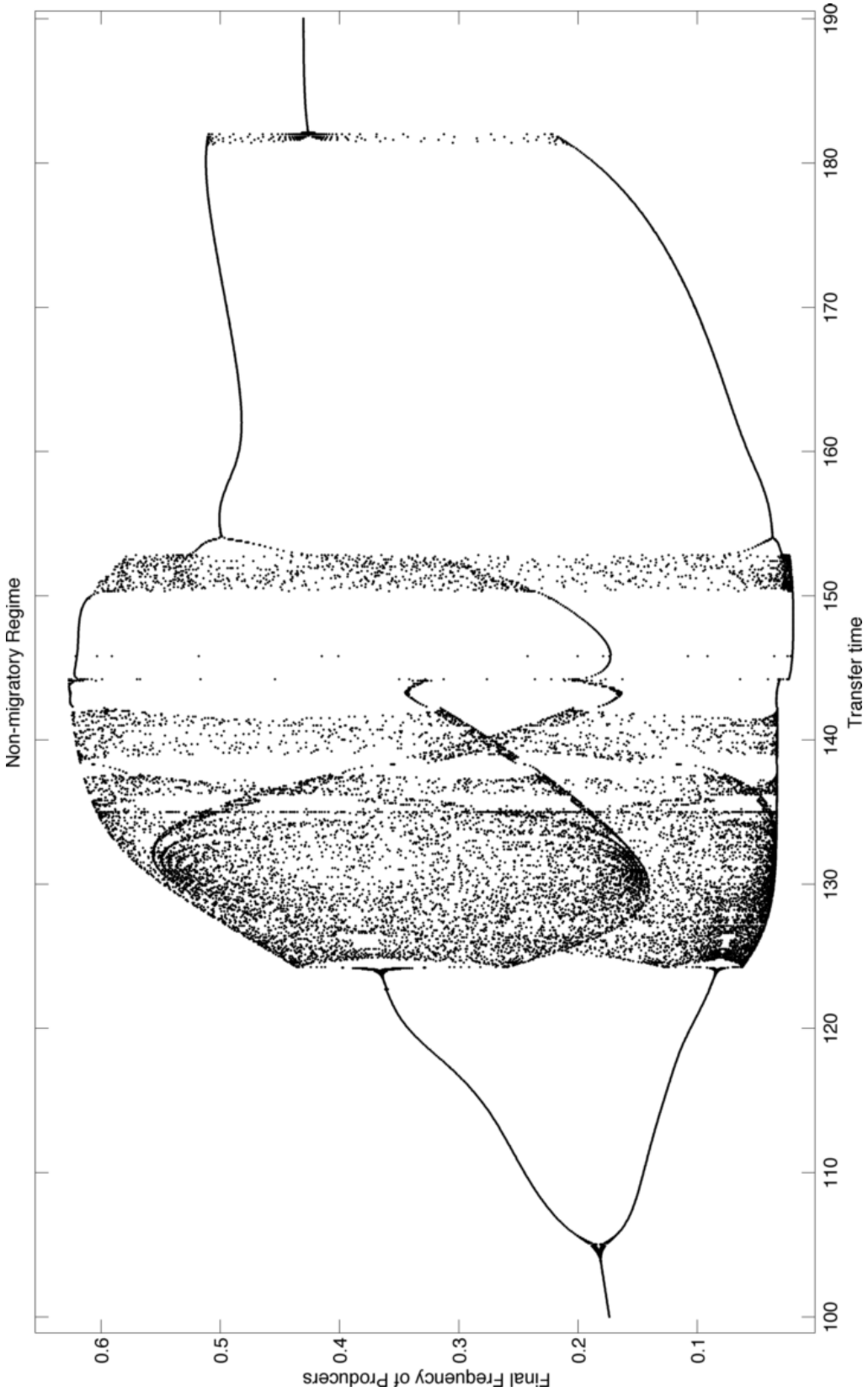

Figure 5-6: Bifurcation diagram of the migratory regime considering as a bifurcation parameter the length of the season, T.

5.4 Simple model

Is the observed chaos a consequence of the transfer regime between seasons? Is it a consequence of the inherent complexity of the detailed invertase model? In order to address these questions, in this section we will study a simplified version of the model presented in Chapter 2.

This toy model is based on the phenomenological approach towards spatial structure discussed in Chapter 2, and its dynamics can be described for a homogeneous environment as follows:

$$\frac{dS}{dt} = -Inv \cdot \frac{S}{k+S} \cdot N_1 - U(S) \cdot (N_1 + N_2) \quad (5.1)$$

$$\frac{dG}{dt} = Inv \cdot \frac{S}{k+S} \cdot N_1 - U(G) \cdot (N_1 + N_2) \quad (5.2)$$

$$\frac{dN_1}{dt} = (1 - Icost) \cdot E_S \cdot U(S) \cdot N_1 + E_G \cdot U(G) \cdot N_1 \quad (5.3)$$

$$\frac{dN_2}{dt} = E_S \cdot U(S) \cdot N_2 + E_G \cdot U(G) \cdot N_2 \quad (5.4)$$

with initial conditions and parameter values as follows:

Parameter	Name	Value
Initial Sugar S	S_0	0.7
Initial inoculation of cells	N_0	1.4×10^{-6}
Efficiency of G	E_G	0.048
Efficiency of S	E_S	0.030
Cost of production of the enzyme I	$Icost$	0.1
Invertase production	$Inver$	77.109
Diffusion parameter	d	0.007

$U(S)$ and $U(G)$ denote the uptake rate of resources S and G respectively, Inv a function representing invertase production, $Icost$ the cost of producing invertase, while E_S and E_G are the efficiencies at which S and G are converted into ATP respectively.

The dynamics between seasons is equivalent to that described in the previous sec-

tion, *i.e.* the initial condition of a given season is determined based on a sample of the terminal condition of the previous season.

For the purpose of this section, we will focus exclusively on the migratory regime, the reason being that under this regime long-term equilibria can be predicted from exploring only one season, thus simplifying considerably the experimental testing and mathematical analysis.

The dynamics of this toy model for low mixing parameter ($m = 0.2$), with $T = 50$ and $T = 150$ is illustrated in Figure 5-7. Note that in Figure 5-7(a) the system presents two different stable equilibria located in the extreme values 0 and 1, and as a consequence no co-existence is found. In contrast, when the length of each season is increased ($T = 150$), the system presents more than two different stable equilibria, as shown in Figure 5-7(b). In particular for the region between 0.6 and 0.8 the system presents an infinity of fixed points that could be an indicator of chaotic behaviour [91].

Figure 5-8(a) shows the bifurcation diagram for a low mixing parameter ($m = 0.2$). Note that this case also presents what appears to be a chaotic dynamic via a period-doubling bifurcation. Therefore we argue that the complex dynamics presented by this model is not a consequence of the transfer protocol nor the metabolic detail, but of the complex ecology that the two competitors are subjected to. However, this result does not hold for every mixing condition, as changing the parameter m can produce a different outcome: at high values of m the system presents a single stable equilibrium, as illustrated in Figure 5-8(b).

In summary, if we combine the results presented for both the simple and the parameterised model, we notice that the system presents chaotic behaviour under different circumstances. For the parameterised model we find chaotic behaviour for the non-migratory regime, which implies that the dynamics between seasons can indeed introduce complex dynamics in the system. We stress that the chaotic regime was found for low and medium values of the mixing parameter m, as can be seen in Table 5.2. Moreover, the behaviour for the migratory regime in the simple model also

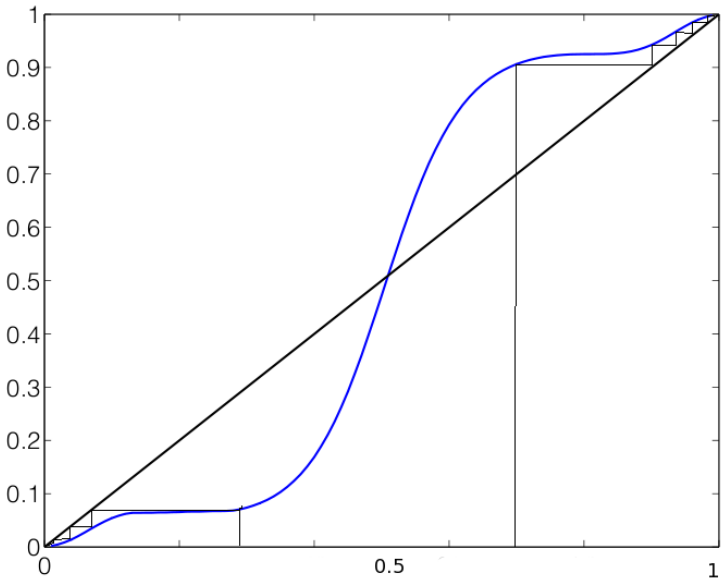

(a) ($m = 0.2$ $T = 50$)

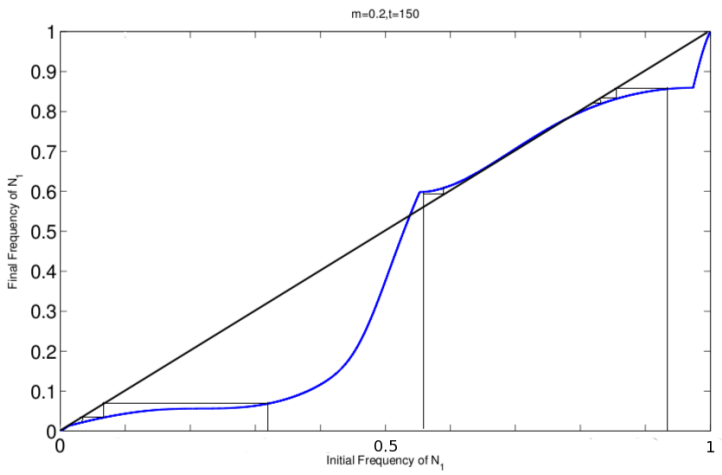

(b) ($m = 0.2$ $T = 150$)

Figure 5-7: Incomplete season dynamics. (a) Two stable equilibria are found in the extremes and no-coexistence are found. (b) Several stable equilibrium are found, in particular the region between 0.6 and 0.8 presents an infinity of fixed points.

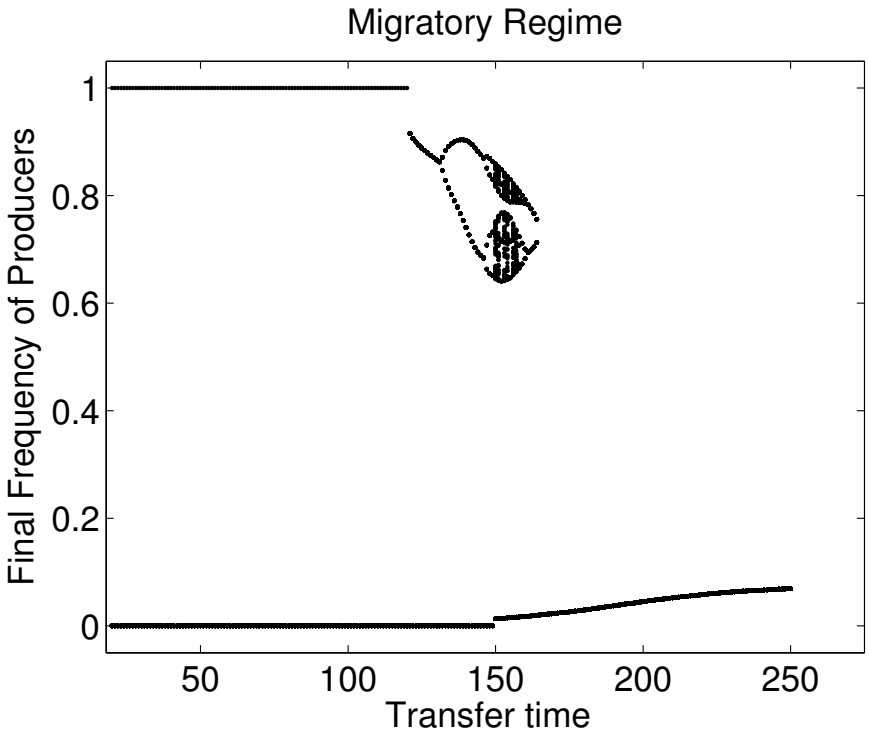

(a) Low degree of mixing ($m = 0.2$)

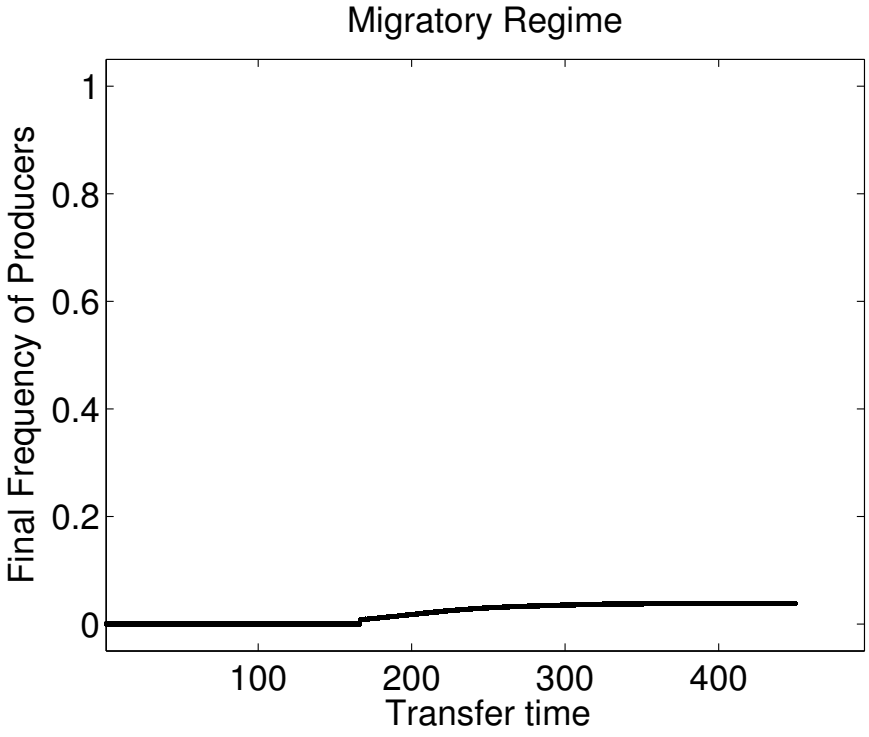

(b) High degree of mixing ($m = 0.8$)

Figure 5-8: Bifurcation diagrams of the migratory regime for values $m = 0.2$ and $m = 0.8$.

presents chaotic dynamics, but in this case only for a low value of the mixing parameter. These observations suggest that spatially structured environments could be an important factor for the system to present a complex dynamics.

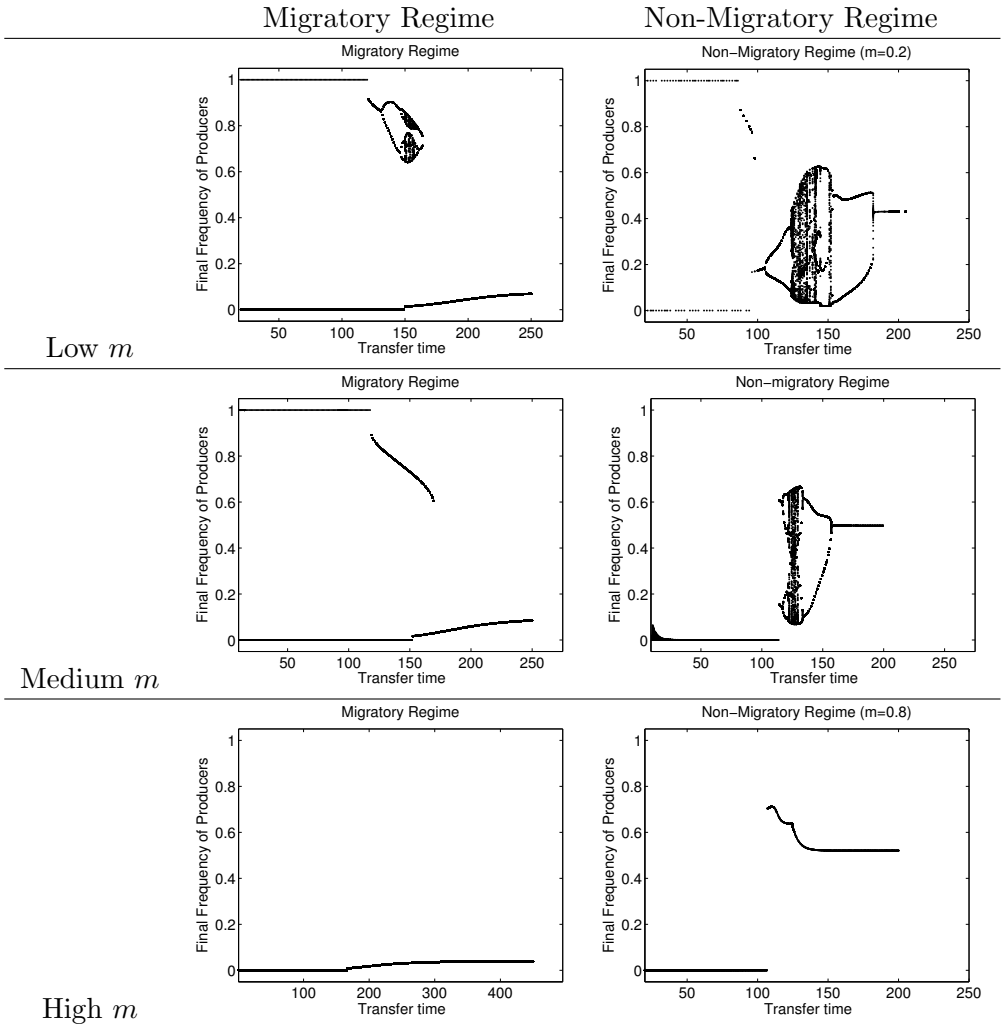

Table 5.2: Panel comparing different degrees of mixing for both the migratory (simple model) and non-migratory regime (parameterised model) showing that for low values of m the system presents chaos.

5.4.1 Final remarks on temporal structure

Here we have investigated the maintenance of diversity in a seasonal structured environment by employing a theoretical approach that utilises a well-known experimental system: invertase production/non-production polymorphism in yeast. Subsequently we asked a range of general ecological questions considering two different regimes for

re-colonisation between seasons: a migratory regime and a non-migratory regime. In the former, the spatial structure is the same at the start of each season, while in the latter the spatial structure at the start of a season is determined by the spatial structure seen at the end of the prior season. We found that for complete seasons (when all the food has been depleted), co-existence between the two different strains of yeast is observed.

Under both regimes, we expect one equilibrium for each m, regardless of the initial condition. This result we thus consider to be potentially of some generality applicable beyond the confines of our particular yeast system. Indeed, this result suggests that in considering the dynamics of co-operation, it would be profitable to consider not just how social structure co-evolves with co-operation but also how co-operators and cheats migrate between seasons.

Surprisingly we found that when not all the resources have been depleted the outcome of the system is rather different. As it is uncommon that resource exhaustion is assayed, it is worth asking whether this might be an important assumption. Moreover, this may also be relevant to cases where migration or over-wintering is initiated on the expectation that resources will be depleted, rather than when they have been exhausted. We showed that the length of the seasons is also important for the maintenance of co-existence. If we explore incomplete seasons, non-producers are able to invade and outcompete producers. This may not be a general result. The producers lose out because early in their growth phase is when they make most of the costly invertase. Hence transferring early gives advantage to the non-producers. Temporal dynamics of cost, while greatly relevant for our case need not be so relevant in other circumstances.

Our results have implications for experimental design. In general these regimes are used to obtain information about maintenance of diversity [42, 64, 99]. It is well recognised that population structure is often important in this context. Whether population structure is something that itself is permitted to evolve is, as we have shown an important issue to consider. Whether the temporal dynamics of resource use matters

and, in turn, whether failure to exhaust resources matters is worth considering on a case-by-case basis.

This chapter has discussed how a seasonal environment can induce a complex dynamics into the system. This unexpected result, however, has produced a series of interesting questions that we expect to address in future research, both theoretical and experimental.

CHAPTER 6

Discussion

Using a classic "cooperative" system based on the polymorphic secretion of invertase in yeast [36, 61], we constructed a mathematical model to study a set of competition experiments between individuals that produce invertase and individuals that do not produce this enzyme. The assumptions of our model are based on the basic biochemistry of yeast and thus the corresponding fitness of different strains was not defined *a priori*.

Interestingly, experimental results showed that when competing these strains in a resource-limited and structured environment, a population composed of producers and non-producers of invertase has a higher fitness (than a population formed of just producers. This result, although counterintuitive, is in agreement with the predictions of our model. Furthermore, our modelling approach allowed us to obtain a mechanistic understanding of the system, identifying the following conditions as necessary to explain this result:

- **Some organisms present a rate-efficiency trade-off [60, 69].** Cells use resources most efficiently when the resources are rare. For this reason, a population consisting only of producers of invertase creates abundant resources and therefore

consumes them inefficiently, lowering the overall fitness of the population.

- **Producing unnecessary invertase, which has a metabolic cost associated.** It is important to notice that, as invertase production is regulated exclusively by glucose, cells produce invertase even when there is no more sucrose to be hydrolysed. Consequently cells waste the extra invertase produced whilst still paying the cost of producing it.

  The wasteful production of invertase, however, only has an impact when sucrose is a limiting resource. The reason why yeast evolves this regulatory system (yeast only has sensors for glucose) is unknown and may be an interesting follow-up of this work. A possible explanation could be that the strain we are using evolved in a laboratory environment, where glucose is the principal carbon source, other possible explanation could be that yeast has also evolved in seasonal environments, and therefore producing extra invertase for the time when sucrose becomes available again could be an effective bet-hedging strategy. A possible follow up could be engineer a strain capable of sensing sucrose and compete it with our strain (just capable of sensing glucose).

- **Spatially structured environments.[39, 74]** The experimental setup is designed in such a way that yeast grows in spatially structured environments (agar plates). Our model includes spatial structure in a phenomenological way, when the same system is tested in homogeneous environments (shaking flasks), both theory and experiments, didn't held the result that mixed populations are fitter than populations exclusively formed of producers.

In our theoretical model we found that mixed population are fitter than populations formed exclusively of producers. We found this result surprising as classical cooperation theory assumes that co-operative behaviour always increases the fitness of the population [70, 19].

We argue that this result could help us understand the coexistence of apparent "cheats" and "cooperators" in a population, and why we observed their coexistence in

nature. In our model system, social interaction between them will increase the benefit for both as a group, instead of as individual strains.

6.0.2 Spatial structure matters

In order to study nature and to understand how organisms have evolved, it is important to understand the consequences of spatially structured environments in their ecological interactions. The competitive exclusion principle states that well-mixed environments are beneficial to species with the higher fitness in that particular environment, not allowing other phenotypes to survive [4]. In a heterogeneous environment , however, it is possible to have different niches supporting organisms with a wide variety of survival strategies. For instance, cooperative strategies benefit from a spatially structured environment.

In Chapter 3 we constructed a spatially explicit model based on the diffusion equation and the parameterisation previously used. With this approach we found the same qualitative results as seen in our competition experiments, and in agreement with the three-region model. In particular, we found that in this model system fitness also peaks at an intermediate frequency, and as a consequence we showed the result is robust to different models of spatial diffusion of resources.

Furthermore, the spatially explicit model is in agreement with previous studies [21, 71, 100] stating that the best way of maintaining coexistence between two competitors is a“patchy structure”. This structure allows producers to keep enough sugar to compensate the cost of producing invertase, but sharing enough and therefore not suffering the effect of the rate-efficiency trade-off by maintaining the levels of sugars low enough to stay in the upper plateau of the function. The optimal scenario for the group is such that part of the sugar has to be shared with non-producers and as a consequence the population (as a group) increments its fitness. Of course there is a fine equilibrium between how much resources producers have to share in order to avoid the rate-efficiency trade-off and having enough to maintain their growth.

Also, by changing the initial population distribution and as a consequence the population structure, we obtained different results regarding the long-term coexistence of producers and non-producers, it is important to notice that spatial structure is not a sufficient conditions for finding coexistence in the long-term in this system.

Having found the phenomenological and the spatially explicit model give the same qualitative predictions, for the remainder of the thesis we decided to use the previous m model as it had the advantage of giving not only qualitative predictions but also to predict quantitatively our experimental data. This was, after all, the principal motivation of using a systems-biology approach instead of a general-model approach.

6.0.3 Temporal Structure also matters

During the first chapters of this thesis we considered a one-season scenario in order to quantify the relative fitness of producers with respect to non-producers. The experimental system we considered is based on each replicate having the same initial conditions (concentration of resources and total density of cells) and the same initial spatial structure. If any of these initial conditions was not preserved, we would not be able to make any objective comparisons between the experiments.

The maintenance of diversity in ecosystems is an important topic in evolutionary biology [16]; temporal structure can be responsible for the complex interactions that we observe in nature. A competition between two actors in one season does not necessarily reflect the outcome of the competition between the same two actors under a seasonal regime.

In experimental evolution serial transfer regimes are used as a proxy of seasonal environments. This is a widely used technique in the study of evolution in microorganisms and one that we have used to study the long-term coexistence between producers and non-producers.

We found that there are at least two different ways of experimentally transferring from one season to another, the difference between them is the way by which the

spatial structure is kept between seasons. An analogy of both transfer protocols can be described as migratory and non-migratory regimes in nature, both being well-studied settings in ecology.

During an academic visit to Greig's lab in the Max Planck Institute in Plön, I performed long-term competition experiments in order to evaluate the long-term consequences of both regimes. Although the results obtained seem to be inconclusive, this motivated a further theoretical study regarding the hybrid dynamics of both transfer protocols. The result of this study, and a possible explanation of the inconclusiveness of the experiments, is discussed in Chapter 5.

Why were the results of the first set of experiments inconclusive? This question can have many answers, first of all, as we show (in theory) this system is highly complex and details of the spatial structure and the timing between transfers can fundamentally affect the resulting dynamics.

For example, if the experimental design allocates a single patch on the centre of a 25 ml agar plate, under a migratory regime this small patch was transferred to a fresh medium maintaining the same size, in contrast uto the non-migratory regime where transfers are performed by replica plating. As a result the patch in the middle is"squeezed" and therefore increases its diameter with each season. It is important to highlight this issue because agar is a semi-solid material and the sugar has to diffuse through it, so it is possible that agar plates that have bigger patches have also better access to sugar in the medium. Although we let yeast grow for 6 days, the remaining sugar at the end of the season was not measured. It could even be the case that in one of the regimes cells were depleting the available sugar while in the other case there was still sugar in the environment. This apparently minor difference may have dramatic consequences.

In our theoretical study, we extended our model in order to introduce a serial transfer regime, and we found that the long-term equilibrium is very sensitive to the length of the season and the timing between transfers. Transferring before all the sugar

has been depleted can lead to multiple steady states and in some cases drive the system into a chaotic regime.

We believe this result could be relevant in the design of experimental protocols. This result, however, is still preliminary, as a rigorous mathematical analysis has to be performed in addition to testing it experimentally. Furthermore, it is important to notice that this result is not contingent upon the model system studied in this thesis; here we argue that this complex dynamics could be a consequence of the underlying seasonal dynamics. In order to test this hypothesis, we constructed a simplified version of the model that ignores the metabolic detail and still recovers the complex dynamics.

Indeed the simple model also found that chaotic behaviour is more robust than expected and not a consequence of the transfer regime under consideration. This is an important observation as it allows us to study the dynamics of the system using a transfer protocol that preserves the population structure between seasons and therefore allowing us to construct a map between different initial conditions.

Performing numerical simulations on the simple model we found that the chaotic behaviour could be found in both transfer regimes, but with different models; the system specific and the toy model, the reason could be the dynamics of the phenomenological spatial mode. To test is this is the case a follow up would be do the transfers with different regimes in the explicit spatial model. We believe the fact that we can found chaos in this system could be relevant to test this phenomenon experimentally, because then it is possible to characterise the long-term dynamics of the system based only on an analysis of the dynamics within one season. Choosing several initial conditions, and using the transfer protocol that preserves population structure between seasons, we can determine the long-term status of each sub-population using a one-dimensional iterated map and a cobweb plot.

6.0.4 How general are the results presented in this thesis?

After the publication of the main result presented in this thesis [61], we have received comments expressing concerns about the generality of our predictions, and criticising our approach for being too system-specific. I agree that using the modelling approach used in this thesis, it would be very difficult, if not impossible, to study co-operative behaviour in more complex systems. Nevertheless, two of the three fundamental conditions discussed in this thesis are general properties present in different co-operative systems [29], being imperfect information the only "system-specific" condition.

Other approaches, for instance those that use game theory as a main theoretical tool, would of course be more flexible as in general they ignore biochemical details of the system. However, it is our contention that using a bottom-up approach gives us a mechanistic understanding of the system that could help us find the biological basis underlying the maintenance of cooperation, fundaments that could eventually be tested in other co-operative systems. Is it too much to suggest that for theoretical models to be useful they should say something new about a system, and not only be used to validate the observer's biological intuition?

Here we have shown that there are circumstances where non-producers of invertase (also known as "cheats") add to the fitness of a group when co-existing with producers (referred to as "cooperators"). So, why is it that non-producers are referred to as cheats? If it would be possible to find situations where this phenomenon occurs in different co-operative systems, it may help us find general answers about the social dilemma related to the co-existence of cheats and cooperators in natural environments, especially in structured environments where components of "group" fitness may be most critical. The language of cooperator and cheat is likely to limit our understanding of the system [23], and therefore it may be time to revisit the co-operation problem without using anthropomorphic terms when speaking about microbes.

APPENDIX A

Appendix

A.1 Experimental Design

The experiments have been conducted using a yeast model system developed in Greig and Travisano [36]. It consists of two isogenic yeast strains, *SUC2 (a/a, leu2/leu2, his5/his5, ura3/ura3, SUC2/SUC2)* and *suc2*, an isogenic diploid strain in which both copies of *SUC2* have been replaced by *KanMX*. *SUC2* secretes the enzyme invertase required to catalyse hydrolysis of sucrose into glucose and fructose and is therefore termed producer or co-operator, while the other strain suc2 does not secrete invertase and is termed non-producer or cheat. For all experiments, yeast were grown in supplemented minimal medium (5 g/L ammonium sulphate, 1.7 g/L yeast nitrogen base, 50 mg/L uracil, 20 mg/L histidine, 50 mg/L leucine) containing agar (16g/L), sucrose, and glucose when necessary. All cultures were grown at a temperature of 30°C and liquid cultures were shaken using an orbital incubator (150 rpm). For further details of strains see [36, 60].

A.1.1 Experimental Design A

SUC2 and suc2 were competed against each other for 24 h in 16 chemostats supplied with glucose-limited culture medium (0.8 g/L) incubated with continuous shaking and aeration. Dilution rate varied between 0.2 and 0.4 per hour. Using these conditions, glucose uptake rate is between 0.2 and 0.4 mmol/gram/hour [104], which induces the secretion of invertase in SUC2 cells [18] so that invertase makes up approximately 0.1% of cell protein. Quantitative PCR and DNA extracted from samples taken from each chemostat before and after competition was used to measure the change in the abundance of suc2 and SUC2 during competition. Fitness was calculated as the ratio of population doublings during competition (w).

A.1.2 Experimental Design B

Starter cultures of SUC2 and suc2 were grown up overnight in liquid YPD medium. Starter cultures were then diluted down $10 \times^{-} 4$ and each strain was inoculated onto 2 μM filters (Milipore, UK) that were placed on agar plates containing 100 g/L sucrose (10%) or 20 g/L sucrose (2%). Each strain was spread onto four filters on two agar plates of each sucrose concentration. One randomly selected filter was removed from each agar plate after 4 h, 24 h, 30 h, and 48 h. Filters were vortexed in sterile saline for approximately 30 s to form a cell suspension that was diluted down and plated out YPD plates to determine cell titre on each disk. Growth rate was calculated as the slope of population doublings against time during the exponential phase of growth. Results from the 10% and 2% sucrose plates were combined because growth rates were equal on these two media for both strains.

A.1.3 Experimental Design C

We established competition cultures of a *SUC2* strain and a *suc2* strain that were grown up overnight in YPD broth. 20 mL agar plates, containing 20 g/L (2%) sucrose, were inoculated with 20 20 mL aliquots of competition cultures in a standardised 5 by

4 array. We consider two population structures. In the mixed population treatment, each aliquot on a plate consisted of the same mix of both *SUC2* and *suc2*. In the structured treatment each aliquot on a plate consisted of either *SUC2* or *suc2*. In total 12 competitions were carried out on mixed as well as structured plates. For the mixed treatment, starter cultures were mixed to form competition cultures where each aliquot consisted of a fixed proportion of *SUC2*, with the following cases being considered 20%, 40%, 60%, and 80% of *SUC2*. For the structured treatment, cases considered were 20%, 40%, 60%, and 80% of aliquots containing only *SUC2* while the rest of respective aliquots contained *suc2*. In this treatment, the position of *suc2* and *SUC2* aliquots on the array was randomised.

After all sugar was exhausted (population growth had ceased) the content of each agar plate was homogenised by washing cells off of the plate in 3 mL of sterile saline. The fitness of *SUC2* and *suc2* was determined by quantitative PCR on DNA extracted from samples taken before and after competition. To estimate net titre, cells were serially diluted and spread on YPD plates to accurately determine cell numbers at the end of the experiment.

A.1.4 Experimental Design D

The methods for this experiment were the same as for Experiment C with the following exceptions. 20 mL agar plates, containing 2% sucrose, were inoculated with single aliquot of competition culture containing 1.2×10^5 cells evenly spread across the entire plate. We considered the cases where each aliquot contained *SUC2* at an initial frequency of 0%, 20%, 40%, 60%, 80%, and 100%. After 2 days of incubation, the content of the agar plate was homogenised by washing off cells in 3 mL of sterile saline. To determine titre, we plated serial dilutions of this homogenised sample on YPD agar plates.

The titre data from Experiments C and D were subsequently normalised to maximum observed titre in each set-up before presenting in Figure 1.

A.1.5 Experimental Design E

Starter cultures of *SUC2* and *suc2* were grown up for 2 days in liquid YPD medium, and then samples were diluted down and plated to yield single colonies on YPD agar, which were counted to determine the original cell density in the starter cultures. Mixtures of these starter cultures were made corresponding to 100%, 80%, 60%, 40%, 20%, and 0% by volume of the *SUC2* culture, and these were diluted 10-fold with sterile water. 13 μL of each of these diluted mixtures was pipetted onto the centre of 20 ml plates containing 0.1% or 0.01% sucrose. These plates were incubated for 7 days, then the patch of cells in the middle of each plate was cut out of the agar using a sterile scalpel and placed into 5 ml of sterile water in a capped test-tube. These test-tubes were vortexed vigorously to wash the yeast cells from the agar, and the resulting suspension was diluted down and plated out on YPD medium to determine the number of cells in each patch.

A.1.6 Experimental Design F

For the experiment in liquid culture, 1.3 μL of each of the diluted cell mixtures, as described in Design E, was pipetted into 2 ml liquid 2% sucrose medium in 25 mm wide test-tubes. These were incubated for 2 days with shaking, before the cultures were diluted down and plated to determine the number of cells in each culture. The experiments were replicated three times.

A.1.7 Quantitative PCR

DNA for use in quantitative PCR was extracted using a Wizard genomic DNA extraction kit (Promega, UK) as per the manufacturer's instructions. DNA was amplified using SYBR Green Master Mix (Applied Biosystems International) or TaqMan Universal PCR master mix (Applied Biosystems International), depending on whether or not a dual-labeled probe was used in the amplification reaction. Amplification reactions contained each primer at a concentration of 900 nM and a dual labeled probe

(where appropriate) at a concentration of 62.5 nM. SYBR Green chemistry was used to detect the SUC2 strain using forward (5'- CGATGATTTGACTAATTGGGAAGA-3') and reverse primers (5'-CCAGAGAAAGCACCTGAATCGT-3') that amplify a section of the SUC2 gene. The suc2 strain was detected using a dual-labeled probe (FAM-CGGGCAATCAGGTGCGACAATCTATC-TAM) that binds between forward (5'-GTATAAATG- GGCTCGCGATAATG-3') and reverse primers
(59-CATC- GGGCTTCCCATACAAT-39) of the KanMX gene. Amplifications were carried out in an ABI 7000 sequence detection under the following reaction conditions: 10 min at 95°C followed by 40 cycles or 95°C for 30 s followed by 60°C for 30 s. The relative copy number of a particular sequence in a given amplification reaction was determined by comparison with standard curves of DNA extracted from known reference strains. Each amplification reaction from a competition culture was carried out with at least 2- to 4-fold replication. Fitness was measured as ratio of doublings of the two strains during competition, such that a value of 1 represents equal competitive ability. Quantitative-PCR based methods have previously been used to measure fitness of yeast during competition, and preliminary experiments revealed that this protocol gives equivalent results to measuring the abundance of *SUC2* and *suc2* by plating samples of competition cultures on YPD and YPD supplemented with geneticin, which selects for the *suc2* strain.

BIBLIOGRAPHY

[1] P. Abbot, J. Abe, J. Alcock, S. Alizon, J. a. C. Alpedrinha, M. Andersson, J.-B. Andre, M. van Baalen, F. Balloux, S. Balshine, N. Barton, L. W. Beukeboom, J. M. Biernaskie, T. Bilde, G. Borgia, M. Breed, S. Brown, R. Bshary, A. Buckling, N. T. Burley, M. N. Burton-Chellew, M. a. Cant, M. Chapuisat, E. L. Charnov, T. Clutton-Brock, A. Cockburn, B. J. Cole, N. Colegrave, L. Cosmides, I. D. Couzin, J. a. Coyne, S. Creel, B. Crespi, R. L. Curry, S. R. X. Dall, T. Day, J. L. Dickinson, L. A. Dugatkin, C. El Mouden, S. T. Emlen, J. Evans, R. Ferriere, J. Field, S. Foitzik, K. Foster, W. a. Foster, C. W. Fox, J. Gadau, S. Gandon, A. Gardner, M. G. Gardner, T. Getty, M. a. D. Goodisman, A. Grafen, R. Grosberg, C. M. Grozinger, P.-H. Gouyon, D. Gwynne, P. H. Harvey, B. J. Hatchwell, J. Heinze, H. Helantera, K. R. Helms, K. Hill, N. Jiricny, R. a. Johnstone, A. Kacelnik, E. T. Kiers, H. Kokko, J. Komdeur, J. Korb, D. Kronauer, R. Kümmerli, L. Lehmann, T. a. Linksvayer, S. Lion, B. Lyon, J. a. R. Marshall, R. McElreath, Y. Michalakis, R. E. Michod, D. Mock, T. Monnin, R. Montgomerie, A. J. Moore, U. G. Mueller, R. Noë, S. Okasha, P. Pamilo, G. a. Parker, J. S. Pedersen, I. Pen, D. Pfennig, D. C. Queller, D. J. Rankin, S. E. Reece, H. K.

Reeve, M. Reuter, G. Roberts, S. K. a. Robson, D. Roze, F. Rousset, O. Rueppell, J. L. Sachs, L. Santorelli, P. Schmid-Hempel, M. P. Schwarz, T. Scott-Phillips, J. Shellmann-Sherman, P. W. Sherman, D. M. Shuker, J. Smith, J. C. Spagna, B. Strassmann, A. V. Suarez, L. Sundström, M. Taborsky, P. Taylor, G. Thompson, J. Tooby, N. D. Tsutsui, K. Tsuji, S. Turillazzi, F. Ubeda, E. L. Vargo, B. Voelkl, T. Wenseleers, S. a. West, M. J. West-Eberhard, D. F. Westneat, D. C. Wiernasz, G. Wild, R. Wrangham, A. J. Young, D. W. Zeh, J. a. Zeh, and A. Zink, *Inclusive fitness theory and eusociality.*, Nature, 471 (2011), pp. E1–4; author reply E9–10.

[2] M. Ackermann, B. Stecher, N. E. Freed, P. Songhet, W.-D. Hardt, and M. Doebeli, *Self-destructive cooperation mediated by phenotypic noise.*, Nature, 454 (2008), pp. 987–90.

[3] M. Archetti and I. Scheuring, *Review: Game theory of public goods in one-shot social dilemmas without assortment.*, Journal of Theoretical Biology, (2012), pp. 9–20.

[4] R. A. Armstrong and R. McGehee, *Competitive exclusion*, The American Naturalist, 115 (1978), pp. 151–170.

[5] R. Axelrod and W. D. Hamilton, *The Evolution of Cooperation*, Evolution, 211 (1981), pp. 1390–1396.

[6] F. Badotti, M. G. Dário, S. L. Alves, M. L. A. Cordioli, L. C. Miletti, P. S. de Araujo, and B. U. Stambuk, *Switching the mode of sucrose utilization by Saccharomyces cerevisiae.*, Microbial Cell Factories, 7 (2008), p. 4.

[7] A. S. Batista, L. C. Mileti, and B. U. Stambuk, *Sucrose fermentation by Saccharomyces cerevisiae lacking hexose transport*, Journal of Molecular Microbiology and Biotechnology, 8 (2006), pp. 26–33.

[8] A. S. Batista, L. C. Miletti, and B. U. Stambuk, *Sucrose fermentation by Saccharomyces cerevisiae lacking hexose transport.*, Journal of Molecular Microbiology and Biotechnology, 8 (2004), pp. 26–33.

[9] R. E. Beardmore, I. Gudelj, D. A. Lipson, and L. D. Hurst, *Metabolic trade-offs and the maintenance of the fittest and the flattest.*, Nature, 472 (2011), pp. 342–6.

[10] M. M. Belinchón and J. M. Gancedo, *Different signalling pathways mediate glucose induction of SUC2, HXT1 and pyruvate decarboxylase in yeast.*, FEMS Yeast Research, 7 (2007), pp. 40–7.

[11] J. J. Boomsma and B. Baer, *The evolution of male traits in social insects*, Annual Review of Entomology, 50 (2005), pp. 395–420.

[12] M. A. Brockhurst, M. G. J. L. Habets, B. Libberton, A. Buckling, and A. Gardner, *Ecological drivers of the evolution of public-goods cooperation in bacteria.*, Ecology, 91 (2010), pp. 334–40.

[13] R. Bshary and A. S. Grutter, *Image scoring and cooperation in a cleaner fish mutualism.*, Nature, 441 (2006), pp. 975–8.

[14] A. Buckling, R. Craig Maclean, M. A. Brockhurst, and N. Colegrave, *The Beagle in a bottle.*, Nature, 457 (2009), pp. 824–9.

[15] J. J. Bull and W. R. Harcombe, *Population dynamics constrain the cooperative evolution of cross-feeding.*, PloS One, 4 (2009), p. e4115.

[16] P. Chesson, *Mechanisms of maintenance of species diversity*, Annual Review of Ecology and Systematics, 31 (2000), pp. 343–366.

[17] T. H. Clutton-Brock, A. F. Russell, L. L. Sharpe, A. J. Young, Z. Balmforth, and G. M. McIlrath, *Evolution and development of sex differences in cooperative behavior in meerkats.*, Science, 297 (2002), pp. 253–6.

[18] R. Craig Maclean and C. Brandon, *Stable public goods cooperation and dynamic social interactions in yeast.*, Journal of Evolutionary Biology, 21 (2008), pp. 1836–43.

[19] J. A. Damore and J. Gore, *Understanding microbial cooperation.*, Journal of Theoretical Biology, (2012), pp. 31–41.

[20] F. B. M. de Waal and M. Suchak, *Prosocial primates: selfish and unselfish motivations.*, Philosophical Transactions of the Royal Society of London. Series B, Biological sciences, 365 (2010), pp. 2711–22.

[21] M. Doebeli and C. Hauert, *Models of cooperation based on the Prisoner's Dilemma and the Snowdrift game*, Ecology Letters, 8 (2005), pp. 748–766.

[22] H. Dong, L. Nilsson, C. Kurland, and C. G, *Gratuitous overexpression of genes in Escherichia coli leads to growth inhibition and ribosome destruction .*, Microbiology, 177 (1995), pp. 1497–1504.

[23] W. W. Driscoll, J. W. Pepper, and L. S. Pierson III, *Spontaneous Gac mutants of Pseudomonas biological control strains: Cheaters or Mutualist?.*, Applied and Environmental Microbiology, 77 (2011), pp. 7227–7235.

[24] Z. Duan, M. Andronescu, K. Schutz, S. McIlwain, Y. J. Kim, C. Lee, J. Shendure, S. Fields, C. A. Blau, and W. S. Noble, *A three-dimensional model of the yeast genome.*, Nature, 465 (2010), pp. 363–7.

[25] K. Elbing, C. Larsson, R. M. Bill, E. Alberts, J. L. Snoep, E. Boles, S. Hohmann, and L. Gustafsson, *Role of hexose transport in control of glycolytic flux in Saccharomyces cerevisiae*, Applied and Environmental Microbiology, 70 (2004), pp. 5323–5330.

[26] K. Elbing, A. Stahlberg, S. Hohmann, and L. Gustafsson, *Transcriptional responses to glucose at different glycolytic rates in Saccharomyces cerevisiae.*, European Journal of Biochemistry, 271 (2004), pp. 4855–64.

[27] S. F. Elena and R. E. Lenski, *Evolution experiments with microorganisms: the dynamics and genetic bases of adaptation.*, Nature Reviews. Genetics, 4 (2003), pp. 457–69.

[28] J. D. Esko and C. R. H. Raetz, *Replica plating and in situ enzymatic assay of animal cell colonies established on filter paper*, Proceedings of the National Academy of Sciences of the United States of America, 75 (1978), pp. 1190–1193.

[29] F. Fiegna, Y.-T. N. Yu, S. V. Kadam, and G. J. Velicer, *Evolution of an obligate social cheater to a superior cooperator.*, Nature, 441 (2006), pp. 310–4.

[30] S. A. Frank, *The trade-off between rate and yield in the design of microbial metabolism.*, Journal of Evolutionary Biology, 23 (2010), pp. 609–13.

[31] J. M. Gancedo, *The early steps of glucose signalling in yeast.*, FEMS Microbiology Reviews, 32 (2008), pp. 673–704.

[32] J. H. Gillespie, *Is the population size of a species relevant to its evolution?*, Evolution; International Journal of Organic Evolution, 55 (2001), pp. 2161–9.

[33] J. Gore and A. van Oudenaarden, *The yin and yang of nature.*, Nature, 457 (2009), pp. 271–2.

[34] J. Gore, H. Youk, and A. van Oudenaarden, *Snowdrift game dynamics and facultative cheating in yeast.*, Nature, 459 (2009), pp. 253–6.

[35] D. Greig, *Population biology: wild origins of a model yeast*, Current Biology, 17 (2007), pp. R251–R253.

[36] D. Greig and M. Travisano, *The Prisoner's Dilemma and polymorphism in yeast SUC genes.*, Proceedings of the Royal Society B. Biological sciences., 271 Suppl (2004), pp. S25–6.

[37] J. H. Koschwanez, K. R. Foster, and A. W. Murray, *Sucrose utilization in budding yeast as a model for the origin of undifferentiated multicellularity*, PLoS Biology, 9 (2011), p. e1001122.

[38] M. G. J. L. Habets, T. Czárán, R. F. Hoekstra, and J. A. G. M. de Visser, *Spatial structure inhibits the rate of invasion of beneficial mutations in asexual populations.*, Proceedingsof the Royal Society B. Biological sciences, 274 (2007), pp. 2139–43.

[39] M. G. J. L. Habets, D. E. Rozen, R. F. Hoekstra, and J. A. G. M. de Visser, *The effect of population structure on the adaptive radiation of microbial populations evolving in spatially structured environments.*, Ecology Letters, 9 (2006), pp. 1041–8.

[40] W. Hamilton, *The evolution of altruistic behavior*, The American Naturalist, 97 (1963), pp. 354–356.

[41] P. Hammerstein, *Why Is reciprocity so rare in social animals? A protestant appeal.*, Genetic Cultural Evolution of Cooperation, (2003), pp. 83–94.

[42] W. R. Harcombe, *Novel cooperation experimentally evolved between species.*, Evolution; International Journal of Organic Evolution, 64 (2010), pp. 2166–72.

[43] C. Hauert and M. Doebeli, *Spatial structure often inhibits the evolution of cooperation in the snowdrift game*, Nature, (2004), pp. 643–646.

[44] M. Hegreness, N. Shoresh, D. Damian, D. Hartl, and R. Kishony, *Accelerated evolution of resistance in multidrug environments.*, Proceedings of the National Academy of Sciences of the United States of America, 105 (2008), pp. 13977–81.

[45] M. E. Hochberg, D. J. Rankin, and M. Taborsky, *The coevolution of cooperation and dispersal in social groups and its implications for the emergence of multicellularity.*, BMC Evolutionary Biology, 8 (2008), p. 238.

[46] W. O. H. Hughes and J. J. Boomsma, *Genetic royal cheats in leaf-cutting ant societies.*, Proceedings of the National Academy of Sciences of the United States of America, 105 (2008), pp. 5150–3.

[47] B. Hunt, L. Ometto, Y. Wurm, D. Shoemaker, V. Soojin, L. Keller, and M. Goodisman, *Relaxed selection is a precursor to the evolution of phenotypic plasticity*, Proceedings of the National Academy of Sciences of the United States of America, 108 (2011), pp. 15936–15941.

[48] P. D. Keightley, *Deleterious Mutations and the Evolution of Sex*, Science, 290 (2000), pp. 331–333.

[49] B. Kerr, M. A. Riley, M. W. Feldman, and B. J. M. Bohannan, *Local dispersal promotes biodiversity in a real-life game of rock-paper -scissors.*, Nature, 2868 (2002), pp. 2865–2868.

[50] N. A. Khan, F. K. Zimmermann, and N. R. Eaton, *Genetic and biochemical evidence of sucrose fermentation by maltase in yeast.*, Molecular & General Genetics, 123 (1973), pp. 43–50.

[51] K. Kiontke, *Evolutionary biology: patchy food may maintain a foraging polymorphism.*, Current Biology, 18 (2008), pp. R1017–9.

[52] T. Köhler, G. G. Perron, A. Buckling, and C. van Delden, *Quorum sensing inhibition selects for virulence and cooperation in Pseudomonas aeruginosa.*, PLoS Pathogens, 6 (2010), p. e1000883.

[53] A. S. Kondrashov, *Deleterious mutations and the evolution of sexual reproduction*, Nature, 336 (1988), pp. 435–440.

[54] J.-U. Kreft and S. Bonhoeffer, *The evolution of groups of cooperating bacteria and the growth rate versus yield trade-off.*, Microbiology, 151 (2005), pp. 637–41.

[55] J. U. Kreft, C. Picioreanu, J. W. Wimpenny, and M. C. van Loosdrecht, *Individual-based modelling of biofilms.*, Microbiology, 147 (2001), pp. 2897–912.

[56] P. Langer, M. A. Nowak, and C. Hauert, *Spatial invasion of cooperation.*, Journal of Theoretical Biology, 250 (2008), pp. 634–41.

[57] J. Lederberg and E. M. Lederberg, *Replica Plating and Indirect Selection of Bacterial Mutants*, Journal of Bacteriology, 63 (1952), pp. 399–406.

[58] R. E. Lenski and G. J. Velicer, *Games Microbes Play*, Selection, 1 (2001), pp. 89–96.

[59] G. M. Santangelo, *Glucose signaling in Saccharomyces cerevisiae*, Microbiology and Molecular Biology Reviews, 70 (2006), pp. 253–282.

[60] R. C. MacLean, *The tragedy of the commons in microbial populations: insights from theoretical, comparative and experimental studies.*, Heredity, 100 (2008), pp. 233–9.

[61] R. C. MacLean, A. Fuentes-Hernandez, D. Greig, L. D. Hurst, and I. Gudelj, *A mixture of "cheats" and "co-operators" can enable maximal group benefit.*, PLoS Biology, 8 (2010).

[62] R. C. MacLean and I. Gudelj, *Resource competition and social conflict in experimental populations of yeast.*, Nature, 441 (2006), pp. 498–501.

[63] C. J. Marx, *Microbiology. Getting in touch with your friends.*, Science, 324 (2009), pp. 1150–1.

[64] A. D. Morgan, S. Gandon, and A. Buckling, *The effect of migration on local adaptation in a coevolving host-parasite system.*, Nature, 437 (2005), pp. 253–6.

[65] C. D. Nadell, K. R. Foster, and J. a. B. Xavier, *Emergence of spatial structure in cell groups and the evolution of cooperation.*, PLoS Computational Biology, 6 (2010), p. e1000716.

[66] J. F. Nash, *Equilibrium Points in N-Person Games.*, Proceedings of the National Academy of Sciences of the United States of America, 36 (1950), pp. 48–9.

[67] G. I. Naumov, E. S. Naumova, E. D. Sancho, and M. P. Korhola, *Polymeric SUC genes in natural populations of Saccharomyces cerevisiae.*, FEMS Microbiology Letters, 135 (1996), pp. 31–5.

[68] L. Neigeborn and M. Carlson, *Genes affecting the regulation of SUC2 gene expression by glucose repression in Saccharomyces cerevisiae.*, Genetics, 108 (1984), pp. 845–58.

[69] M. Novak, T. Pfeiffer, R. E. Lenski, U. Sauer, and S. Bonhoeffer, *Experimental tests for an evolutionary trade-off between growth rate and yield in E. coli.*, The American Naturalist, 168 (2006), pp. 242–51.

[70] M. A. Nowak, *Five rules for the evolution of cooperation.*, Science, 314 (2006), pp. 1560–3.

[71] M. A. Nowak, S. Bonhoeffer, and R. M. May, *Spatial games and the maintenance of cooperation.*, Proceedings of the National Academy of Sciences of the United States of America, 91 (1994), pp. 4877–81.

[72] M. A. Nowak, C. E. Tarnita, and E. O. Wilson, *The evolution of eusociality.*, Nature, 466 (2010), pp. 1057–62.

[73] T. Ohta and J. Gillespie, *Development of neutral and nearly neutral theories*, Theoretical Population Biology, 49 (1996), pp. 128–42.

[74] H. Ohtsuki, C. Hauert, E. Lieberman, and M. A. Nowak, *A simple rule for the evolution of cooperation on graphs and social networks.*, Nature, 441 (2006), pp. 502–5.

[75] K. Otterstedt, C. Larsson, R. M. Bill, A. Stahlber, E. Boles, S. Hohmann, and L. Gustafsson, *Switching the mode of metabolism in the yeast Saccharomyces cerevisiae*, EMBO Reports, 5 (2004), pp. 532–537.

[76] S. Ozcan, J. Dover, and M. Johnston, *Glucose sensing and signaling by two glucose receptors in the yeast Saccharomyces cerevisiae*, EMBO Journal, 17 (1998), pp. 2566–2573.

[77] S. Ozcan and M. Johnston, *Three different regulatory mechanisms enable yeast hexose transporter (HXT) genes to be induced by different levels of glucose.*, Molecular and Cellular Biology, 15 (1995), pp. 1564–72.

[78] M. Pagel, *Natural selection 150 years on.*, Nature, 457 (2009), pp. 808–11.

[79] L. Perfeito, M. I. Pereira, P. R. A. Campos, and I. Gordo, *The effect of spatial structure on adaptation in Escherichia coli.*, Biology Letters, 4 (2008), pp. 57–9.

[80] T. Pfeiffer and S. Bonhoeffer, *An evolutionary scenario for the transition to undifferentiated multicellularity.*, Proceedings of the National Academy of Sciences of the United States of America, 100 (2003), pp. 1095–8.

[81] T. Pfeiffer and S. Bonhoeffer, *Evolution of cross-feeding in microbial populations.*, The American Naturalist, 163 (2004), pp. E126–35.

[82] T. Pfeiffer, S. Schuster, and S. Bonhoeffer, *Cooperation and competition in the evolution of ATP-producing pathways.*, Science, 292 (2001), pp. 504–7.

[83] W. C. Ratcliff, F. Denison, M. Borello, and M. Travisano, *Experimental evolution of multicellularity*, Proceedings of the National Academy of Sciences of the United States of America, 5 (2012), pp. 1595–600.

[84] E. Reifenberger, E. Boles, and M. Ciriacy, *Kinetic characterization of individual hexose transporters of Saccharomyces cerevisiae and their relation to the triggering mechanisms of glucose repression.*, European Journal of Biochemistry, 245 (1997), pp. 324–33.

[85] C. F. Roberts, *A replica plating technique for the isolation of nutritionally exacting mutants of a filamentous fungus (Aspergillus nidulans).*, Journal of General Microbiology, 20 (1959), pp. 540–8.

[86] C. P. Roca, J. A. Cuesta, and A. Sánchez, *Effect of spatial structure on the evolution of cooperation*, Physical Review E, 80 (2009), pp. 1–16.

[87] F. Rolland, J. Winderickx, and J. M. Thevelein, *Glucose-sensing and -signalling mechanisms in yeast.*, FEMS Yeast Research, 2 (2002), pp. 183–201.

[88] K. G. Ross and L. Keller, *Ecology and evolution of social organization: insights from fire ants and other highly eusocial insects*, Annual Review of Ecology and Systematics, 26 (1995), pp. 631–656.

[89] A. Ross-Gillespie, A. Gardner, A. Buckling, S. A. West, and A. S. Griffin, *Density dependence and cooperation: theory and a test with bacteria.*, Evolution; International Journal of Organic Evolution, 63 (2009), pp. 2315–25.

[90] J. L. Sachs, U. G. Mueller, T. P. Wilcox, and J. J. Bull, *The Evolution of Cooperation*, The Quarterly Review of Biology, 79 (2004), pp. 135–160.

[91] A. N. Sarkovskii, *Coexistence of cycle of a continuos map of the line into itself.*, Ukrain Mat. Zh., 16 (1964), pp. 61–71.

[92] S. Schuster, J.-U. Kreft, N. Brenner, F. Wessely, G. Theissen, E. Ruppin, and A. Schroeter, *Cooperation and cheating in microbial exoenzyme production–theoretical analysis for biotechnological applications.*, Biotechnology Journal, 5 (2010), pp. 751–8.

[93] M. L. Sogin, H. G. Morrison, J. A. Huber, D. M. Welch, S. M. Huse, P. R. Neal, J. M. Arieta, and G. J. Herndl, *Microbial diversity in the deep sea and the underexplored "rare biosphere"*., Proceedings of the National Academy of Sciences of the United States of America, 32 (2006), pp. 12115–12120.

[94] B. U. Stambuk, A. S. Batista, and P. S. de Araujo, *Kinetics of active sucrose transport in Saccharomyces cerevisiae*, Journal of Bioscience and Bioengineering, 89 (2000), p. 212.

[95] E. Szathmary and J. Maynard Smith, *The major evolutionary transitions*, Nature, 374 (1995), pp. 227–232.

[96] C. E. Tarnita, T. Antal, H. Ohtsuki, and M. A. Nowak, *Evolutionary dynamics in set structured populations.*, Proceedings of the National Academy of Sciences of the United States of America, 106 (2009), pp. 8601–4.

[97] A. M. Turing, *The Chemical Basis of Morphogenesis*, Philosophical Transactions of the Royal Society B: Biological Sciences, 237 (1952), pp. 37–72.

[98] J. P. van Dijken, J. Bauer, L. Brambilla, P. Duboc, J. M. Francois, C. Gancedo, M. L. F. Giuseppin, J. Heijnen, M. Hoare, H. C. Lange, E. A. MAdden, P. Niederberger, J. Nielsen, J. L. Parrou, T. Petit, D. Porro, M. Reuss, N. van Riel, M. Rizzi, H. Y. Steensma, C. T. Verrips, J. Vindelov, and J. T. Pronk, *An interlaboratory comparison of physiological and genetic properties of four Saccharomyces cerevisiae strains*, Enzyme and Microbial Technology, 26 (2000), pp. 706–714.

[99] P. A. Venail, R. C. MacLean, T. Bouvier, M. A. Brockhurst, M. E. Hochberg, and N. Mouquet, *Diversity and productivity peak at intermediate dispersal rate in evolving metacommunities.*, Nature, 452 (2008), pp. 210–4.

[100] J. Y. Wakano, M. A. Nowak, and C. Hauert, *Spatial dynamics of ecological public goods.*, Proceedings of the National Academy of Sciences of the United States of America, 106 (2009), pp. 7910–4.

[101] C. Wedekind and M. Milinski, *Cooperation through image scoring in humans*, Science, 288 (2000), pp. 850–852.

[102] S. A. West and A. Buckling, *Cooperation, virulence and siderophore production in bacterial parasites.*, Proceedings of the Royal Society B. Biological sciences, 270 (2003), pp. 37–44.

[103] S. A. West, A. S. Griffin, A. Gardner, and S. P. Diggle, *Social evolution theory for microorganisms.*, Nature Reviews Microbiology, 4 (2006), pp. 597–607.

[104] R. A. Weusthuis, J. T. Pronk, P. J. Van Den Broek, and J. P. van Dijken, *Chemostat cultivation as a tool for studies on sugar transport in yeasts*, Microbiological Reviews, 58 (1994), pp. 616–630.

[105] G. S. Wilkinson, *Reciprocal food sharing in the vampire bat*, Nature, 308 (1984), pp. 181–184.

[106] M. Woolfit and K. Wolfe, *The gene duplication that greased society's wheels*, Nature Genetics, 37 (2005), pp. 566–567.

[107] J. B. Xavier and K. R. Foster, *Cooperation and conflict in microbial biofilms.*, Proceedings of the National Academy of Sciences of the United States of America, 104 (2007), pp. 876–81.

[108] S. Zaman, S. I. Lippman, X. Zhao, and J. R. Broach, *How Saccharomyces responds to nutrients.*, Annual Review of Genetics, 42 (2008), pp. 27–81.

[109] C. Zeyl, *Budding yeast as a model organism for population genetics.*, Yeast, 16 (2000), pp. 773–84.